Summer 6-25-2014

Development and Validation of a Postural Controller for Advanced Myoelectric Prosthetic Hands

Jacob Lionel Segil
University of Colorado Boulder, jacob.segil@colorado.edu

Development and Validation of a Postural Controller for Advanced Myoelectric Prosthetic Hands

by

JACOB LIONEL SEGIL

B.S., University of Illinois at Urbana-Champaign, 2008

M.S., University of Colorado at Boulder, 2012

A thesis submitted to the

Faculty of the Graduate School of the

University of Colorado in partial fulfillment

of the requirement for the degree of

Doctor of Philosophy

Department of Mechanical Engineering

2014

This thesis entitled:

Development and Validation of a Postural Controller

for Advanced Myoelectric Prosthetic Hands

written by Jacob Lionel Segil

has been approved for the Department of Mechanical Engineering

_____

Richard F. *ff.* Weir, Ph.D.

_____

Mark Rentschler, Ph.D., P.E.

Date _____

The final copy of this thesis has been examined by the signatories, and we find that both the content and the form meet acceptable presentation standards of scholarly work in the above mentioned discipline.

IRB protocol # 11-0152

Segil, Jacob Lionel (Ph.D., Mechanical Engineering)

Development and Validation of a Postural Controller for Advanced Myoelectric Prosthetic Hands

Thesis directed by Professor Richard F. *ff*. Weir

Myoelectric control systems (MECs) remain the technological bottleneck in the development of advanced prosthetic hands. MECs should provide a human machine interface that deciphers user intent in real-time and operates effectively in daily life. Current MECs like finite state machines and pattern recognition systems require physiologically inappropriate commands to indicate intent and/or lack effectiveness in a clinical setting. The work of this dissertation aims to develop and validate a novel MEC architecture, namely postural control, in order to supplant the current state of the art MECs and recreate more of the characteristics of the intact limb. Specifically, the development of the postural control systems builds upon previous work based on principal component analysis of human grasping. Novel attributes of the postural control system were then added to the MEC, empirically tested, and validated with able limbed subjects using a virtual hand interface. Further investigation of the postural controller was performed by comparing it to state of the art commercial and research MECs with able limbed subjects using a physical prosthesis during activities of daily living. The dissertation concludes by verifying the increased effectiveness and robustness of the postural controller compared to other MECs when used by persons with transradial limb loss to perform activities of daily living with a physical prosthesis.

<u>Dedication</u>

For my wife, Carrie. To my father, Laurence J. Segil who inspired my love of science.

<u>Acknowledgements</u>

I owe much gratitude to my advisor Professor Richard F. *ff.* Weir for his substantial time and effort dedicated to this project and many others during the past six years. Also, my committee members Professor Derek Reamon, Professor Mark Rentschler, Professor Lawrence Carlson, and Professor Alena Grabowski contributed advice and encouragement throughout this project. Several other people were helpful with specific challenges throughout the project. Dr. Christian Cipriani was a great mentor and collaborator. Stephen Huddle provided extensive help in preparing the experimental apparatus in Chapter 6. Nick Stites, Darren McSweeney, Tim May, Jared Wampler, and Jay Franklin from the Integrated Teaching and Learning Laboratory aided the software and electronic designs throughout the project. Professor Alena Grabowski, Professor Rodger Kram, and Professor Alaa Ahmed donated laboratory space and equipment as well as offered encouragement and advice. Finally, many friends volunteered their time as subjects in all of the experiments and they all deserve acknowledgement as well. This work was mainly supported by Award Number I01BX007080 from the Rehabilitation Research & Development Service of the VA Office of Research and Development. Additional support was provided by the Whitaker Foundation, the Italian Ministry of Education University and Research under the FIRB-2010 MY-HAND Project [RBFR10VCLD], and by the European Commission under the WAY project (FP7-ICT-228844).

<u>Content</u>

Figures

Abbreviations

ABLE = able-bodied subjects

ADL = activity of daily living

AMP = subject with limb loss

C1/C2/C3 = controller 1/2/3

CR = completion rate

CNS = central nervous system

DoA = degree of actuation

DoF = degree of freedom

E = extension electromyographic signal

EMG = electromyography

F = flexion electromyographic signal

FP = functionality profile

HF = hand flat

HK = hook

HMI = Human-machine interface

IMES = implantable myoelectric sensors

JAT = joint angle transform

LP = lateral prehension

MCP = metacarpophalangeal joint

MECs = myoelectric control systems

MES = myoelectric signals

MT = movement time

OP = opposition

P3/P4/P12 = 3, 4, 12-site position control

PC = postural control

PCA = principal component analysis

PE = path efficiency

PIP = proximal interphalangeal joint

PP = palmar prehension

PT = pointer

RMS = root mean square

SHAP = southampton hand assessment procedure

S_S = SHAP score

T = trigger

TC = time to completion

TMR = targeted motor reinnvervation

TP = tip prehension

U = ulnar deviation electromyographic signal

UPLOM = upper limb prosthetic outcome measures

V3/V4/V12 = 3, 4, 12-site velocity control

VH = virtual hand

VSA = vector summation algorithm

"In the absence of any other proof, the thumb alone would convince me of God's existence."
Sir Issac Newton

Chapter 1 - Motivation and Specific Aims

The development of advanced prosthetic limbs is an active and highly visible field of research. Much attention in this field has focused on brain machine interfaces [1], [2], [3], peripheral nerve implants [4], [5], [6] and surgical techniques to augment the neuromuscular system [7], [8]. These technologies promise revolutionary therapies for persons with limb loss and other neuromuscular disorders however are far from clinical relevance today. There is a great need for near term, clinically focused research. A large portion of upper limb prosthetic device users still prefer body-powered, split hook devices [9], a World War II era technology. New multifunctional commercial prosthetic hands have recently become more prevalent [10] due to advances in microprocessor technology, electric motor design, and battery power. Now, the technological bottleneck in the development of clinically viable advanced prosthetic limbs is the human machine interface.

The prevailing clinically relevant human machine interfaces in the field of upper limb prosthetic control are myoelectric control systems. Myoelectric control systems (MECs) should provide a human machine interface that deciphers users intent in real-time and operates effectively in daily life. Many MECs have been developed including direct control schemes, pattern recognition systems, and finite state machines, however no MECs can recreate the fluidity, intuitiveness, and dexterity of the intact neuromuscular system. In this dissertation, a novel MEC architecture, namely postural control, was developed and validated by the authors in

order to supplant the current state of the art MECs and recreate more of the characteristics of the intact limb. **This works aims to answer the hypothesis that postural control systems provide a more effective and clinically robust interface compared to state of the art systems in the commercial and research realms for persons with transradial limb loss using myoelectric prosthetic hands.**

This dissertation investigated this hypothesis in four aims. More specifically, the original development of the postural control systems built upon previous work based on Santello et al.'s [11] study using principal component analysis of human grasping. Novel attributes of the postural control system were then added to the postural controller, empirically tested, and validated with able limbed subjects using a virtual hand interface. Further validation of the postural controller was performed by comparing it to state of the art commercial and research MECs with able limbed subjects using a physical prosthesis during activities of daily living. The dissertation concludes by validating the effectiveness and robustness of the postural controller when used by persons with transradial limb loss. The specific aims for this dissertation are:

Specific Aim 1: Design and Validation of a Morphing Myoelectric Hand Posture Controller Based on Principal Component Analysis of Human Grasping[1]

The principal component analysis (PCA) of human grasping performed by Santello et al. [11] provided the motivation for the development of a postural controller. Santello et al., found that two principal components described the majority of the variance in human joint angles

---

[1] Segil, J.L.; Weir, R.F.F., "Design and Validation of a Morphing Myoelectric Hand Posture Controller Based on Principal Component Analysis of Human Grasping," *Neural Systems and Rehabilitation Engineering, IEEE Transactions on* , vol.22, no.2, pp.249,257, March 2014 doi: 10.1109/TNSRE.2013.2260172

during grasping. In other words, most grasps performed during activities of daily living could be mapped to a two dimensional domain. This finding inspired the design of a novel MEC, namely postural control. This aim describes the design and validation of a morphing myoelectric hand controller based on principal component analysis of human grasping. The postural controller commands continuously morphing hand postures including functional grasps using between two and four surface electromyography (EMG) electrodes pairs. Four unique maps were developed to transform the EMG control signals in the principal component domain. A preliminary validation experiment was performed by 10 non-amputee subjects to determine the map with highest performance. The subjects used the myoelectric controller to morph a virtual hand between functional grasps in a series of randomized trials.   The number of joints controlled accurately was evaluated to characterize the performance of each map. Additional metrics were studied including completion rate, time to completion, and path efficiency. The highest performing map controlled over 13 out of 15 joints accurately.

Specific Aim 2: A Novel Postural Control Algorithm for Simultaneous and Proportional Control of Multi-Functional Myoelectric Prosthetic Hands[2]

The design of the postural controller developed in aim 1 was further advanced in this aim. Most significantly, the algorithm that allows for customizable, dynamic postural control domain maps was developed and integrated into the postural controller. This attribute was previously impossible when the postural control domain was based solely on the PCA of human grasping. Additional design attributes were added including various cursor control techniques and potential wells. Design parameters of the postural controller were empirically tested including

---

[2] Intended publication with *Journal of Neural Engineering* submitted January 2014 with co-author Richard F. *ff.* Weir, Ph.D.

position/velocity cursor control techniques, the necessary number of EMG control signals, and the robustness of the system to donning/doffing. Here the novel algorithm for a postural controller is presented and tested during two experiments with eleven total able bodied subjects. The first experiment consisted of a center-out target acquisition task using various configurations of the myoelectric postural controller in order to empirically determine suitable design parameters. The second experiment involved a hand posture matching exercise using a virtual hand interface and quantified subject performance and learning using the postural controller over a period of three days. In the first experiment, we found that the performance increased when using a velocity cursor control technique versus a position cursor control technique. Also, the performance did not change when using three, four, or twelve surface electrodes. In the second experiment, subjects commanded a six degree of freedom virtual hand into seven functional postures without training with completion rates of 82% ± 4%, movement times of 3.5s ± 0.2s, and path efficiencies of 45% ± 3%. Subjects retained the ability to use the postural controller at a high level across days after a single one-hour training session. Our results substantiate the novel algorithm for a postural controller as a robust and advantageous design for a MEC of multi-function prosthetic hands.

Specific Aim 3: A Comparative Study of State of the Art Myoelectric Controllers for Multi-Grasp Prosthetic Hands[3]

The design of the postural controller was shown to be robust and effective during virtual hand posture matching tasks, however the efficacy of the system when implemented on a physical device required further evidence. Here a comparative study of two types of finite state

---

[3] Intended publication with *Journal of Rehabilitation Research and Development,* submitted February 2014 with co-authors Marco Controzzi, Ph.D., Richard F. *ff.* Weir, Ph.D., and Christian Cipriani, Ph.D.

machines and a postural control scheme using both virtual and physical assessment procedures with seven able-limbed subjects is presented. The Southampton Hand Assessment Procedure was used in order to compare the effectiveness of the controllers during activities of daily living using a multi-grasp artificial hand. Also, a virtual hand posture matching task was used to compare the controllers when reproducing six target postures. The performance when using the postural control scheme was significantly better ($p < 0.05$) than the finite state machines during the physical assessment when comparing within subject averages using the SHAP percent difference metric. The virtual assessment results described significantly greater completion rates (97% and 99%) for the finite state machines but the movement time tended to be faster (2.7s) for the postural control scheme. Our results substantiate that postural control schemes rival other state of the art myoelectric controllers during object manipulation tasks and other activities of daily living

Specific Aim 4: Functional Assessment of Persons with Transradial Limb Loss Using a Myoelectric Postural Controller and Multi-functional Prosthetic Hand[4]

Finally, the postural controller was tested by persons with transradial limb loss in order to answer the overarching hypothesis that the system provides a more effective and clinically robust interface when compared to state of the art systems in the commercial and research realms. Persons with transradial limb loss present additional complications with regards to the design of the postural controller due to the differences in residual limb size, musculature, and neural control. Several design modifications were made in order to address these challenges and then

---

[4] Intended publication with *Myoelectric Controls Symposium,* submitted March 2014 with co-authors Stephen Huddle, M.S. and Richard F. *ff.* Weir, Ph.D.

tested. Here a functional assessment of persons with transradial limb loss with a myoelectric postural controller and multi-functional prosthetic hand is presented. Persons with transradial limb loss performed the Southampton Hand Assessment Procedure with a modified Bebionic hand and a postural controller. Able-limbed subjects also performed the test with the identical prosthesis and controller for comparison. The results describe that the transradial amputees and able-limbed subjects achieved the same performance indicating that the postural controller is a valid myoelectric control system after transradial limb loss. The transradial amputees restored 55% of typical hand function on average. Also by deduction, the postural controller would perform better than the other state of the art MECS tested for persons with limb loss as well. The results show that the postural controller compared favorably to other myoelectric controllers in the commercial and research realms and demonstrate the clinical efficacy of the postural controller for transradial amputees.

Chapter 2 - Background

A brief overview of the neuromuscular system with an emphasis on upper limb anatomy, motor control theory, and grasp taxonomy is presented along with an introduction to myoelectric control systems. A detailed review of the state-of-the-art myoelectric prosthetic hand control schemes concludes the section.

Neuromuscular System

Upper Limb Anatomy

The human arm and hand is a complex and robust system capable of powerful grasps and fine manipulation. In particular, the human hand has been described as nature's most wondrous machine. Sir Issac Newtwon once said, 'In the absence of any other proof, the thumb alone would convince me of God's existence' [12]. The musculoskeletal system of the hand consists of at least 18 joint articulations controlled by over 30 muscles [13]. The hand has proprioceptors that sense the position of the hand in space and sensory receptors capable of sensing temperature, vibration, shear, and movement [14].

Skeletal muscles are composed of muscle fibers that can be volitionally controlled. A neural command causes the actin and myosin filaments within the myofibrils to ratchet along the length of the sarcomere and produce a muscle contraction. The flow of ions across the muscle cell membrane during the contraction creates electric potentials that can be measured using electrodes. This naturally occurring voltage produces a quasi-Gaussian distributed random noise electric field called the electromyogram. Electromyography (EMG) is the study of these muscle, or myoelectric, signals (MES). The EMG signal can be measured from the surface of the skin

using surface electrodes and/or within the muscle fiber using intramuscular electrodes. The EMG signal is a composite, or superposition, of the all of the electric potentials created within the electrode detection volume. The measured signal is generally monotonic and is proportional to the amount of muscle activity in the detection volume [15]. The use of EMG in the control of prosthetic devices is discussed more thoroughly in the *Introduction to Myoelectric Control Systems* section.

Grasp Taxonomy

The complexity of the human hand has led to extensive research into its typical uses. Grasps taxonomies have been developed since the mid-20th century in order to organize the ways the human hand is used [12], [16], [17]. In general, there is consensus on the six most common grasp patterns which include lateral prehension, tip prehension, power prehension, extension, tripod, and spherical prehension (Figure 1, [18]). More specifically, palmar, lateral, and tip prehension are the most used grasps [16]. These six functional grasps can be organized further into opposed and unopposed grasps. Opposed grasps including tripod, tip prehension, and extension are formed with the thumb adducted across the palm. Unopposed grasps including lateral prehension, power, and spherical are formed with the thumb abducted away from the palm. Other grasps can be included in order to target typical modern day uses like clicking a computer mouse (pointer) and/or pressing against a table to stand up (hand flat) [19], [20]. Some functional grasps are ignored when applied to a multi-function prosthesis because of the mechanical constraints of the device. For example, the extension grasp is not possible with kinematic coupled joints in the digits of many prosthetic hands since the mechanical coupling forces all joints in the digits to flex in unison [10]. In general, grasp taxonomies inform the design of multi-function prosthetic hands as well as the associated myoelectric control systems.
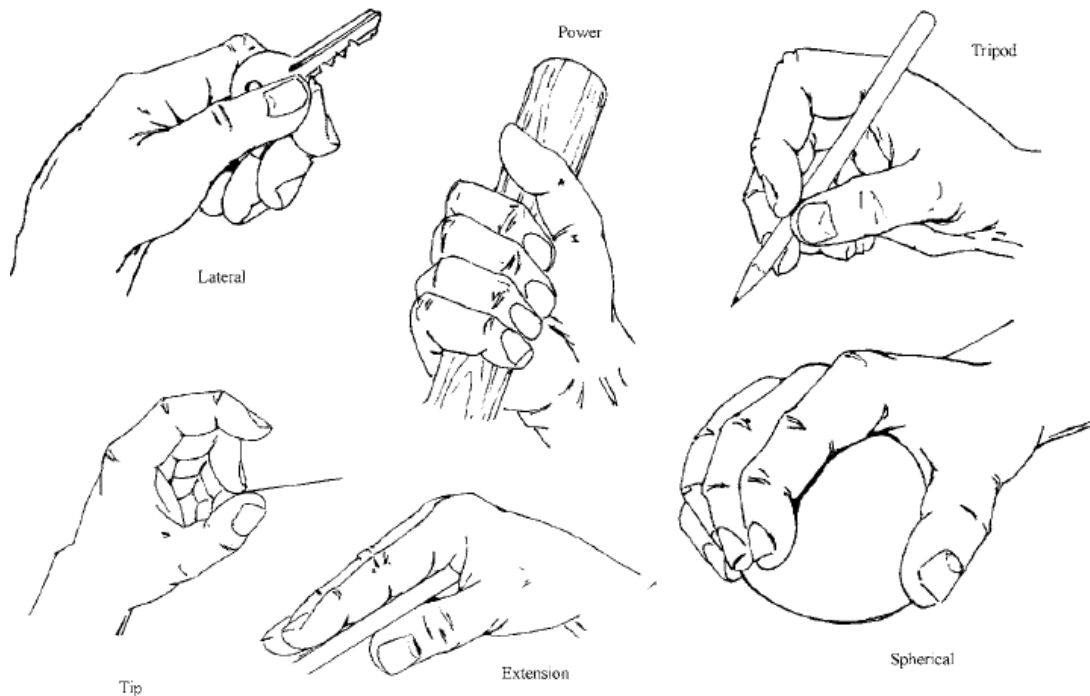
Figure 1. – The six most common grasp patterns including lateral prehension, tip prehension, power prehension, extension, tripod, and spherical prehension. Image reproduced from Light et al [18].

Motor Control

The neuromuscular system integrates sensory information and motor commands into coordinated skill and movements, namely the study of motor control. Even a seemingly simple task, like drinking a cup of coffee, requires an incredible harmonization of motor commands to redundant biomechanical systems and analysis of sensory information which all occurs in real-time without excessive mental burden. It is important to understand motor control in the intact system in order to better design replacements when part of the neuromuscular system is lost due to amputation.

The anatomy of the human neuromuscular system forms a redundant biomechanical machine where there are more degrees of actuation (DoA – muscles) and degrees of freedom (DoF – joints) than are necessary to achieve any given task [21]. As a result, tasks can be accomplished with a variety of kinematic, kinetic, and muscle activation strategies. This feature is defined as motor variability and is a critical concept in the field of motor control. As Bernstein described best, motor variability is 'repetition without repetition'.

Many theories exist today to explain the control method used to command this redundant biomechanical system with motor variability. The uncontrolled manifold hypothesis describes a control strategy that allows for high variability among certain variables (i.e. – joint angles, muscle activations, etc.) as long as the desired task is accomplished [22],[23]. A similar theory, optimal feedback control, describes the use of feedback to optimally correct the deviations that affect the task goal and ignore the variability of the irrelevant variables [24]. The concept of muscular synergies describes the reduction of the number of control signals necessary to produce movement by grouping muscles into temporal or spatial sets [25], [26]. These muscle synergies are activated in a fixed balance (linear combination) such that specific tasks can be accomplished with a minimal amount of commands from the central nervous system (CNS).

The synergy concept has been thoroughly investigated with regards to the control of grasping. The work of Santello *et al.* [11] described the postural synergies that were present during human grasping trials. A postural synergy, like a muscular synergy, is a pattern of joint angles that varies together (i.e. – a kinematic coupling). Santello *et al.* found that two postural synergies described 80% of the variance in human grasping. In other words, grasping is a low (~2) dimensional task. Many studies further investigated the muscular and postural synergies used during grasping as reviewed by [27] and [28]. This work from the field of neuroscience has

created a translational topic in the field of robotic and prosthetic grasping and is discussed in more detail in the *Postural Control Schemes* section below.

Introduction to Myoelectric Control Systems

History of Myoelectric Control and Upper Limb Prosthetic Design

Myoelectric control systems (MECs) were developed in order to control externally powered prosthetic devices. Externally powered prostheses use battery power and motors to cause a desired function (e.g. – flex elbow, grasp cup). Powered prostheses have been commercially available since the 1980s [29] and contained only a single DoA, (i.e. – number of actuators in device). Only recently have multi-function, or advanced, prosthetic hands become commercially available (Figure 2). These devices contain many DoAs and can produce multiple grasping postures. In comparison, body-powered prostheses use cabling and harnesses to convert body motion into the same functions [30]. Both methodologies are attempting to recreate the lost function after an upper-limb amputation. In 2005, there were an estimated 41,000 Americas living with major upper limb loss [31]. These users describe similar areas of improvement for both methodologies including more intuitive control schemes and the ability to cause simultaneous and coordinated motion of multiple joints [32]. An intuitive MEC recreates the lost function using physiologically appropriate neural commands. Powered prosthetic devices and MECs will be superior to body-powered devices (especially once appropriate sensory feedback is incorporated) and is therefore the focus of this work.

Figure 2. – Examples of (a) body-powered (b) single degree of actuation and (c) multifunction prosthetic hands. The hands shown are the Hosmer Hook, the Otto Bock MyoHand VariPlus Speed, the Motion Control ProControl hand, the Touch Bionics iLimb hand, the RSL Steeper Bebionic hand, and the Otto Bock Michelangelo hand respectively.

Myoelectric control systems have been clinically available for over 30 years [33]. This first evidence of a MEC was in 1948 used to control a Hufner hand and was then further developed by separate groups, the Russian hand and the French hand, in the 1950's [29], [34]. Over time, these systems have become more prevalent because they can be controlled using easily prepared and noninvasive techniques. In addition, advances in micro-electronics, miniature-actuators, and battery technology have accelerated the number of developments in powered prostheses. Figure 3 compares an able-bodied control system with a myoelectric control system.
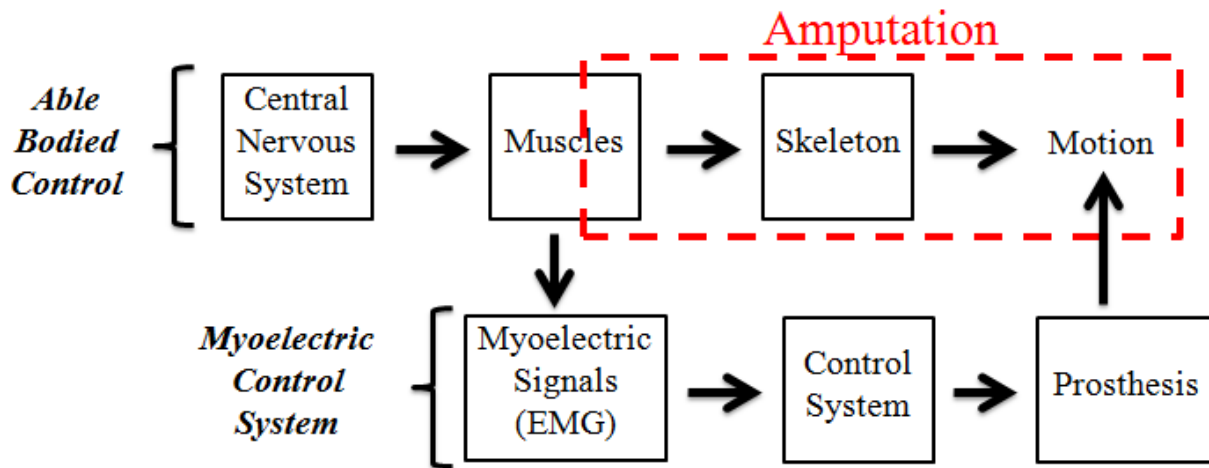
Figure 3. – Comparison between able-bodied and myoelectric control

As seen in Figure 3, the MEC uses the muscles as sources of control of signals. The muscle contraction is measured using electrodes. The site on the body where a myoelectric electrode is placed to measure an EMG signal is referred to as a control site. The EMG signal can then be processed and used as a control signal to control the prosthesis. This process has been extensively studied and is covered more thoroughly in several reviews [35],[36],[37].

In general, the goal of a MEC is to *decipher user intent.* However, the subgoals of MECs are numerous. Childress and Weir [15] define the objectives as the following: (1) low mental loading or subconscious control, (2) user-friendliness, (3) independence in multifunctional control, (4) simultaneous and coordinated control of multiple functions, (5) near-instantaneous response, (6) noninterference with the individual's remaining functional abilities, and (7) a natural appearance and quiet movement. While some of these goals are more or less important to the user, the objective that most research has focused on is goal (4) simultaneous and

coordinated control of multiple functions. This objective is far from being achieved and is the motivation for this work as well as many others today.

The Myoelectric Paradox

MECs have a technological bottleneck in the communication between the user and the prosthesis. Parker *et al.* [33] describe this phenomenon as the myoelectric paradox: "the functionality and thus control site requirements increase with the level of amputation while the number of sites decreases…" The myoelectric paradox is the primary limitation on the development of more dexterous prosthetic limbs. While a prosthetic limb with almost all the degrees of freedom of an anatomical arm [38] has been built, no myoelectric control strategy can operate such a complex device with dexterity.

The myoelectric paradox can also be posed as a Multiple Input, Multiple Output (MIMO) control challenge. As described by the myoelectric paradox, the number of inputs to the controller is less than the required number of outputs when using advanced multifunction prosthetic limbs. The methods used to solve this inherent imbalance in MEC have been studied for decades and are the foundation of the postural controller discussed below.

Direct Myoelectric Control

The original type of MEC used a direct control scheme. Direct control schemes map a single EMG control signal to a single control variable like joint position or motor speed [39], [40]. Direct control schemes require little cognitive effort from the user, can occur with minimal computational delay, and a minimal number of EMG control sites are necessary. Many commercial devices on the market today successfully implement direct control schemes like the Motion Control ETD [41], Hosmer Terminal Device [42], and the Otto Bock System Electric

Hand [43]. However, these devices have a single DoA; they are considered 'open-close' prostheses. Users indicate that multiple grasps and increased articulation are highly desirable design considerations [9], [32] but these functions are not possible when using single DoA prostheses with a direct MEC.

In order to take advantage of the intuitive nature of direct MEC schemes, several techniques have been developed in order to increase the number of control signals to the MEC and thereby solve the myoelectric paradox. Targeted Motor Reinnervation (TMR) is a surgical technique which increases the number of available control sites for myoelectric control [7]. TMR rewires the efferent nervous system so that the musculature remaining after amputation is reinnverated with efferent nerves that used to control the amputated joints. The result is an increase in the number of intuitive EMG control sites to be used in a direct MEC scheme. TMR has been performed on dozens of patients so far with positive and dramatic results. Another methodology to increase the number of input control signals is the use of implantable myoelectric sensors (IMES) [8]. The IMES are implanted inside the residual limb and communicate through wireless telemetry to the MEC. Intuitive control sites can be created by implanting IMES into specific muscles within the residual limb that then control the physiologically appropriate joint in the prosthesis. The localized EMG activity measured by the IMES is not possible to detect using standard-of-care surface electrodes. Conclusive results have been produced verifying the efficacy of the IMES in human subjects using fine wire needle intramuscular electrodes [44], [45]. Current work at Walter Reed Medical Center is studying the ability of the first human subject using IMES to control a hand and wrist prosthesis.

Clinical Assessment Protocols

The clinical assessment of MECs requires both reliable and validated testing protocols as well as reproducible hardware/software interfaces in order to make robust comparisons across studies. Many clinical assessment procedures have been proposed in the previous decades using both virtual interfaces and physical testing protocols. Virtual testing interfaces typically entail subjects matching a virtual limb/hand to a target posture. Birdwell [44] used intramuscular fine wire electrodes to command a virtual hand posture matching exercise using both direct control and pattern recognition MECs. Dalley et al. [46] used a state machine architecture in a posture matching exercise to command multiple functional postures. Hargrove et al., [47] used a virtual clothespin task to quantify the efficacy of a pattern recognition MEC as opposed to standard offline metrics like classification accuracy and error. Simon et al., [48] developed the Target Achievement Control Test in order to evaluate real-time pattern recognition MEC with various controller and task complexities. Virtual assessment procedures can be advantageous since the need to use standardized prosthetic hardware is removed. However, a virtual assessment procedure cannot perfectly simulate a real-world environment where grasp stability, load on the body due to limb position, temporal coordination of the digits within the prosthesis, and compensatory movements increase the complexity of a physical task compared to a virtual task.

Physical assessment procedures more closely reproduce clinical situations and tasks. The Academy's State of the Science Conference on Upper Limb Prosthetic Outcome Measures (ULPOM) identified parameters that contribute to the usability of a prosthesis [49], [50]. The ULPOM group described three domains including the functional, activity, and participation domains which require differing assessment techniques like technical tasks, clinical assessment, and self-rating respectively. Other reviews describe both objective and subjective protocols to

measure functional outcomes [18], [51]. The Assessment of Capacity for Myoelectric Control (ACMC) is a subjective protocol that judges subjects as they perform activities of daily living (ADLs) focusing on four main types of tasks: gripping, holding, releasing, and coordinating. The box and blocks test as well as the clothespin test provide objective measures of a single ADL using a time based performance metric [52], [53]. Finally, the Southampton Hand Assessment Procedure (SHAP) test is an objective, time-based test that includes 26 ADL tasks which span the functional grasps detailed in Table 1 [16]. The SHAP was shown to be reliable and was validated so that results of independent studies can be compared [18]. This fact has led the field of prosthetic hand control and design to adopt it as a tool to assessment prosthetic hand and MEC function. It is an easily reproducible test however it only requires planar motions/tasks (i.e. – no tasks that require reaching overhead or below the waist). As examples, the i-LIMB and DMC hand was compared by Van Der Niet et al., [54] using the SHAP test and Dalley et al., [55] used the SHAP test to perform a functional assessment of the Multigrasp Myoelectric Controller using the Vanderbuilt Multigrasp Hand

Table 1 – Southampton Hand Assessment Procedure (SHAP) tasks

Type	Number	Name	Grasp	Type	Number	Name	Grasp
Abstract Object Tasks	1	Spherical (lightweight)	PP	Activities of Daily Living	13	Pick up coins	TP
	2	Tripod (lightweight)	TP		14	Button board	PP
	3	Power (lightweight)	PP		15	Food cutting	LP
	4	Lateral (lightweight)	LP		16	Page turning	LP
	5	Tip (lightweight)	TP		17	Jar lid	PP
	6	Extension (lightweight)	TP		18	Jug pouring	PP
	7	Spherical (heavyweight)	PP		19	Carton pouring	PP
	8	Tripod (heavyweight)	TP		20	Heavy object lift	PP
	9	Power (heavyweight)	PP		21	Light object lift	TP
	10	Lateral (heavyweight)	LP		22	Tray lift	LP
	11	Tip (heavyweight)	TP		23	Rotate key	LP
	12	Extension (heavyweight)	TP		24	Open/close zip	LP
					25	Rotate a screw	PP
					26	Door handle	LP

State-of-the-Art Myoelectric Control Systems

Pattern Recognition Control Schemes

Pattern recognition is a widely researched topic for the control of multifunctional prosthetic limbs [56],[57],[58]. It is based on measuring patterns of surface EMG signals and assigning each pattern to the desired posture/motion. The EMG measurement of multiple control sites is preprocessed and segmented into windows over time. Features are extracted from each window which contain information on the EMG signal. The classifier then decides upon the desired posture/motion from the extracted features. The pattern recognition system can recognize many patterns but must be trained for each pattern before use. The postures/motions are predefined and cannot vary during use.

Pattern recognition provides an intuitive method for controlling multiple degrees of freedom but sacrifices coordinated movement (e.g. each DoF must be actuated sequentially) and practical robustness. Extensive research focused on the type of statistical algorithm to use as the classifier (a thorough review is provided by Scheme and Englehart [59]). Most classifiers seem to produce similar classification accuracy and therefore secondary parameters like robustness to clinical conditions are more critical measures of a systems performance. Scheme and Englehart [59] discuss many of the pitfalls towards clinical robustness of the current state of the art pattern recognition techniques including electrode shift, variation in force of the contraction, limb position, and transient changes in the EMG signal. Young et al., [60] documented the negative effects of electrode shift on the performance of pattern recognition systems. Several studies have shown the negative impact various limb positions can have on the performance of pattern recognition systems [61], [62]. Other work focused on the development of simultaneous, coordinated motion across DoFs, but showed a decrease in performance compared to sequential

control pattern recognition schemes [63]. A technique to retrain the classifier 'on the fly' was developed in order to compensate for the deteriorating effects of the pitfalls described above [64]. This technique has shown promise and may enable these systems to move from the lab to the clinic.

State/Binary Control Schemes

Event driven finite-state schemes (also referred to as state machines or binary control schemes) consist of many predefined states each with a unique function (i.e. – posture or motion) that can be selected sequentially [65], [66], [67], [68]. The EMG input signal commands a transition between the states until the desired state is selected. Then, the predefined function is performed. The EMG input can be considered a 'trigger' which steps the prosthesis through various functions. This type of control requires memorization but is a more clinically robust interface compared to pattern recognition schemes. In fact, several commercially available prosthetic hands integrate simple state machines today [69], [19]. Of course, there are several pitfalls to state control schemes including a limited, predefined set of functions, time delays due to transitions between states, and most importantly an unintuitive control paradigm. Several studies have shown that users can learn to control a prosthetic hand using a state machine control scheme to a high level of performance [55], [70] however these studies do not address the increase in mental burden due to the lack of intuitive control caused by the state machine control scheme. Inherently, a state machine will never be intuitive because the physiological result of the measured EMG activity does not correspond whatsoever to function of the prosthesis. Nonetheless, state machine control schemes allow for a high level of performance and have commercial implementation as well.

Postural Control Schemes

Postural control is a burgeoning technique that transforms the EMG input signals into an array of joint angles (i.e. – a posture) using a linear transformation (a kinematic coupling). The relative magnitude of each EMG signal modulates the contribution of each corresponding postural vector. It could be considered a type of direct control except that it includes a dimensionality reduction step caused by the linear transform. Several studies in both the robotic and prosthetic control literature used Principal Component Analysis (PCA) to derive the postural vectors (principal components - PCs). These studies were motivated by the observations made by [11] that 80% of the variance in grasping of everyday objects can be explained using 2 principal components as described in the *Motor Control* section. Ciocarlie and Allen [71] used mathematical coupling based on principal components in the control of advanced robotic hands. The reduced dimensionality of the control system allowed for computational advantages when interfacing between the human and robot. Ciocarlie and Allen focused on complex tasks like dexterous grasping and grasp stability which further demonstrates the utility of postural control schemes in the control of multi-DOF prosthetic hands. Matrone *et al.* [72], [73] showed the efficacy of a postural control system for a myoelectric prosthetic hand based on principal component analysis. In their work, principal components were derived in order to drive a 6 DOA prosthetic hand using only two input command signals and single map onto the PC domain. The experimental results proved the ability of this type of controller to drive a prosthetic hand into typical grasping postures using computer and myoelectric control. However, postural control schemes are also limited by the kinematic coupling. For example, the postural controller used in *Specific Aim 1* cannot command the posture used when describing the number two (or the 'peace' sign). This posture cannot be accomplished using the postural

controller since the mathematical coupling described by the principal components flexes all four digits in near unison. Therefore, design of a postural controller must take into account the grasps/postures that are desirable to reproduce. This dissertation describes the development and validation of a postural control scheme for advanced prosthetic hands that better recreates what was lost due to amputation.

Chapter 3 - Design and Validation of a Morphing Myoelectric Hand Posture Controller based on Principal Component Analysis of Human Grasping[5]

Introduction

The idea that grew into the postural controller stems from the work of Santello et al., study entitled *Postural hand synergies for tool use* [11]. Santello et al., measured the joint angles of the human hand while grasping and performed a principal component analysis on the resulting dataset. The result proved that grasping was a low-dimensional task. More specifically, Santello et al., showed that only two variables (principal components[6]) could describe over 80% of the variance in the hand postures. The two principal components are two vectors that describe a kinematic coupling of the joints in the hand. The linear combination of the two principal components could describe many of the hand postures used in activities in daily living. In effect, the two principal components reduce the dimensionality of the hand and thereby the number of input commands necessary to command a hand posture.

The first PC describes the flexion of the metacarpophalangeal (MCP) joint of the digits and the rotational/adduction of the thumb. The second PC describes the extension of the MCP joints and flexion of the proximal interphalangeal joint (PIP) of the digits while the thumb follows the same pattern as in the first PC. Figure 4 depicts the two dimensional domain (referred to hereafter as the principal component domain or postural control domain) and the coordinates of 57 different grasps tested in [11].

---

[6] Depending on the field of research, the literature uses the terminology principal components, postural synergies, and eigengrasps to describe the mathematical coupling of joints in human hand. This study uses the term principal components in all cases.
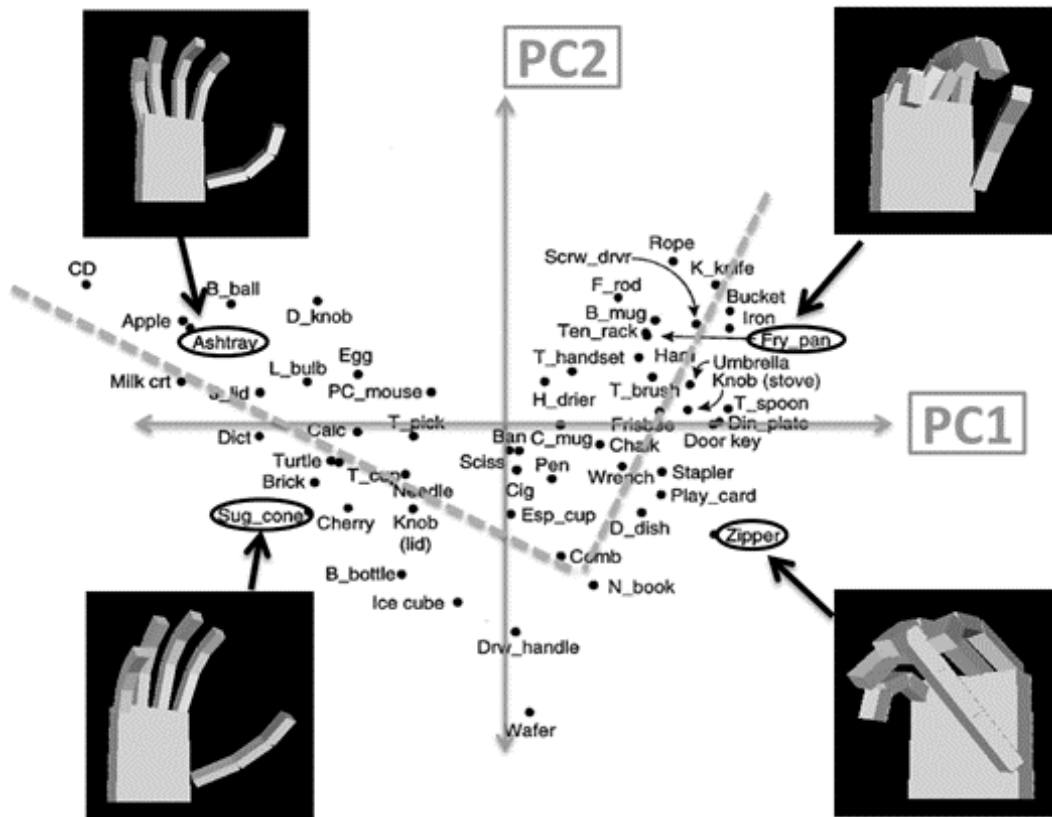
Figure 4 – The distribution of grasping postures in the principal component domain found by Santello et al., 1998. Santello et al. found that the 1st and 2nd principal components (PC1 and PC2) accounted for more than 80% of the variance in the joint angles of grasping postures. Therefore mapping two control input signals to PC1 and PC2 provides a means to command a prosthetic hand into numerous grasping postures using just two control inputs. The four target postures used in this study are circled and shown. The target postures were chosen because they are evenly distributed between the four quadrants of the PC domain and constitute 4 of the 6 functional grasps described by [4]. The bimodal trend in the distribution of postures is shown by the dashed lines.

Other researchers integrated Santello's technique into the control of robotic and prosthetic hands. Ciocarlie and Allen [71] used mathematical coupling based on principal components in the control of advanced robotic hands. The reduced dimensionality of the control system allowed for computational advantages when interfacing between the human and robot. Ciocarlie and Allen focused on complex tasks like dexterous grasping and grasp stability which

further demonstrates the utility of PCs in the control of multi-DOF hands. Matrone *et al*. [72]–[74] showed the efficacy of a control system for a myoelectric prosthetic hand based on PCs. In their work, PCs were derived in order to drive a 6 DOA prosthetic hand using only two input command signals and single map onto the PC domain. The experimental results proved the ability of this type of controller to drive a prosthetic hand into typical grasping postures using computer and myoelectric control.

The bimodal distribution of postures in the PC domain suggests that better (i.e. – faster/more accurate) control might be achieved if the EMG inputs were aligned to the distribution. We tested this hypothesis by implementing novel transformations (maps) of the EMG signals on the PC domain [75]. The use of novel mappings motivated additional questions including the benefit of additional control sites (i.e. – a 2 DOF mapping versus a 4 DOF mapping). This chapter details the control system architecture based on principal component analysis of human grasping, the experimental methods, and the ability of the control system to drive a high DOM virtual hand into functional grasps in a continuously morphing fashion.

Development of Controller Architecture

A block diagram of the controller architecture based on principal components is shown in Figure 5 The EMG control signals are processed using standard EMG processing techniques. The PC domain maps transform the EMG signals into a PC coordinate (PC1, PC2). The Joint Angle Transform produces an array of 15 joint angles from the PC coordinate which is then sent to the virtual hand model for visualization. It should be noted that the controller does not require any training unlike MECs based on pattern recognition techniques. The following section describes the controller architecture in more detail.
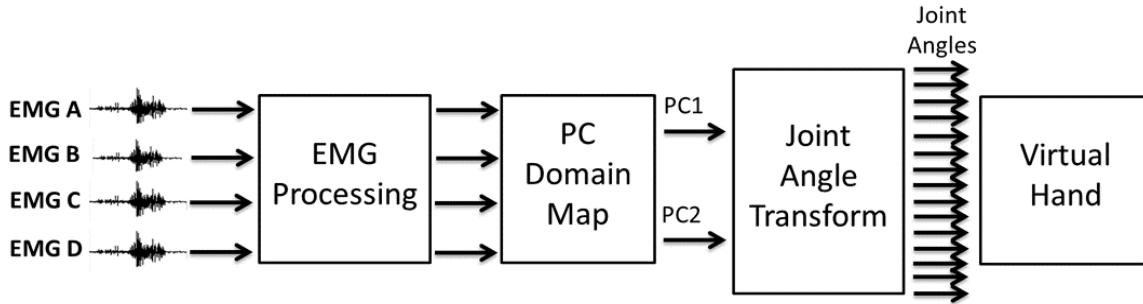
Figure 5 - Block diagram of the controller architecture based on principal components of human grasping. The raw EMG control signals are processed using standard EMG processing techniques. Four different PC domain maps are tested using various transformations of the EMG control signals on the PC domain. The output of the maps is a PC coordinate (PC1, PC2). The joint angle transform converts the PC coordinate into an array of 15 joint angles. The virtual hand visualizes the 15 joint angles in real time.

EMG Processing

The four EMG signals were acquired using ProControl2 electrode pairs (Motion Control, Inc.) and self-adhesive Ag/AgCl snap electrode stickers (Noraxon USA, Inc.). Electrodes were placed on flexor digitorum superficialis (EMG A), extensor digitorum (EMG B), extensor carpi ulnaris (EMG C), and flexor carpi ulnaris (EMG D). The location of the control sites were based on previous work [76] which found four independent surface EMG sites on the forearms of non-amputee subjects. The measured raw EMG signals from four control sites were amplified by the ProControl2 electrode and sent to a NI USB-6008 data acquisition device (National Instruments, Inc.). The raw analog EMG signal was sampled at 1 kHz. Then the signal was band pass filtered (30-450 Hz), notch filtered at 60 Hz, rectified, smoothed with a 200ms moving average filter, and normalized individually to the signal input range of the data acquisition device. A tuning process was performed for each subject before the myoelectric sessions took place. The tuning process included adjusting the gain and activation threshold for all EMG signals in order to produce the most comfortable control system for each subject. The gains were adjusted to ensure

that every task was achievable without overdue effort including co-contraction tasks (i.e. when postures lie far from the EMG signal axes in the PC domain). The activation thresholds were adjusted to negate quiescent EMG signals. All of the processing techniques described above are typical clinical practices and can be implemented when using many commercial prosthetic hands.

PC Domain Maps

The controller is based in the PC domain. Various maps between the EMG control signals and the PC domain were investigated. All maps as well as the target postures used in the experimental protocol are depicted in Figure 6. The generalized equation of the mappings is described by equation ((1). Table 2 specifies the unique transformation matrix [**A**] and offset vector [**B**] implemented by each map.
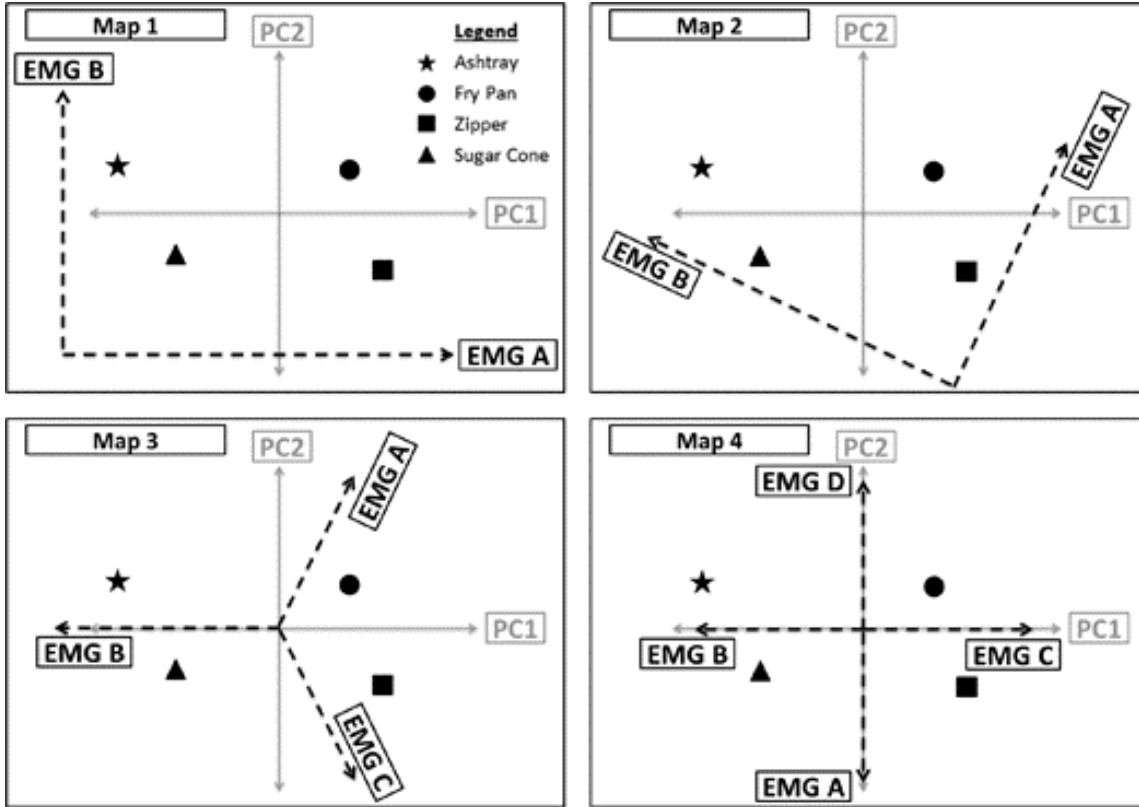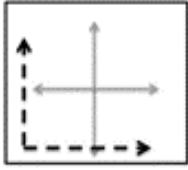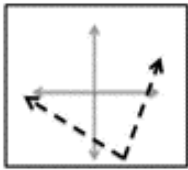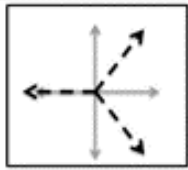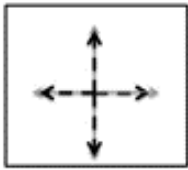
Figure 6 - Maps 1-4 on the PC domain. Map 1 translates the EMG signals to the third quadrant and aligns EMG A with PC1 and EMG B with PC 2. Map 2 translates and rotates the EMG A and EMG B signals. The rotation mimics the bimodal pattern seen in the grasping posture distribution from Santello et al. Map 3 divides the PC domain into three equal portions using EMG A, B, and C. Map 4 divides the PC domain into four equal portions using EMG A, B, C, and D.

$$\begin{bmatrix} PC1 \\ PC2 \end{bmatrix} = [A] \begin{bmatrix} EMG\ A \\ EMG\ B \\ EMG\ C \\ EMG\ D \end{bmatrix} + [B]$$

(1)

Table 2 - Definitions of Maps 1-4

Maps	Transformation Matrix - [A]	Offset Vector – [B]
1	$\begin{bmatrix} 0.20 & 0 & 0 & 0 \\ 0 & 0.12 & 0 & 0 \end{bmatrix}$	$\begin{bmatrix} -0.30 \\ -0.14 \end{bmatrix}$
2	$\begin{bmatrix} 2.97 & 0 & 0 & 0 \\ 0 & -0.34 & 0 & 0 \end{bmatrix}$	$\begin{bmatrix} 0.15 \\ -0.20 \end{bmatrix}$
3	$\begin{bmatrix} 0.40 & -2.50 & 0.40 & 0 \\ 1.67 & 0 & -1.17 & 0 \end{bmatrix}$	$\begin{bmatrix} 0 \\ 0 \end{bmatrix}$
4	$\begin{bmatrix} 0 & -0.35 & 0.20 & 0 \\ -0.20 & 0 & 0 & 0.16 \end{bmatrix}$	$\begin{bmatrix} 0 \\ 0 \end{bmatrix}$

Map 1 only utilizes EMG A and B and projects the EMG control signals to the third quadrant of the PC domain. The EMG A and B axes correspond to the positive PC1 and PC2 directions respectively. This map was considered to be the simplest method of maneuvering in the PC domain. Map 2 only utilizes EMG A and B as well. However, Map 2 projects the EMG control signals to the fourth quadrant of the PC domain. This map was developed to mimic the bimodal distribution of the postures in the PC domain (see dashed lines in Figure 4). A set of vectors that best fit the distribution of postures in the PC-domain was derived using Principal Component Analysis and used as the transformation matrix [A] for map 2 (Table 2). The vectors were then translated to ensure that the entire principal component domain was accessible using this map. Map 3 utilizes EMG A, B, and C and divides the PC domain into three equal portions.

The EMG A axis is projected to the first quadrant of the PC domain. The EMG B axis projects onto the negative PC1 axis. The EMG C axis is projected to the fourth quadrant of the PC domain. Map 4 utilizes all four EMG signals (A, B, C, and D) and divides the principal component domain into four equal portions. The EMG A, B, C, and D axes follow the negative PC2 axis, negative PC1 axis, positive PC1 axis, and positive PC2 axis respectively.

For all mappings, EMG signals were assigned in order to follow the most physiologically realistic maps by applying the following rules: 1) flexor digitorum superficialis (EMG A) drives the hand to close 2) extensor digitorum (EMG B) drives the hand to open 3) extensor carpi ulnaris (EMG C) drives towards lateral prehension/Zipper 4) flexor carpi ulnaris (EMG D) drives towards power grasp/Fry Pan. In all cases, the result of the ((1) is a PC coordinate (PC1, PC2) which is the input to the Joint Angle Transform.

Joint Angle Transform

The joint angle transform converts the PC coordinate into a 15 element joint angle vector using a mathematical coupling based on the PCs of human grasping. Each principal component vector ($\overrightarrow{PC_1}$ and $\overrightarrow{PC_2}$) is a 15-element vector describing a pattern of joint angles. The principal component vectors are derived from physiological human grasping data, as calculated by [11], and are the source of the biomimetic characteristics of this control algorithm. The linear combination of the two PC vectors and the PC coordinate (PC1,PC2) equals a joint angle command vector which controls the posture of the hand as described by ((2).

$$\begin{bmatrix} Joint\ Angle\ 1 \\ Joint\ Angle\ 2 \\ ... \\ Joint\ Angle\ 15 \end{bmatrix} = \begin{bmatrix} \overrightarrow{PC_1}, \overrightarrow{PC_2} \end{bmatrix} * \begin{bmatrix} PC1 \\ PC2 \end{bmatrix}$$

(2)

The control algorithm described by ((2) converts the EMG input signals into a continuously variable joint angle command vector. In other words, the posture of the hand can continuously morph from posture to posture by varying the EMG control signals. It should be noted that the input to the Joint Angle Transform (the PC coordinate) has two elements whereas the output of the transform (the joint angle vector) has 15 elements. The Joint Angle Transform produces a dimensionality transformation between the PC domain and the joint angle domain. The mathematical coupling defined by the principal components of grasping enables this transformation to take place using biomimetic patterns. However, the resulting posture is also limited by this coupling. For example, the posture used when describing the number two (or the 'peace' sign) cannot be accomplished using this controller since the mathematical coupling described by the principal components flexes all four digits in near unison. This controller is designed to command grasping postures and can achieve all the functional grasps as shown in Figure 4.

Experimental Methods

Subject Information

An experimental protocol was developed to validate the performance of the controller and to determine a preferred map. Ten healthy, non-amputee subjects aged 22-58 were selected for the study. All experiments were conducted using the dominant arm (nine subjects were right-hand dominant and one was left-hand dominant). The study took place over a single three hour meeting in the Integrated Teaching and Learning Laboratory at the University of Colorado at Boulder for each subject. The Institutional Review Board at the University of Colorado at Boulder reviewed and approved the experimental protocol.

Experimental Protocol

The experiment was separated into 3 sessions. First, a joystick control session developed a performance benchmark for each subject using a Parallax 2-axis joystick (DigiKey Corporation). Then a practice session where the subjects were first introduced to each map and posture using myoelectric control. The experimental session produced the dataset analyzed in Section V using myoelectric control.

Each session presented the subject with a randomized series of trials. The task was to match the controlled posture to the target posture in ten seconds or less. The subjects were provided instantaneous feedback on the number of joints controlled accurately through the testing interface. The feedback was produced by comparing the joint angle command vector (calculated in real time using ((1) and ((2)) and the target posture. The four target postures (lateral prehension – "zipper", power grasp – "fry pan", cylindrical prehension – "sugar cone", and hand flat – "ashtray") are shown in Figure 4. These grasps were chosen because they are evenly distributed between the four quadrants of the PC domain and constitute 4 of the 6 functional grasps described by [4]. The target posture and the map used in each trial were varied for a total of 16 unique combinations. The target postures were randomized within each map. The order of the maps was randomized between subjects. The 10 second trial was followed by a 5 second break before the next trial. The joystick control session, practice session, and experimental session consisted of 16, 16, and 64 trials respectively for each subject as prescribed by a power analysis [77].

Testing Interface and Virtual Hand Model

The testing interface developed in LabView is shown in Figure 7. The target posture is static image that varies across trials. The maximum accuracy score displays the highest number

of joints controlled accurately at any time during the trial. The pause button allows the subject to pause the experiment at any time. The controlled posture morphs as the subject manipulates control signal. The current accuracy instantaneously displays the number of joints controlled accurately. The four normalized EMG waveforms are displayed in real time.
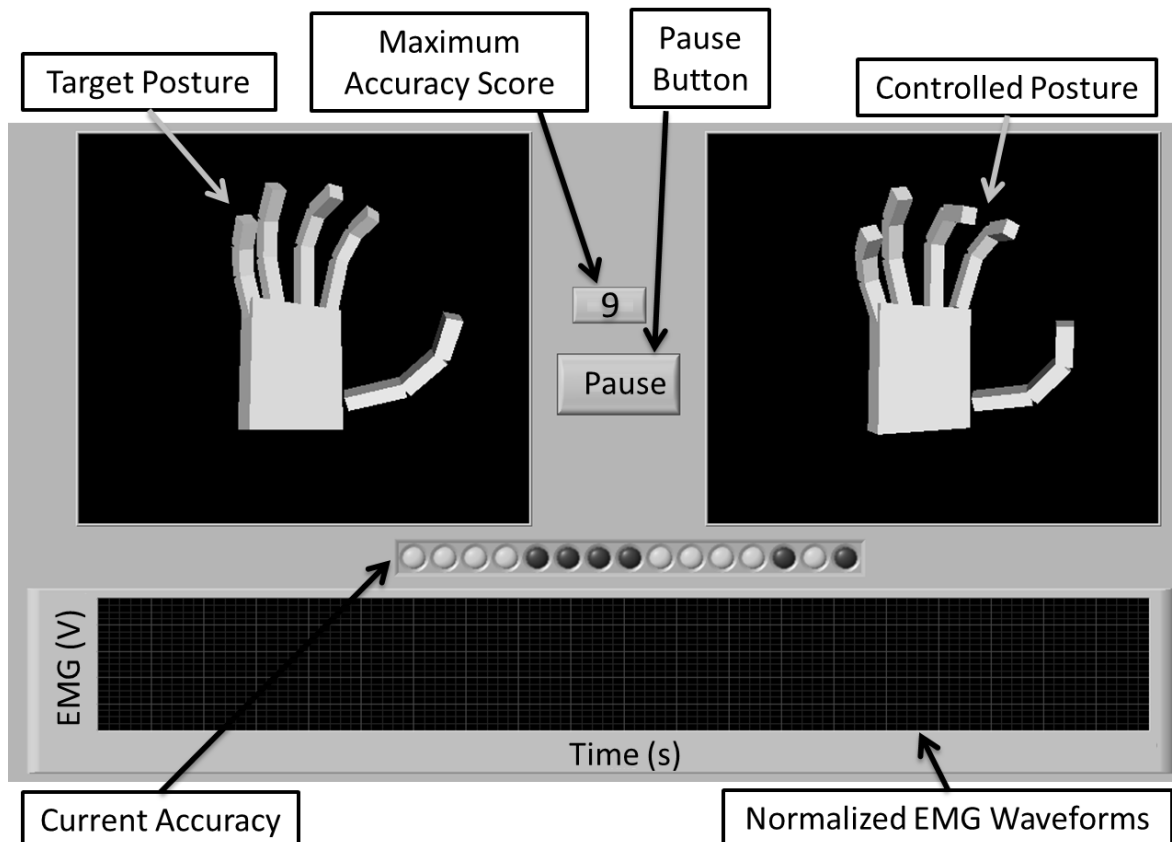
Figure 7 - The testing interface seen by the subjects. The target posture is stationary during the trial but changes after each trial. The maximum accuracy score displays the highest number of joints controlled accurately at any time during the trial. The pause button allows the subject to pause the experiment at any time. The controlled posture morphs as the subject manipulates the control signals. The current accuracy instantaneously displays the number of joints controlled accurately throughout the trial. The two-four normalized EMG waveforms are displayed in real time.

The custom-built, virtual hand model can be controlled using a variety of interfaces (joystick, EMG, computer mouse, etc). The model has 15 articulating joints corresponding to the

15 joints measured in [11]and is further described in Table 3. All 15 joints can be manipulated in real time. Joint angle limits corresponding to their anatomical range of motion were developed in order to disallow non-anthropomorphic motions [78]. The hand dimensions and joint ranges of motion are modeled after a 50% percentile male hand [78]. The thumb joint locations and axes of rotation were based upon anthropometric data and modeling studies of the thumb [79], [80].

Table 3- Joints of the virtual hand model

Joint Number	Joint Name	Joint Abbreviation	Joint Description	Range of Motion (degrees)
1.	Thumb Rotation	TR	Rotation about CMC joint	180
2.	Thumb MCP	TM	Flexion about length of thumb	90
3.	Thumb PIP	TP	Flexion about length of thumb	90
4.	Thumb Abduction	TA	Abducts towards palm	90
5.	Index MCP	IM	Flexion about length of digit	90
6.	Middle MCP	MM	Flexion about length of digit	90
7.	Ring MCP	RM	Flexion about length of digit	90
8.	Little MCP	LM	Flexion about length of digit	90
9.	Index PIP	IP	Flexion about length of digit	90
10.	Middle PIP	MP	Flexion about length of digit	90
11.	Ring PIP	RP	Flexion about length of digit	90
12.	Little PIP	LP	Flexion about length of digit	90
13.	Index Abduction	IA	Abducts away from middle	30
14.	Ring Abduction	RA	Abducts away from middle	30
15.	Little Abduction	LA	Abducts away from middle	30

Metrics

Several metrics were used to study the performance of each subject. All the metrics were based on the *postural envelope*. The postural envelope was defined as 25% of the total range of motion of each joint [46]. If a commanded joint angle was within the postural envelope, then that joint was considered to be controlled accurately. The *number of joints controlled* was

defined as the maximum number of joints (out of 15 possible joints) that were ever simultaneously within the postural envelope during the 10 second trial. The *completion rate (CR)* metric was defined as the number of successful trials per total number of trials. A successful trial was when all 15 joints were held in the postural envelope for 0.5 seconds. The *time to completion (TC)* metric measured the duration of the trial (in seconds) before a success occurred. Finally, the *path efficiency (PE)* metric was defined the measured rotational distance (denominator in (3)) compared to the shortest possible rotational distance (numerator in (3)) between the starting posture and the target posture to produce an efficiency measure between 0 - 100%. The measured rotational distance was found by summing the difference in joint angle between sequential updates of the hand posture. The total number of updates (N) depended on the length of the trial in time.

$$PE(\%) = \frac{\sum_{i=1}^{15}\left(\theta_{i,final} - \theta_{i,initial}\right)}{\sum_{i=1}^{15}\sum_{j=2}^{N}\left(\theta_{i,j} - \theta_{i,j-1}\right)} \times 100 \qquad (3)$$

The various maps altered the distance between the EMG axes and the postures in the PC domain. A correlation analysis was performed to study the relationships between the distance between the EMG axes and the postures in the PC domain. The *diagonal distance* is defined as the distance between the origin and the posture (shown in Figure 8 by dashed lines). The *perpendicular distance* is the distance between the posture and the closest point along any axis (shown in Figure 8 by solid lines). MATLAB (The Mathworks, Inc.) was used to analyze the results. One way analysis of variance tests and Tukey-Kramer comparisons were used to determine significance. The error bars in the figures represent one standard deviation. A least square fit line was used in the correlation analysis and was derived by minimizing the sum of the squared residuals. The goodness of fit (R^2) measure describes the variance of the data about the

least square fit line and was found by subtracting the ratio of the sum of squared residuals over the total sum of squares from one. The p-value describes the significance of the correlation and was considered statistically significant when having a value less than 0.05.
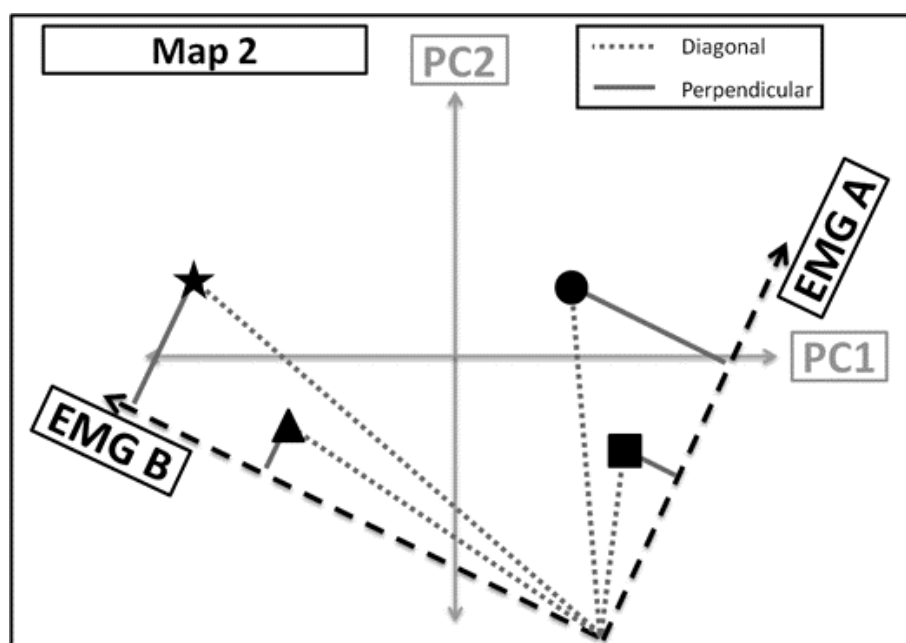
Figure 8 - Example of diagonal and perpendicular distance definition using Map 2. The diagonal distance is measured from the origin of the map to the posture. The perpendicular distance is the shortest distance from the posture to the nearest axis. The amount of co-contraction necessary to acquire off axis target postures is quantified by the perpendicular distance metric.

Experimental Results and Discussion

Joystick Control vs. Myoelectric Control

The number of joints controlled accurately for both myoelectric control and joystick control trials across maps for all subjects is compared in Figure 9. There was not a significant difference between the performance of each control method within each map or across maps. This is an interesting finding since joystick control was developed to be a benchmark for the best

possible performance. Joystick control provides independent, or co-activation free, command input signals as compared to EMG signals. Also, subjects using joystick control could command any PC coordinate free of bias to the location of the posture in the PC domain. In contrast, subjects had to co-contract in order to reach regions of the PC domain not close to an EMG axis when using myoelectric control. The results in Figure 9 show that the bias in the PC domain introduced when using myoelectric control did not significantly change the performance when compared to joystick control. In other words, the use of myoelectric command signal is equally as effective as a joystick command signal in this experimental paradigm.
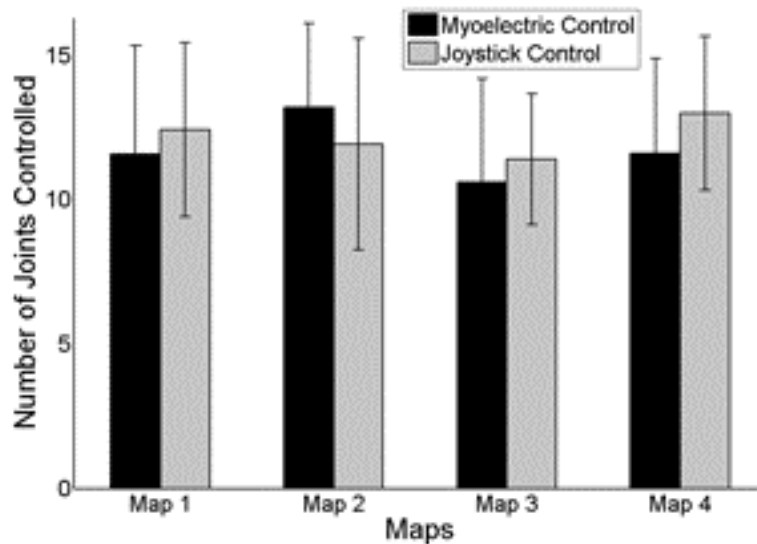
Figure 9- The number of joints controlled accurately for both myoelectric control and joystick control trials across maps and all subjects.

Highest Performing Map

The performance of all four maps for all metrics is displayed in Figure 10. The maps respectively directed over 11, 13, 10, and 11 joints accurately. The completion rate for each map was over 21, 37, 21, and 14 percent respectively. The performance of Map 2 was statistically

more accurate ($p < 0.05$) and had a statistically higher completion rate than any of the other maps ($p < 0.05$). The seemingly low completion rates (less than 50%) are due to the complexity of the task. The subject must position all 15 joints into the postural envelope at the same time in order for a successful trial. These values were expected to be in this range. The time to completion metric shows a similar trend in that Map 2 had the fastest average time to completion. However, Maps 3 and 4 tended to have the highest path efficiency measures. This result led to the correlation analysis discussed below. In general, an increase number of control sites (Maps 3 and 4) do not increase performance using the postural controller.
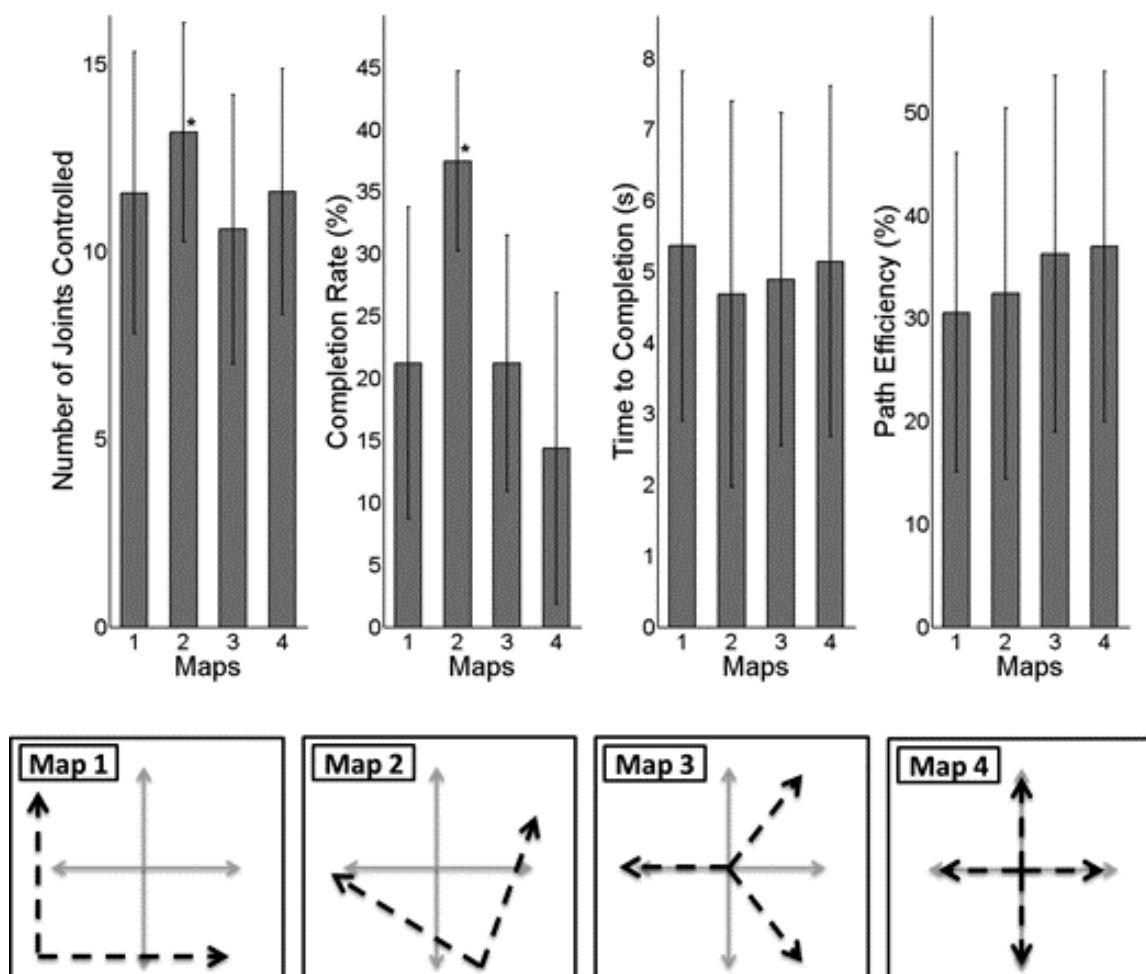
Figure 10 - Comparison of performance metrics over all maps. The performance of Map 2 was statistically greater than the other maps for both the number of joints controlled and completion rate metrics ($p < 0.05$).

The design of Map 2 stemmed from the bimodal distribution of postures in the PC domain (see Figure 4). Santello *et al*. describe that the trends seen in the distribution of the postures in the PC domain "points to the possible existence of two main synergies through which hand shape is modulated". Map 2 transforms the PC domain to align the 2 EMG control axes with these two main synergies. This transformation yielded the highest performing map. The other maps do not follow the distribution of postures in the PC domain and do not perform as

well. This result motivates further investigation into the optimization of the projections of EMG input signals onto the PC domain for specific users.

Correlation Analysis of Distance versus Performance

In light of the results described in Part B, we posit that having to co-contract to reach postures lying far from EMG control axes was more difficult to achieve and therefore would tend to bias our results. To test this hypothesis a correlation analysis was performed in order to determine if the *diagonal* and *perpendicular distances* from the EMG axes to the postures in the PC domain affected the performance of the controller (see Figure 8). The scatter plots[7] of the diagonal and perpendicular distances compared to each performance metric are shown in Figure 11.

The trends of the least square fit lines all show an inverse relationship between the performance and the Euclidian distance but only the correlation between path efficiency (PE) and the distance from the origin shows a statistically significant correlation ($p < 0.05$). This result mirrors the trend shown in Figure 10 where the PE for Maps 3 and 4 were highest and have the shortest diagonal distances.

This finding does not substantiate the hypothesis that an increase in distance from the control axes makes the task more difficult to achieve. This finding suggest that subjects were able to use co-contraction to achieve the target postures readily enough and that co-contraction did not adversely affect their performance as was shown in Figure 10.

---

[7] Not all scatter plots contain the same number of datum. Missing datum are due to unsuccessful combinations of postures and maps across all subjects.
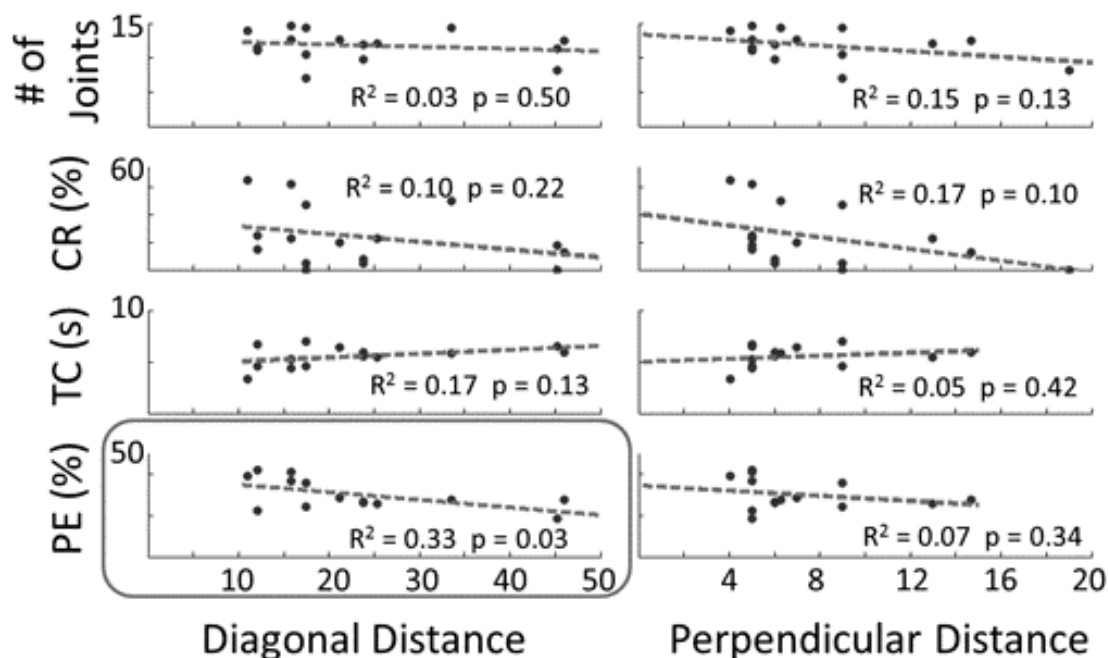
Figure 11 - A correlation analysis between distance and all performance metrics. The four rows correspond to the four performance metrics (Number of Joints Controlled, Completion Rate (CR), Time to Completion (TC), and Path Efficiency (PE)) and the two columns correspond to the two distance metrics (diagonal and perpendicular distance). The least square fit line, goodness of fit measure, and p-value are shown for all comparisons. The correlation between path efficiency (PE) and diagonal distance (circled) is the only relationship with a significant correlation. This finding mirrors the trend shown in Figure 10 where PE was greatest for Maps 3 and 4 which have the shortest diagonal distances to all target postures.

The correlation between PE and diagonal distance shows the greatest goodness of fit (R^2) and is the only correlation of statistical significance ($p < 0.05$). This trend suggests that Maps 3 and 4 have greater PE because they have on average lower diagonal distances than Maps 1 and 2. The distance between the origin and the postures is shortened because the origin for Maps 3 and 4 is centered on the origin of the PC axes and therefore closer to the postures. The path efficiency metric describes the amount of 'wandering' in the PC domain that the subject performs during a successful trial (3). The results suggest that the less wandering occurs when

the required distance is shorter. This analysis also confirmed that the other performance metrics (accuracy, time to completion, and completion rate) were not significantly correlated to the diagonal or perpendicular distance metrics. The metrics measured performance independent of the location of the target posture in the PC domain.

Practice Session versus Experimental Session

The average number of joints controlled accurately during the experimental session (11.7 +/- 0.3) was significantly greater ($p < 0.01$) than during the practice session (10.5 +/-0.4) across all subjects. This result indicates a brief practice session (i.e. less than 10 minutes in duration) increases the performance of the subjects significantly. It should also be noted that the subjects were not provided any instruction as to how to best perform the task for each posture/map combination. The subjects were naïve to the map used in each trial and therefore were not able to learn strategies for how to accomplish each specific map/posture combination. This protocol forced the subjects to guess the function of each control site at the beginning of the trial before determining the best strategy. As shown in [73], the authors would expect that additional instruction would increase the performance of the subjects.

Future Development

The development of the postural controller based on principal component analysis of human grasping enlightened the authors to the benefits of the joint angle transform (JAT) as a dimensionality augmentation technique. This work used a JAT that was composed of the principal components empirically found by Santello et al. The JAT can be composed of customizable kinematic couplings and could vary based on the location of the PC coordinate (a dynamic JAT). The benefits of various mappings within the PC domain was shown with this work and motivated further investigation into customizable and dynamic JATs in order to

provide a more effective and intuitive MEC. Chapter 4 focuses on these developments as well as others.

Conclusion

This aim verifies that a myoelectric controller based on principal components of human grasping can control a multi-multifunctional virtual hand in a continuously morphing fashion. A validation experiment studied the performance of the controller using clinically practiced techniques including myoelectric control site selection, commercially available surface electrodes, and standard EMG filtering. The map that mimicked the bimodal distribution of postures in the PC domain (Map 2) achieved the highest performance by directing over 13 joints accurately. A correlation analysis was performed in order to understand the relationship between distance in the PC domain and performance. The experimental results presented indicate that the controller based on PCA of human grasping provides an effective method for non-amputee subjects to morph a high DOM virtual hand into functional grasps.

Chapter 4- A Novel Postural Control Algorithm for Simultaneous and Proportional Control of Multi-Functional Myoelectric Prosthetic Hands[8]

As demonstrated in Chapter 3, postural control is a technique that uses simultaneous and proportional surface EMG signals to drive a cursor in a two-dimensional domain which contains an arrangement of functional postures. The controller outputs a continuously varying hand posture and does not require a training dataset like other MECs. Several studies in both the robotic and prosthetic control literature used Principal Component Analysis (PCA) to derive the postural vectors [71]–[73]. These studies were motivated by Santello *et al.* [11] who found that 80% of the variance in grasping everyday objects can be explained using the first two principal components. In other words, the linear combination of two postural vectors could accurately reproduce the hand postures needed for grasping of everyday objects. Other studies project EMG signals to a two-dimensional domain similar to the PC domain. De Rugy *et al.* [81] used forearm EMG signals for a two-dimensional target acquisition task in order to study muscle coordination under various biomechanical conditions. Pistohl *et al.* [82] controlled individual digits of a virtual and prosthetic hand using intrinsic hand EMG by maneuvering a cursor in a two-dimensional domain allowing for simultaneous and proportional control of multiple DoFs. Radhakrishnan *et al.,* [83] studied the ability to learn novel myoelectric control interfaces using a two-dimensional center-out target acquisition task. However, none of these studies focuses on the clinical implementation like producing functional postures and using clinically available surface EMG control sites.

---

[8] Intended publication with *Journal of Neural Engineering,* submitted January 2014

In the previous chapter, it was shown that a specific mapping of the EMG signals in the PC domain augmented the ability of subjects to drive a virtual hand into functional postures when using the principal components derived by Santello *et al*. This work builds upon that finding by developing a novel algorithm for a postural controller that is not dependent on PCA to derive the postural vectors. Namely, the postural vectors that compose the JAT are assigned dynamically as the user navigates the PC domain and are dependent on the two nearest posture within the PC domain map. The novel algorithm of the postural controller is detailed here. Also, two experiments were performed to empirically derive other design parameters of the controller and to quantify the performance of the subjects across days. The experimental results and a discussion of the implications of these results on the efficacy of the novel algorithm for a postural controller are presented.

Postural Control Algorithm

The novel algorithm of the postural controller is detailed Figure 12. In general, the controller transforms an array of EMG signals into a joint angle array (i.e. – a hand posture). Many parameters within this algorithm can be adjusted in order to build the most effective and intuitive interface. The experiments discussed here compared several design parameters and quantified the clinical efficacy of the controller with able bodied subjects. All components within this algorithm are discussed in more detail below.
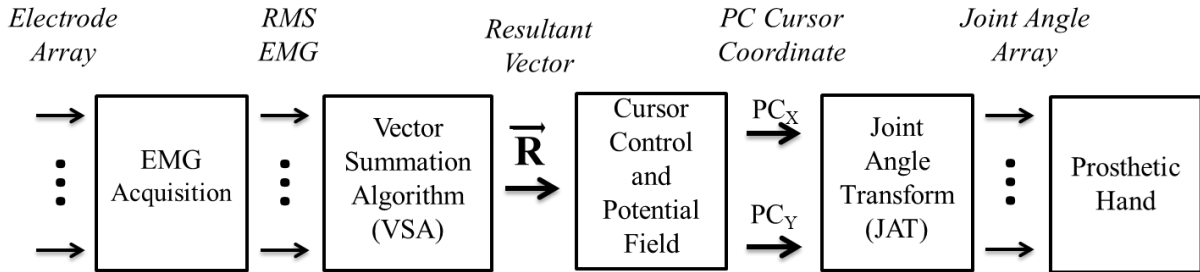
Figure 12 – Novel algorithm for a postural controller. An untargeted surface electrode array acquires electromyographic (EMG) signals. The filtered root mean square average (RMS) EMG values are passed to the VSA which produces a resultant vector ($\vec{R}$). The resultant vector is used to calculate the PC Cursor coordinate (PC_X,PC_Y) using various cursor control schemes and potential field designs. Finally, the JAT transforms the PC cursor coordinate to a joint angle array which is sent to the prosthetic hand.

EMG Acquisition

An untargeted surface electrode array on the dominant forearm (Figure 13a) acquires myoelectric signals. The array spans the circumference of the proximal third of the forearm with *N* electrodes in the longitudinal direction. The humeral epicondyles locate the north-south axis and therefore orientate the array with respect to the arm. The untargeted array distinguishes that specific muscles are not targeted by each electrode. Standard clinical techniques process raw EMG signals into an array of root mean square (RMS) averages over 100ms non-overlapping time windows. The EMG acquisition results in a 'snap-shot' of EMG activity within the forearm which the Vector Summation Algorithm further deciphers.

Vector Summation Algorithm

The vector summation algorithm (VSA) interprets the 'snap-shot' of EMG activity using a uniformly spaced vector summation map (Figure 13b). Electrodes on the dorsal/ventral side of the limb (wrist extension/flexion) correspond to the y-axis of the PC domain and electrodes on the medial/lateral side of the limb (ulnar/radial deviation) correspond to the x-axis of the PC

domain (for a right-sided limb). The RMS EMG value determines the magnitude of each corresponding vector (represented by gray outline in Figure 13b). The summation of all vectors produces a resultant vector, $\vec{R}$. Equation (4) describes the calculation of $\vec{R}$ where RMS_i is the RMS value of the EMG_i signal, θ_i is the control site angle in the PC domain, and N is the number of control sites. The direction of the resultant vector indicates the area in the forearm with the most EMG activity and the magnitude indicates the relative amount of EMG activity. In short, the VSA reduces the RMS EMG array into a single resultant vector $(\vec{R})$ that subsequently drives the PC cursor coordinate (PC_x, PC_y)

$$\vec{R}(t) = \begin{bmatrix} R_x(t) \\ R_y(t) \end{bmatrix} = \sum_{i=1}^{N} \begin{bmatrix} RMS_i(t)\cos\theta_i \\ RMS_i(t)\sin\theta_i \end{bmatrix} \tag{4}$$

Cursor Control Schemes and Potential Field

The resultant vector produced by the VSA $(\vec{R})$ controls the PC cursor coordinate (PC_x, PC_y) using a position or velocity cursor control scheme (compared in Experiment A of Chapter 4). The position control scheme interprets the resultant as a positional command vector (i.e. – units of distance). In the position cursor control scheme the end point of the resultant vector equals the PC cursor coordinate (5).

$$\begin{bmatrix} PC_x(t) \\ PC_y(t) \end{bmatrix} = \begin{bmatrix} R_x(t) \\ R_y(t) \end{bmatrix} = \vec{R}(t) \tag{5}$$

The velocity cursor control scheme interprets the resultant as a velocity command vector (i.e. – units of distance/time). A discrete integration over time determines the cursor position (6) where $(\vec{R}_j)$ is the instantaneous resultant vector, Δt_j is the loop time, V_{gain} is the velocity gain, and j is the software loop count. The velocity gain adjusts the maximum allowable speed (i.e. –

a speed limit). In practice, the magnitude of the resultant corresponds to the speed of the cursor and the direction of the resultant corresponds to the direction the cursor moves.

$$\begin{bmatrix} PC_x(t) \\ PC_y(t) \end{bmatrix} = V_{gain} * \sum_{j=1}^{J} \left(\overrightarrow{R}_j(t) * \Delta t_j \right) \tag{6}$$

The potential field (Figure 13c) preferentially attracts the cursor coordinate to certain regions in the PC domain using a position feedback loop with proportional-derivative controller. The purpose of the potential field is to augment the ability of the user to perform functional grasps using the postural controller. The potential field consists of potential wells surrounding the target positions and potential wedges emanating from the origin to the targets (targets are further detailed in the *Joint Angle Transform* section below). The feedback controller forces the cursor to the areas of lowest potential (i.e. – the bottom of the wells and wedges). All parameters of the potential field (diameter of the wells, width of the wedges, and depth of wells and wedges) can be adjusted in order to best aid the user in performing functional grasps. In effect, the potential field adds a third dimension to the PC domain as visualized in Figure 13c where the light/dark gray areas have zero/negative potential, respectively. The design of the potential fields was determined during pilot studies where various geometries (i.e. – only wells, only wedges, both wells/wedges) were compared. The sequential processing of the resultant vector by the cursor control scheme and then the potential field produces a PC cursor coordinate (PC_x, PC_y) which the JAT converts into a hand posture.

Joint Angle Transform

The JAT converts the PC cursor coordinate into a hand posture based on the postural map at a rate of 10Hz. The postural map defines the number and location of the grasps available to the user in the PC domain. Points (targets) in the PC domain correspond to grasps. When the

PC cursor coordinate equals the target, then the controller reproduces the grasp identically. As the PC cursor coordinate moves between two targets, the controller produces a linear combination of those two postures. A representative postural map is shown in Figure 13d (the hand flat posture is located at the origin of the PC domain but is not shown). This algorithm allows for a large number of postures and freedom to position the postures within the PC domain unlike the controller used in Chapter 3

The Joint Angle Transform (JAT) is a temporally and spatially dependent linear transform that converts the PC cursor coordinate into a joint angle array. The generalized equation (7) defines the JAT where $(PC_x(t), PC_y(t))$ is the temporally dependent PC cursor coordinate based on the acquired EMG signals, $JAT_{k,l}$ are the joint angles for the two closest postures to the current PC cursor coordinate as determined by the postural map (k = 1-6 for a 6 degree of freedom hand, l = 1-2 corresponding to the two closest postures), and $\boldsymbol{\theta}$ is the joint angle array. At any moment in time, the columns of the JAT are made up of two columns of Table 4 depending on the two nearest target postures. A novel aspect of this postural control scheme is that the JAT is spatially dependent (i.e. − the columns of the JAT change depending on the PC cursor coordinate). This fact differentiates this work from previous myoelectric control algorithms. Also, the spatial dependence of the JAT allows for the freedom to position postures within PC domain without limitation. This algorithm allows for any number of target postures and can be placed in any arrangement with in the PC domain. The JAT ensures that the hand posture morphs as the cursor moves between targets in the PC domain.

$$\boldsymbol{\theta} = \begin{bmatrix} \theta_1 \\ \theta_2 \\ \theta_3 \\ \theta_4 \\ \theta_5 \\ \theta_6 \end{bmatrix} = JAT * \begin{bmatrix} PC_x(t) \\ PC_y(t) \end{bmatrix} = \begin{bmatrix} JAT_{1,1}(PC_x, PC_y) & JAT_{1,2}(PC_x, PC_y) \\ JAT_{2,1}(PC_x, PC_y) & JAT_{2,2}(PC_x, PC_y) \\ JAT_{3,1}(PC_x, PC_y) & JAT_{3,2}(PC_x, PC_y) \\ JAT_{4,1}(PC_x, PC_y) & JAT_{4,2}(PC_x, PC_y) \\ JAT_{5,1}(PC_x, PC_y) & JAT_{5,2}(PC_x, PC_y) \\ JAT_{6,1}(PC_x, PC_y) & JAT_{6,2}(PC_x, PC_y) \end{bmatrix} \begin{bmatrix} PC_x(t) \\ PC_y(t) \end{bmatrix} \qquad (7)$$

Table 4 - Joint angles for a 6 DoF prosthetic hand for 7 functional grasps (LP – lateral prehension, TP – tip prehension, PP – palmar prehension, HK – hook, PT – pointer, CP – cylindrical prehension, HF – hand flat.

	LP	TP	PP	HK	PT	CP	HF
Thumb Rotation (°)	20	90	90	0	0	90	0
Thumb Flexion (°)	90	65	65	90	90	65	0
Index Flexion (°)	70	70	70	70	0	45	0
Middle Flexion (°)	80	0	80	80	80	55	0
Ring Flexion (°)	80	0	80	80	80	65	0
Index Flexion (°)	80	0	80	80	80	65	0

This novel algorithm for a postural controller includes many customizable features (number of electrodes, cursor control schemes, potential field designs, postural map designs, etc.) This fact motivated Experiment A where the preferred number of electrodes and cursor control scheme was determined. Afterwards, Experiment B was designed in order to study the clinical efficacy of the postural controller by quantifying t he controller performance in a simulated real world setting. Experiment B also studied the effects of visual feedback on performance and the learning rate across days.

(a)

(b)

(c)

(d)
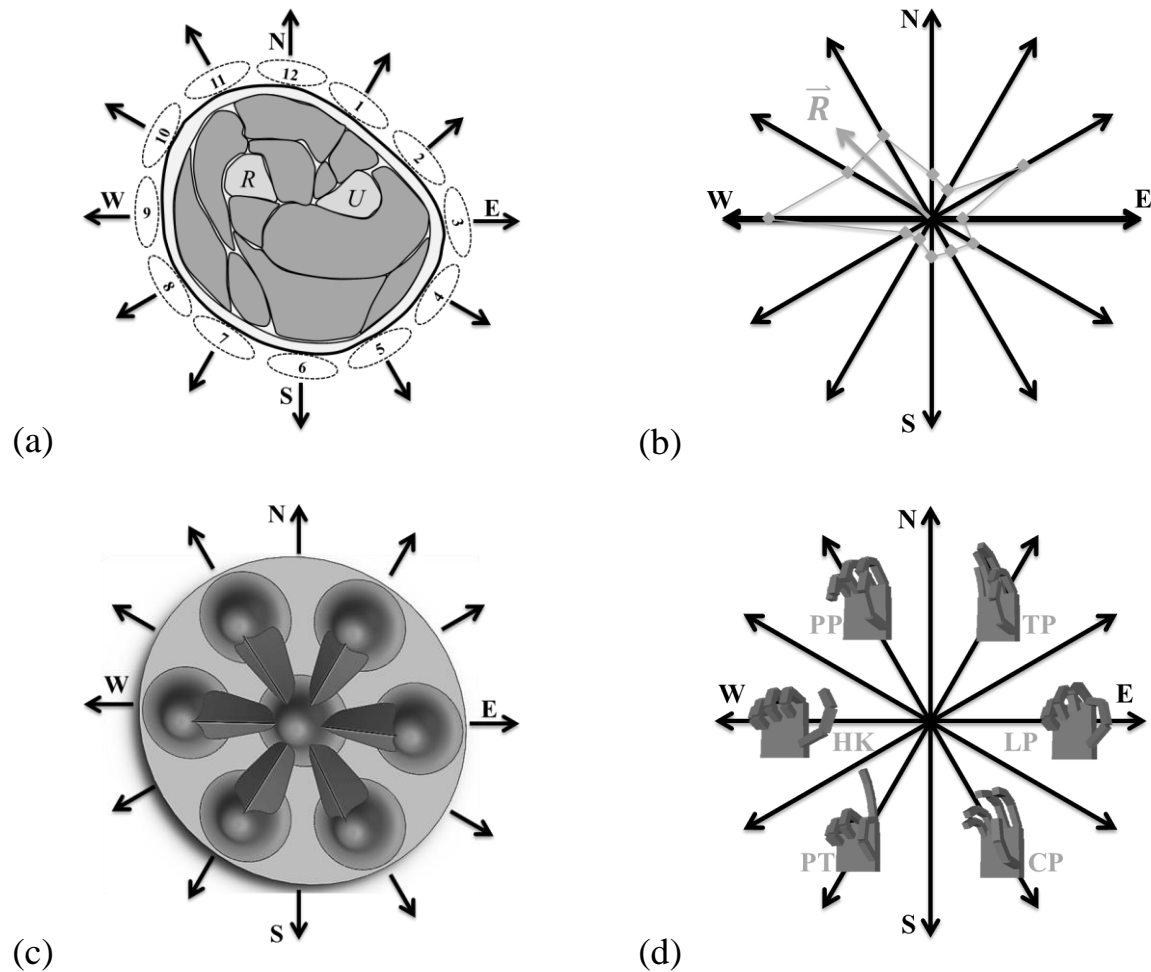
Figure 13 – Components of a postural controller. (a) An untargeted electrode array is arranged about the cross-section of the forearm. Radius bone (R), ulnar bone (U), north (N), south (S), west (W), east (E). (b) The vector summation map depicts exemplary RMS EMG activity as measured by the electrode array. The VSA calculates the resultant vector ($\vec{R}$). (c) An example potential field design where the light/dark gray areas distinguish areas of zero/negative potential, respectively. This potential field design was used in Experiment B (d). An exemplary postural map design with seven postures arranged in a symmetric distribution about the PC domain (hand flat posture not shown at origin). This postural map design was used in Experiment B. TP – tip prehension, LP – lateral prehension, CP – cylindrical prehension, PT – pointer, HK – hook, PP – palmar prehension

Methods

Eleven total subjects naïve to myoelectric control completed an experiment using the described postural controller. Experiment A consisted of a target acquisition task using various

configurations of the controller and was completed by seven subjects. Experiment B consisted of a posture matching exercise using various forms of visual feedback across three days and was completed by four subjects (S1 - S4). All subjects were healthy and claimed to have normal vision/upper limb function. They conducted the experiment using the dominant limb (10 right-hand dominant). An experimental meeting took approximately two hours. The Institutional Review Board at the University of Colorado at Boulder reviewed and approved all experimental protocols. Informed consent was obtained before each experiment.

Apparatus

Subjects sat in an upright position with their dominant arm bent at the elbow and forearm pronated on the armrest of the chair in front of a computer monitor. Experiments were carried out using an untargeted electrode array as described previously (Figure 13a). Self-adhesive snap electrode pairs with 2 cm spacing (Noraxon #272) comprised the electrode array. The array spanned the circumference of the proximal third of the forearm with the electrodes in the longitudinal direction. A Noraxon Telemyo DTS system acquired the signals with a hardware sampling rate of 1.5 kHz. A National Instruments data acquisition device 9205 interfaced with the analog output module of the Noraxon system and was controlled using a custom built LabView interface. The LabView interface processed the EMG signals using standard processing techniques (band pass 30-450Hz, rectification, RMS moving average). Individual gains, thresholds, and offsets tuned the system to produce a symmetric and comfortable system (i.e. – equivalent effort causes equivalent RMS average for all sites).

Experiment A

Experiment A took place in a single experimental meeting. During a single trial, subjects performed a center out target acquisition task using one of two cursor control scheme and one of

three electrode configurations for a total of six control methods: 12-site position control (P12), 12-site velocity control (V12), 4-site position (P4), 4-site velocity (V4), 3-site position (P3), 3-site velocity (V3). The sequence of control methods was presented in a pseudorandom fashion where the velocity and position control sessions and the order of electrode configurations within each session was randomized for each subject (an example protocol is shown in (Figure 14). The 4-site sessions used electrode numbers 3, 6, 9, and 12 and the 3-site sessions used electrode numbers 3, 7, and 11 as described in (Figure 13a). The visual feedback paradigm for all sessions consisted of the PC domain including the target circle and PC cursor coordinate. Twelve equally spaced targets with radii of 14% of the PC domain were set at a radius 70% between the origin and the edge of the PC domain [83] and aligned with the vector summation map. Three randomized blocks of twelve targets were presented for each session. No potential field was applied during Experiment A in order to isolate the differences between the experimental conditions. A trial consisted of directing the cursor from the origin to the target within ten seconds (including the hold time) otherwise the trial was considered a failure. Each session consisted of 36 trials and tested a single control method.
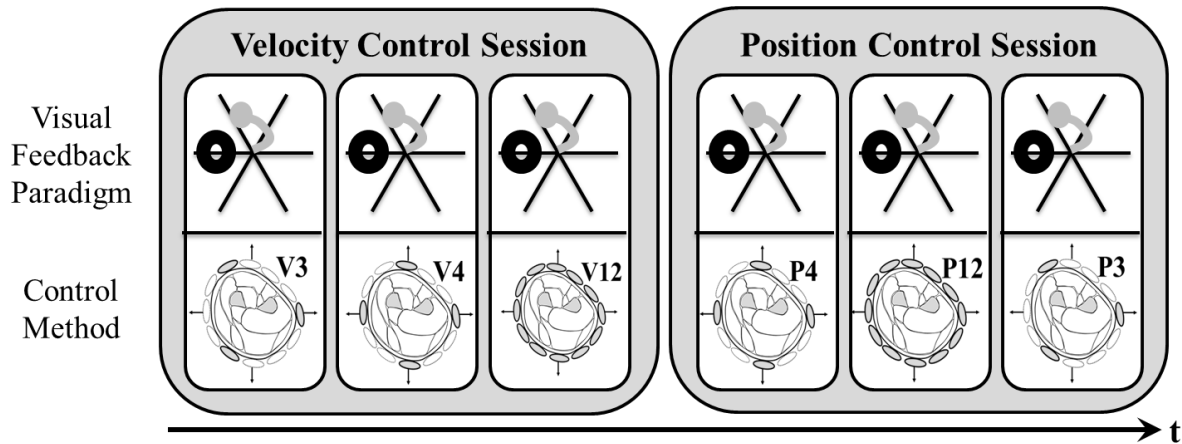
Figure 14 –Experiment A protocol for an exemplary single meeting. The visual feedback paradigm for all sessions consisted of the PC domain including the target circle and PC cursor coordinate. The sequence of control methods was presented in a pseudorandom fashion where the velocity and position control sessions and the order of electrode configurations within each session was randomized for each subject. 3-site velocity (V3), 4-site velocity (V4), 12-site velocity (V12), 4-site position (P4), 12-site position (P12), 3-site position (P3).

Experiment B

Experiment B took place across three experimental meetings on three separate days (D1-D3). In a single trial, subjects were asked to command a six DoF virtual hand into one of seven functional postures using a 3-site electrode array and velocity cursor control scheme. Each experimental meeting comprised of the same sequence of four sessions which presented differing visual feedback paradigms: 1) PreTest (PT) session, 2) Target Training session (Tar), 3) No Target Training session (nTar), and 4) Test (T) session. During all sessions, a computer monitor presented a virtual hand (VH) prosthesis that responded to the real-time output of the postural controller and a target posture. The additional visual feedback differed between experimental sessions (Figure 15). The PC domain was hidden during the PT session. The PC domain with the real time cursor position as well as the target position was presented in the Tar session. The PC domain with the real-time cursor position but not the target position was presented in the nTar

session. The PC domain was hidden during the T session. The sequence of the sessions (PT, Tar, nTar, T) was designed to allow for the assessment of learning [84]. The PT and T session simulated a real-world environment where a screen displaying the PC domain would not be present thereby assessing the clinical efficacy of the system. The Tar and nTar sessions used visual feedback to help teach the subjects to perform the task. Six equally spaced targets with radii of 14% of the PC domain were located at a radius 70% between the origin and the edge of the PC domain (the seventh target posture, hand flat, was located at the origin of the PC domain, Figure 13d). A trial consisted of matching the VH to the target posture within 10 seconds (including one second hold time) otherwise the trial was considered a failure. The VH matched the target posture when the cursor was within the 14% radii of the target in the PC domain and was provided using a visual indicator. The PT/T sessions consisted of 35 trials (5 attempts at each target) and the Tar/nTar sessions consisted of 70 trials (10 attempts at each target). The identical potential field was applied during all experimental meetings and is depicted in Figure 13c. The EMG tuning parameters (gains, offsets, and thresholds) were defined during the first meeting and not altered during the second or third meetings.
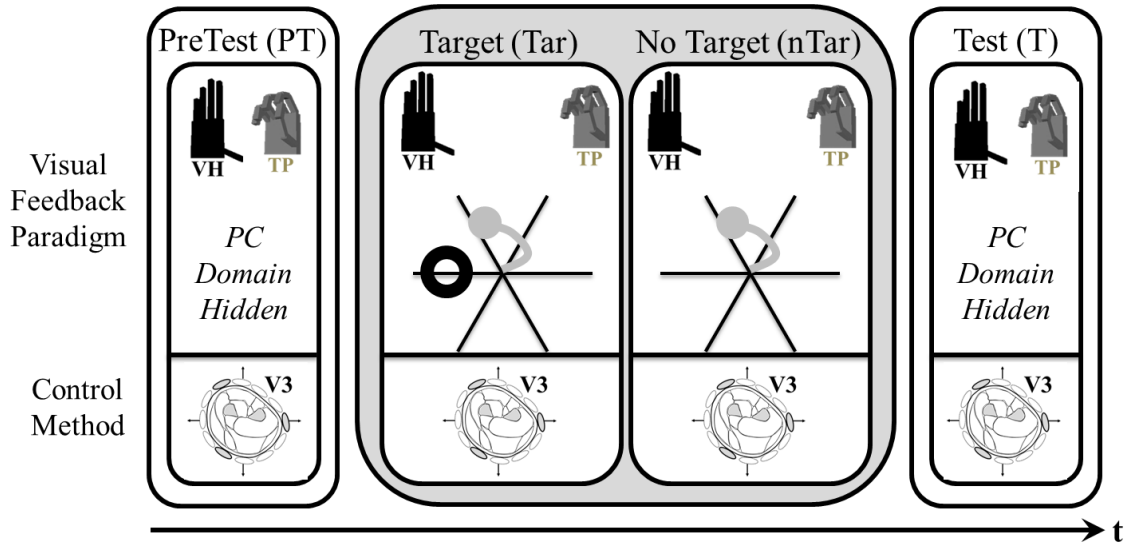
Figure 15 –Experiment B single meeting protocol. This protocol was repeated on D1-D3. During all sessions, a computer monitor presented a virtual hand (VH) prosthesis that responded to the real-time output of the postural controller and a target posture (TP). The additional visual feedback differed between PT/T, Tar, and nTar sessions. All sessions used the same control method (3-site velocity, V3).

Performance Metrics

Several performance metrics were used to study the performance during experiments A and B. The *completion rate* (CR) is the number of successful trials per total number of trials. The *movement time* (MT) is the duration of the successful trial in seconds not including the one second hold time. The *path efficiency* (PE, equation ((8)) describes the degree to which the cursor trace erred from the most direct path between the origin and target during successful trials. The traveled distance is the discrete integral of the PC cursor coordinate path. The ideal distance is the straight line distance between the target coordinate and the origin. A PE equal to 100% signifies that the cursor traveled along a straight line between the origin and target.

$$PE\ (\%) = \frac{Traveled\ Distance}{Ideal\ Distance} * 100 = \frac{\sum_{j=1}^{N}\sqrt{\left(PC_{x,j} - PC_{x,j-1}\right)^2 + \left(PC_{y,j} - PC_{y,j-1}\right)^2}}{\sqrt{(Target_x)^2 + (Target_y)^2}} * 100 \qquad (8)$$

MT and PE were only reported for successful trials. Better performance is quantified by higher CR, lower MT, and higher PE. One/two-factor ANOVA's and Tukey-Kramer post-hoc analyses were used when appropriate with a significance level of 0.05. Experimental results report means ± standard error of the mean.

Results

Experiment A

The PC cursor coordinate traces using the six control methods for a single subject are shown in Figure 16. Each window displays the 36 trials performed using each control method. The twelve targets are shown as well as the vector summation map. The red traces depict a failed trial while the blue traces depict a successful trial. The top row of windows displays the position control trials and the bottom row of windows displays the velocity control trials. Figure 16 depicts qualitatively an increase in CR and PE of the velocity control sessions compared to the position control sessions shown by the increase in straighter blue traces. Also, performance does not seem to change when using 3, 4, or 12-site electrode array. These qualitative observations are tested statistically using the performance metrics described previously.
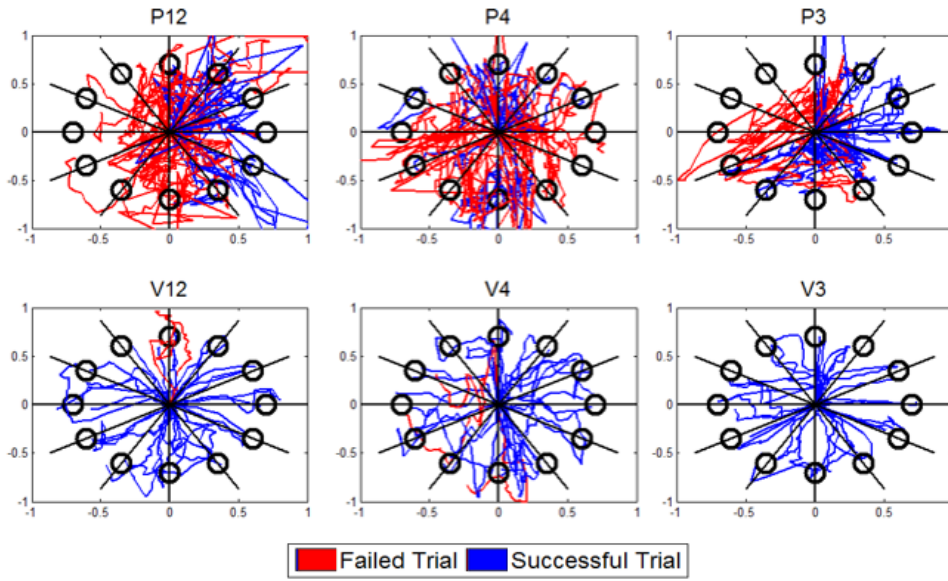
Figure 16 – Raw PC cursor coordinate traces by a single subject. Each window displays 36 attempts corresponding to a single experimental session. The targets are shown as circles. The twelve axes correspond to the twelve electrodes on the limb.

The across subjects average performance metrics for each experimental session are shown in Figure 17. All metrics described the same two findings; the velocity control method allowed for better control than the position control and the number of control sites did not change the performance. In detail, the CR was significantly greater using velocity control (84% ±3%) than position control (45%±3%, $p < 0.0001$). The MT was significantly lower using velocity control (5.3s ± 0.2s) than position control (6.1s ± 0.1s, $p = 0.0002$). The PE was significantly greater using velocity control (69% ± 3%) than position control (27% ± 2%, $p < 0.0001$). In addition, the number of control sites used during each session did not affect the CR, MT, and PE ($p = 0.57$, $p = 0.34$, $p = 0.32$ respectively).
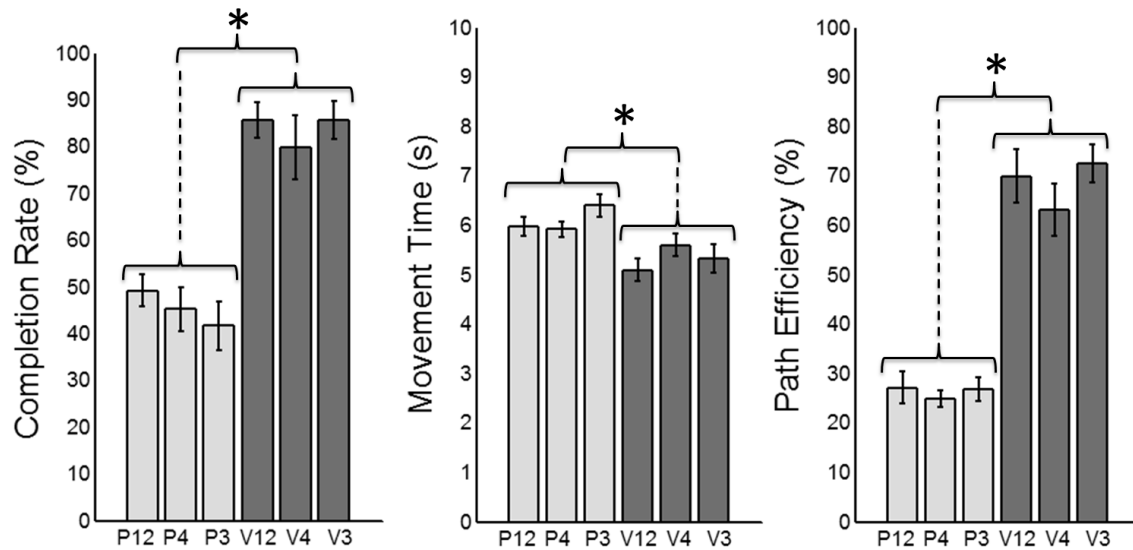
Figure 17 – Experiment A performance metrics averaged across subjects for each control method. No difference was found when comparing the 12-site, 4-site, and 3-site electrode array sessions. * indicates a $p<0.05$.

Experiment B

The ability of subjects to volitionally command a six degree of freedom virtual hand into seven functional postures was quantified (Figure 18) using the average CR, MT, and PE performance metrics for each subject (S1,...,S4). During the testing session the average CR, MT, and PE across subjects was $82\%\pm4\%$, $3.5s\pm0.2s$, and $45\%\pm3\%$. The CR for S4 is a statistical outlier ($p = 0.01$) and is discussed in more detail below. The average CR without S4 is $88\%\pm2\%$.
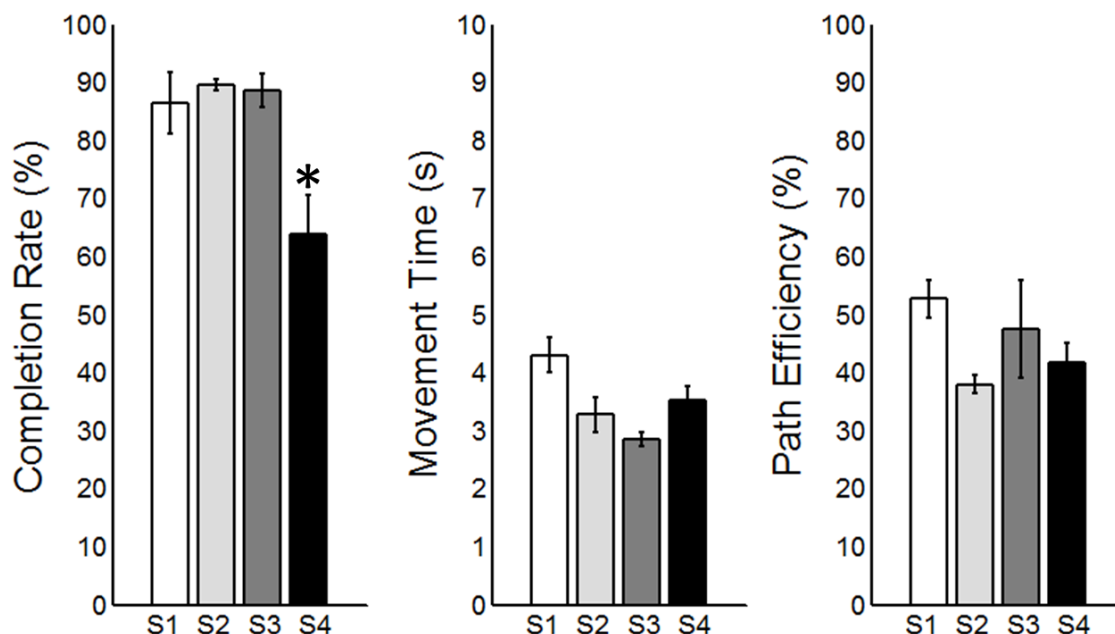
Figure 18– Experiment B Testing (T) session performance metrics averaged over days for each subject. * indicates a $p<0.05$.

The retention of the ability to use the postural controller was tested by comparing performance metrics produced during the PT sessions for all subjects across days (Figure 19). The PT session occurred before the training sessions and thereby tested the retention of the ability to use the postural controller from the previous day. The CR and PE results were significantly different across days ($p \ll 0.001$ and $p = 0.002$ respectively). Post-hoc analysis showed that the CR and PE for day 1 was significantly lower than days two and three. The CR and PE results showed no difference between days two and three ($p = 0.47$ and $p = 0.08$ respectively). The MT results showed no difference across days ($p = 0.98$).
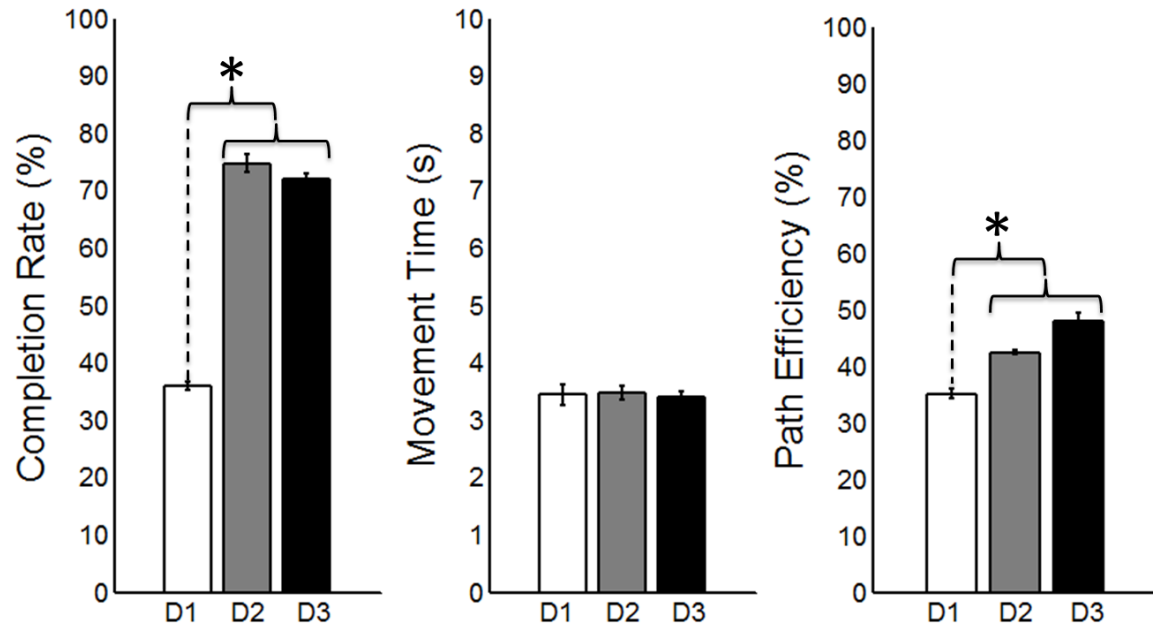
Figure 19 – Experiment B PreTest (PT) session performance metrics averaged over subjects for each day. * indicates a $p < 0.05$.

The effect of visual feedback on performance was tested by comparing average metrics across days for the Tar, nTar, and T sessions (Table 5). The CR during Tar and nTar sessions was significantly greater than T session for three out of four subjects. The MT and PE did not change for any subjects across visual feedback paradigms (average p-values of 0.50 ± 0.05 and 0.83 ± 0.08. These results indicate the additional visual feedback provided during Tar and nTar sessions augments CR, but not MT or PE. In other words, the additional visual feedback increased the frequency of successful trials but did not increase the speed or precision of the successful trials.

Table 5– Experiment B performance metrics averaged across days for each subject. Results are shown for target training (Tar), no target training (nTar), and test (T) sessions. P-value indicates statistical difference between sessions.

		Tar	nTar	T	p		Tar	nTar	T	p		Tar	nTar	T	p
S1	CR (%)	82	84	86	0.84	MT (s)	4.6	4.1	4.3	0.36	PE (%)	52	55	53	0.95
S2		98	95	89	**0.01**		3.0	3.3	3.3	0.63		38	40	38	0.59
S3		99	97	89	**0.04**		2.7	2.6	2.8	0.54		46	50	48	0.92
S4		91	99	64	**0.01**		3.5	3.2	3.5	0.46		39	41	42	0.86

Discussion

Experiment A

The results of Experiment A described a significant increase in performance using a velocity cursor control scheme compared to a position cursor control scheme. Several factors were observed that differentiate the two cursor control schemes. The position control scheme requires continuous activation of specific musculature in order to complete a successful trial since quiescent EMG activity (i.e. – rest) equates to the PC cursor coordinate position at the origin. It was observed that subjects had difficulty holding specific muscular contractions in order to maintain the cursor in the target position. The velocity control scheme allowed for sequential activations of specific musculature in order to complete a successful trial since quiescent EMG activity equates to a stationary PC cursor coordinate position. As a result, subjects were observed using a 'pulsing' strategy where sequential muscle contractions moved the cursor small distances towards the target followed by a pause/rest to ensure an accurate completion of the task. Similar observations were described by Jiang *et al.* when comparing a position and velocity control scheme when using a non-negative matrix factorization algorithm [85]. This result designates velocity control as the favored cursor control scheme for the system.

However, we acknowledge that the preferred cursor control technique may depend on the task (e.g. – a center out target acquisition task using a virtual hand versus an object manipulation task using a physical prosthesis) and should be studied further.

The results of Experiment A found no difference in performance between the different electrode arrays tested. The 12-site untargeted electrode array is assumed to measure redundant EMG activity therefore a subset of electrodes could measure the equivalent information. Previously, we found that three statistically independent electrodes could be determined by performing a cross correlation analysis of the EMG activity measured using a 12-site untargeted surface electrode array for nine out of ten subjects tested [86]. For this task, the EMG activity collected by three electrodes provided sufficient information for the controller to decipher user intent with similar accuracy to the four and twelve electrode arrays. The 3-site electrode array is thereby the preferred electrode array configuration for this system. This finding has noteworthy clinical implications as well. The number of electrodes necessary to control a myoelectric prosthesis should be minimized in order to reduce cost and complexity of a prosthetic hand system.

Experiment B

The clinical efficacy of the postural controller was studied using the T session performance metrics. The average CR, MT, and PE during the T sessions are comparable to many of the current state-of-the-art myoelectric controllers [58], [59], [73]. Pistohl *et al.* used similar control architecture, but did not test a clinically viable system since the control sites were intrinsic to the hand and functional postures were not produced [82]. However, Dalley *et al.*, reported better performance (higher CR and lower MT) than the work presented here using a state machine architecture [67] in a clinically viable system. The state machine architecture

provides a more restrictive environment within which the user controls the hand posture as compared to the postural control architecture. The state machine limits the user to specific transitions between neighboring postures using a physiologically inappropriate trigger command while the postural controller allows for direct transitions between all postures in the PC domain without a trigger command. The state machine is a single dimensional architecture (i.e. − a linear arrangement of postures) whereas the postural control architecture is a two-dimensional architecture (i.e. − a planar arrangement of postures). The added dimension in the postural control architecture provides additional freedom while, in this case, sacrificing performance as compared to the state machine in [67]. Chapter 5 presents a more in depth study of this tradeoff by comparing state machine and postural control architectures directly.

The CR for S4 is significantly different compared to the three other subjects (p = 0.01). We feel that the EMG acquisition gains and thresholds were poorly tuned (the gains too high and thresholds too low) during D1 for S4. The subject repeatedly overshot the target in the PC domain and lacked the precision to direct the cursor to the target consistently without visual feedback. The experimental protocol disallowed for the EMG acquisition system to be reset after the first meeting. The performance of S4 indicates the sensitivity of the system to the initial tuning of the EMG acquisition system.

The pretest session allowed for an analysis of retention of the ability to use the postural controller across days. The performance of subjects (specifically CR and PE) increased and then persisted after only a single day of training. In other words, a single training session is sufficient for high level use. This implies that clinical implementation of the postural controller could occur during a single training session between the prosthetist and user. Another important outcome when comparing performance across days is that performance is not affected by

donning/doffing of the myoelectric system. The myoelectric interface was removed completely between days; however, the performance on average increased and then stabilized without retraining/tuning the myoelectric interface. Specifically, this observation differentiates the postural controller from many pattern recognition systems previously developed which show deteriorating performance from donning/doffing [59].

The effect of visual feedback on performance was shown to significantly augment the CR for three out of four subjects. This finding was expected as the visual feedback provided during the training sessions was meant to assist the subjects complete the task. The information provided by the real-time cursor position enabled the subjects to modulate the muscular activity in order to acquire the target in the PC domain. The MT and PE metrics were unaffected by the various visual feedback paradigms. This suggests that visual feedback assisted in the overall completion of the task (i.e. – matching postures) but not in the speed (MT) or precision (PE). However, this study did not test whether subjects would learn more effectively by exploring the PC domain without any visual feedback.

Novel Aspects

The postural controller presented here integrates several novel aspects with respect to previous work [71]–[73], [87]. Here, the postural map is fully customizable due to the novel derivation of the dynamic JAT. Previously, principal component vectors were used to derive the JAT and dictated the number and locations of the postures in the PC domain. Now, the locations of the postures are defined by the postural map and implemented using equations (7). The number and location of the postures in the PC domain is unlimited. The exemplary postural map (Figure 13d) depicts a PC domain with 6 unique postures, however additional postures could be added circumferentially between the given postures, radially in front/behind the postures, etc.

The freedom provided by this architecture is greater than previous postural controllers due to the advancement in the derivation of the JAT.

The development of the potential field also distinguishes this work. The potential field effectively adds a third dimension to the PC domain. The topography of the PC domain is determined by the design of the feedback controller and the tuning of the proportional and derivative gains. The proportional gain adjusts the 'steepness' of the well/wedge while the derivative gain 'flattens' the bottom of the well. An interesting viewpoint is that the potential field transforms the PC domain into a 'soft' state machine. The preferred states are located at the areas with lowest potential and the harshness of the states is determined by the depth of the wells/wedges. The exemplary potential field (Figure 13c) is a preliminary attempt to design a potential field that augments to performance of the postural controller. Pilot studies indicated the utility of the potential field used here; however, the design of more optimal potential field requires further investigation. Nonetheless, this chapter substantiates the novel algorithm for a postural controller as an effective and robust design for a MEC of multi-function prosthetic hands. Many questions remain concerning the efficacy of the controller during object manipulation tasks and the benefits/pitfalls of the postural controller when directly compared to the state of the art MECs in the commercial and research realms. These questions are addressed directly in Chapter 5.

Chapter 5 - A Comparative Study of State of the Art Myoelectric Controllers for Multi-Grasp Prosthetic Hands[9]

Introduction

As described in Chapter 4, the postural controller was effective at matching virtual hand postures with clinically realistic visual feedback and was robust to donning/doffing across days. However, it must be proven that the postural controller is also effective when implemented on a physical device and used to perform activities of daily living. Additional challenges including stable grasp forces, temporal coordination of the digits in the hand, and co-activity of the EMG control sites due to the weight of the prosthesis must be overcome. Here the postural control (PC) scheme is first implemented on a physical device and able-limbed subjects first use the postural controller to manipulate objects.

In general, MECs address the challenge of an intuitive human machine interfaces with differing strengths and weaknesses. Although comparisons across architectures are essential in order to assess the efficacy of each MEC, only few studies actually addressed this issue in a systematic manner. Previous works have compared pattern recognition MECs [63] and finite state machine MECs [88], but not the more recently proposed PC schemes. Thus, in this work two types of finite state machines and a PC scheme are compared using both virtual and physical assessment procedures with seven able-limbed subjects. Pattern recognition systems were not compared since they have not been shown to be viable to clinical conditions like electrode shift, limb position, sweat, etc. We used the Southampton Hand Assessment Procedure (SHAP) [18] in order to study the effectiveness of each MEC to perform ADLs with a physical multi-grasp

---

[9] Intended publication with *Journal of Rehabilitation Research and Development,* submitted February 2014 with co-authors Marco Controzzi, Ph.D., Richard F. *ff.* Weir, Ph.D., and Christian Cipriani, Ph.D.

artificial hand as well as a virtual hand posture matching task in order to measure the ability of subjects to reproduce six target postures [87].

Methods

Three MEC architectures were compared in this study using a physical assessment (experiment A) and a virtual assessment (experiment B). The experimental setup consisted of a three-site EMG acquisition system and a laptop running a custom application (written using LabView, National Instruments, Inc). The latter processed the EMG signals, implemented the MEC algorithms (i.e.- generated control commands as outputs) and stored the data for off-line analysis. The outputs of the MECs were physically implemented by a multi-grasp artificial hand, connected to the laptop (during experiment A) or a virtual hand displayed on the laptop screen (during experiment B).

The EMG signals were acquired using two surface electrodes targeting the flexor digitorum superficialis (F) and extensor digitorum (E) and a third surface electrode targeting extensor carpi ulnaris (U) muscles when necessary (cf. below). Self-adhesive snap electrode pairs with 2 cm center-to-center inter-electrode spacing were placed on the target muscle in a longitudinal orientation (Noraxon #272). A Noraxon Telemyo 2400R system sampled the EMG signals (3 kHz) with an analog low pass cut-off frequency of 500 Hz while a data acquisition board (NI-USB 6211) connected to the laptop digitized them. These signals were processed using standard techniques (band-pass 10-450Hz, rectification, 100ms moving average) and were used to produce control commands based on the specific MEC. Individual EMG gains and thresholds could be tuned for each subject.

Each of the three MECs had a unique architecture while all other parameters were standardized in order to ensure a robust comparison. The hand posture was initialized to hand flat throughout each experiment for all MECs. The closing speed of the finger for all controllers and postures was set to ~1 second. The temporal coordination for each posture (i.e., the timing of the digit movements when closing the hand) was standardized across controllers. The six target postures and hand flat were identical in each MEC (Table 6) which ensured equal grip forces across each MEC. The six postures comprised functional postures and grasps used in ADLs [16] and were chosen in order to replicate the experimental setup used by Dalley et al., [67]. Finally, the gains on the EMG signals were normalized to the maximum voluntary contraction of each subject.

Table 6 –Target postures included in each MEC

	Palmar Prehension	Tip Prehension	Lateral Prehension	Hook	Pointer	Opposition	Hand Flat
Thumb Rotation (˚)	90	90	20	0	0	90	0
Thumb Flexion (˚)	65	65	90	0	90	0	0
Index Flexion (˚)	70	70	70	70	70	0	0
Middle Flexion (˚)	80	0	80	80	80	0	0
Ring Flexion (˚)	80	0	80	80	80	0	0
Little Flexion (˚)	80	0	80	80	80	0	0
Posture Image							

Controller 1: Commercially available finite-state machine

Controller 1 (C1) replicated the finite state machine implemented in a commercially available device: the iLIMB prosthetic hand (Touch Bionics, ltd. Livingstone, UK, Figure 20). This type of state machine is typical among available commercial prostheses [19], [20], [89]. The architecture consisted of six states corresponding to the six target postures, not including HF. A

trigger (T) iteratively changed states in a specified order. The trigger allowed for a progression in the sequence of states in a single direction. The trigger command occurred when both EMG signals (F, E) supersede a tuned threshold (a brief co-contraction). An audible beep was provided by the experimental apparatus to indicate that a trigger command was recognized (like in the iLIMB prosthetic hand). Once inside a state, the magnitude of the difference between F and E was proportional to the speed of the hand and the sign of the difference corresponded to the opening/closing of the hand (a velocity control scheme). The fully closed posture of each state coincided to one of the target postures while the fully opened posture coincided to HF (full extension of all digits). Therefore, the only available postures within a state were a linear combination of the corresponding target posture and HF.
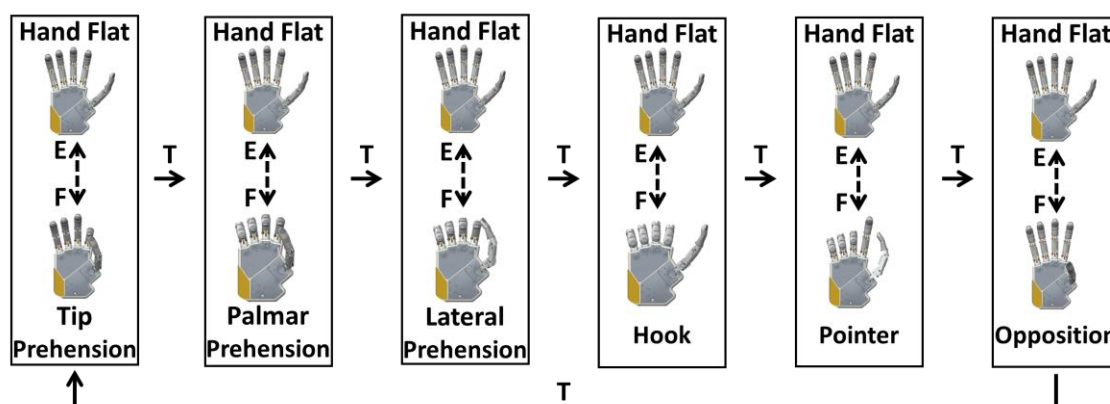
Figure 20 – Controller 1 (C1). A finite state machine based on the iLIMB prosthetic hand.

Controller 2: Vanderbilt University controller

Controller 2 (C2) replicated the Multigrasp Myoelectric Controller developed by Dalley *et al.* [67] (Figure 21) at Vanderbilt University. The architecture consisted of two states (opposition and reposition) with multiple target postures within each state. The two states were distinguished by the abduction position of the thumb: opposition and reposition. A co-

contraction trigger (T) switched between the two states. The trigger command and the hand opening/closing occurred identically to C1. The sequence of postures within each state ensured that the digits closed/opened in a coordinated manner. The transition logic between postures was not reproduced exactly as described in [67] due to mechanical constraints of the artificial hand used in the present study. Specifically, the actuator displacement and force thresholds were not available to use in the transition logic in our study. Instead, the transitions between the states were solely dependent on the volitional EMG input signals. The hand posture when transitioning between targets was a linear combination of the two nearest target postures.
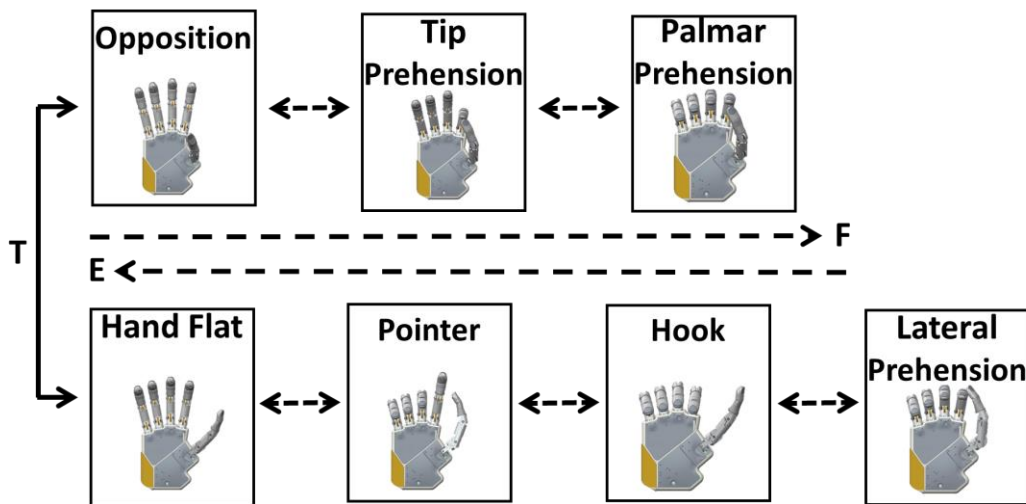
Figure 21 – Controller 2 (C2). A finite state machine based on the Multigrasp Myoelectric Controller developed by Dalley *et al*.

Controller 3: Postural controller

Controller 3 (C3) was a postural controller based on previous work by the authors [87], [90] (Figure 22) as described in Chapter 4. The architecture used EMG signals like a joystick to morph the hand posture. As described previously, the EMG signals are mapped into two control parameters that can be represented by a coordinate in the PC domain. All locations in the PC domain corresponded to a hand posture. In this work, the three EMG signals were mapped in a

radial fashion about the origin of the PC domain (Figure 22). The vector summation of the RMS EMG values equaled the coordinate position in the PC domain. A position control scheme was used where quiescent EMG signals corresponded to the coordinate at the origin. The coordinate, [PC_X, PC_Y], was converted into a joint angle array, **θ**, by a linear transform, the Joint Angle Transform (*JAT*, (9)). The JAT varied depending on the closest target postures to the coordinate at any given time (i.e., the JAT was spatially dependent). At all times, the hand posture (i.e., the joint angle array) was a linear combination of the two closest target postures where when the coordinate equaled a target posture position, the MEC reproduced the target posture identically. The architecture did not include discrete states and therefore did not require a trigger signal.

$$\mathbf{\theta} = \begin{bmatrix} \theta_1 \\ \vdots \\ \theta_6 \end{bmatrix} = \mathbf{JAT} * \begin{bmatrix} PC_x(t) \\ PC_y(t) \end{bmatrix} \tag{9}$$
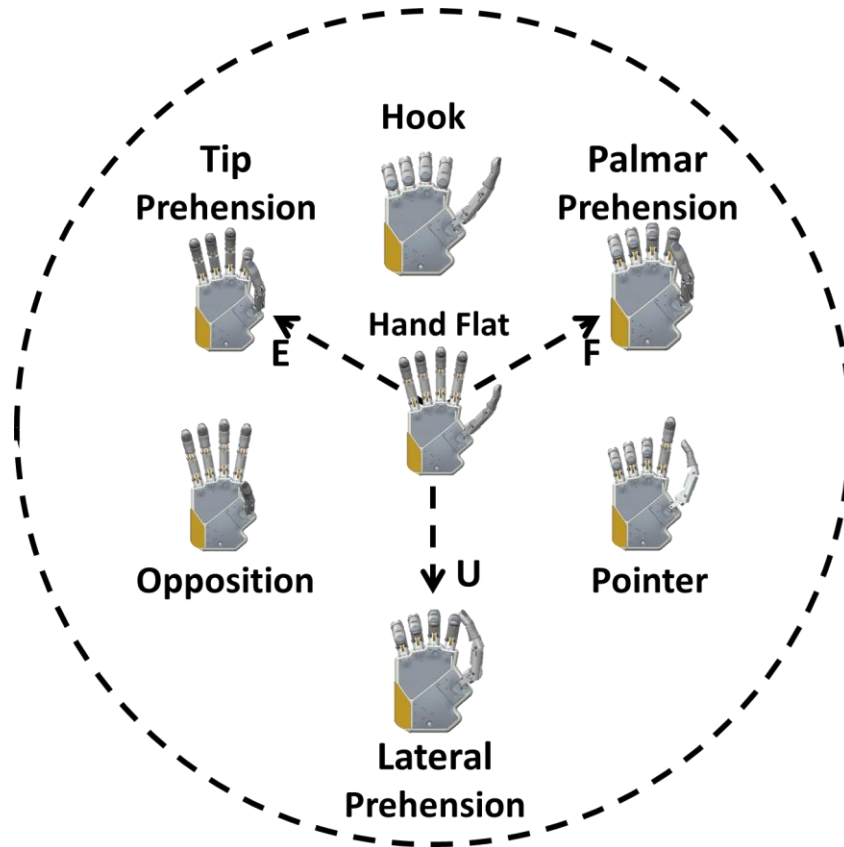
Figure 22 – Controller 3 (C3). A postural controller developed as described in Chapter 4. An arrangement of the target postures in the Postural Control domain is shown as well as the radial mapping of the EMG signals (F, E, and U).

Experimental Methods

Seven able-bodied subjects (aged 26 years ± 3years, all right handed) completed two experiments (A and B) using the three MECs. Experiment A consisted of the SHAP [18] using a modified Azzurra IH2 artificial hand (Prensilia Srl, Pisa, Italy) mounted onto a splint. Experiment A tested the ability of the subjects to manipulate physical objects. Experiment B instead consisted of a virtual hand posture matching task (as in [87]) in order to test the full range of postures for each MEC. In a single (two hour) experimental session both experiments were performed using a single controller (either C1, C2, or C3) with experiment A occurring first. Three sessions were scheduled on three different days for each subject. The order of the

controllers tested across the three days was randomized across subjects. All subjects claimed to have normal vision/upper limb function and were not practiced at myoelectric control. All subjects conducted the experiment using their left arm to match the handedness of the robot hand available. Informed consent according to the Declaration of Helsinki (BMJ 1991; 302:1194) was obtained before conducting the experiments.

Experiment A

In experiment A, the subjects performed the SHAP wearing the artificial hand. The hand was mounted on an able-bodied splint which included a handlebar so that the physiological limb would maintain an anatomically neutral position. The SHAP is a standardized time-based hand assessment procedure that measures the hand function relative to normal able-bodied function using 26 ADL tasks which span the functional grasps (Table 1, [18]). It was shown to be reliable and was validated so that results of independent studies can be compared [18]. For example, it was used by Van Der Niet and colleagues to compare the i-LIMB and DMC hands [54] and by Dalley *et al.* to functionally assess the Multigrasp Myoelectric Controller (i.e. the controller replicated in this work) [55]. As instructed by the SHAP protocol, subjects were asked to complete tasks consisting of the physical manipulation of abstract objects (cylinders, spheres, tabs, etc.) and physical ADLs (turning a door handle as in Figure 23a, picking up coins, moving containers, lifting a tray, etc.). The 26 tasks were performed as quickly as possible and were self-timed by the subject using a start/stop button as prescribed by the SHAP Only a subset of grasps (palmar, tip, and lateral prehension) in each MEC was necessary to perform the SHAP (Table 1). The duration of each task was used to calculate a SHAP score which described the overall function of the subject. The calculation of the SHAP score occurred by inputting the duration of the each task in seconds into the proprietary algorithm provided by the SHAP organization

through their website (http://www.shap.ecs.soton.ac.uk/index.php).   Since the SHAP used a time-based protocol, the best performance equated to the fastest average performance across all tasks.

The artificial hand used during the SHAP was a modified IH2 Azzurra hand. The unmodified version of this hand consists of five underactuated digits (two joints per digit) driven by five motors which actuated the flexion/extension of the thumb, index, middle, ring/little as a pair and the ab/adduction of the thumb. The hand was modified in order to improve grasp stability during TP and LP. In particular the thumb and index fingers were splinted so that they became a single jointed digit about the metacarpophalangeal joint (Figure 23b) and compliant material was added to the fingertips.

Before the experiment, the EMG control sites were located by palpating the forearm and the electrodes were fixed as described previously. Then the splint with the robot hand was fitted to the subjects' forearms using adjustable straps in an anatomically correct position. As a standard procedure, the gains on the EMG signals were normalized to the maximum voluntary contraction of each subject as the subject suspended the hand and splint in order to best compensate for the nominal EMG activity due to the weight of the system. For all controllers, there was a balance between too little gain (i.e., the tasks were too effortful for the subjects) and too much gain (i.e. the controller was unusable due to false triggers and/or poor cursor control in C3). The experimenter tuned the EMG signals with the goal of finding the balance between these two extremes.

During the experiment subjects sat in an upright position in front of a table where the SHAP materials were placed. The subject rehearsed each SHAP task until he/she was able to

reliably perform it as suggested by the SHAP assessor's manual [91]. The subject performed the task until satisfied that the fastest possible time was achieved. Five tasks of the original SHAP were not included in our study (button board, food cutting, rotate key, zipper, and screwdriver tasks) due to mechanical limitations of the hand available and were given the maximum time, 100 seconds, as prescribed by the SHAP assessor's manual. Subjects were instructed to rest between SHAP tasks as needed.

(a)   (b)
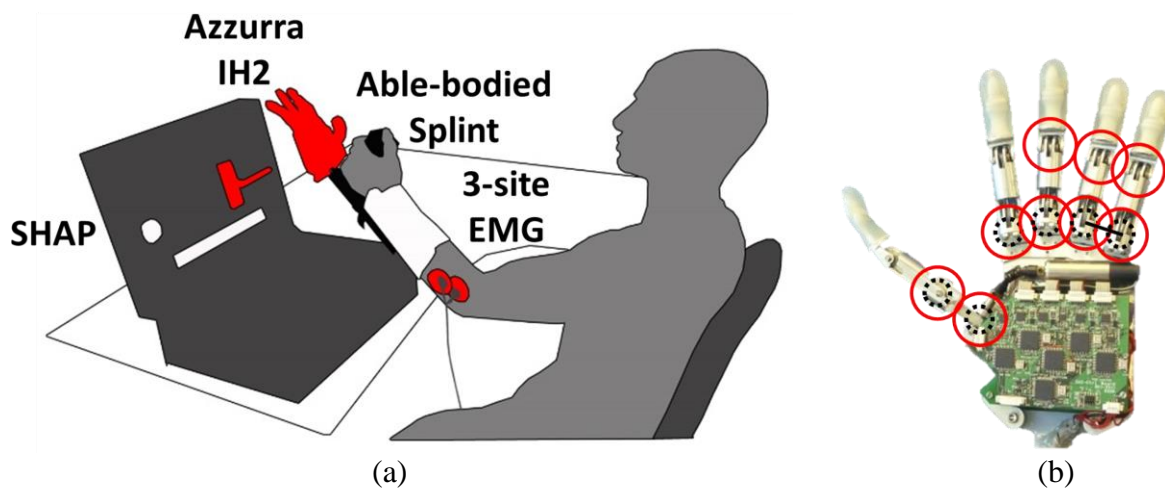
Figure 23 – a) The experimental platform consisting of Azzurra IH2 artificial hand mounted onto an able-bodied splint, a three-site surface EMG acquisition system, and the SHAP. b) The Azzurra IH2 artificial hand with nine joints (red circles) and five motors (dashed black circles, the ring and little fingers are coupled as shown by solid line).

Experiment B

In experiment B, the subjects performed a virtual hand posture matching task by controlling the movements of a virtual hand (VH) displayed on the laptop using the same EMG control sites as in experiment A. The VH posture matching task was meant to quantify the ability of the subjects to reproduce all six functional grasps available in each MEC (as opposed to the subset of grasps used during the SHAP). The VH had the same physical architecture of the IH2 Azzurra hand and responded in real-time to the output of the MECs. During the experiment

subjects sat in an upright position in front of the laptop (the splint and the robot hand were not used). The subjects were asked to match the posture of the VH to one out of six randomly presented target postures as quickly as possible. The random presentation of target postures was implemented in order to simulate everyday use when users choose between hand postures in a pseudo-random fashion. The target posture was displayed as a static image of the VH in the appropriate position [87]. A successful trial consisted of matching the VH to the target posture in ten seconds or less (including a one second hold time) otherwise the trial was considered a failure. The VH matched the target posture when the coordinate was within the 14% radii of the target position in the PC domain [83] and was indicated by the visual interface. The experiment consisted of 60 trials (10 attempts at each target posture). The sequence of target postures was randomized across subjects. Before experiment B the EMG acquisition was retuned. The VH task tested the ability of each subject to produce the specified target postures as opposed to the SHAP which required the completion of the task and not a specific posture.

Performance Metrics

In experiment A, the *SHAP Score* (S_S) as defined by Light et al. [18] was used as one of the performance metrics. The S_S was designed to measure a subject's artificial hand function and was derived from the time to complete the SHAP tasks; a score of 100 corresponded to normal, able-bodied hand function while a score of 0 equated to minimal function [18]. The S_S was calculated as an across subject average (unpaired) and was reported in order to compare the prosthetic system to previous studies using the SHAP.

In this work, we introduced the *SHAP Percent Difference* (S_D) which was the percent difference from the subject average S_S as described by equation (10) where N was the total number of subjects and c was the MEC. Positive S_D occured when the S_S for the MEC was

greater than the subject's average and vice versa. The S_D was the preferred performance metric compared to the S_S since it was a within subject comparison and therefore was a more sensitive measure of the relative utility of the MECs.

$$S_D^c = \frac{\sum_{n=1}^{N}\left(\frac{S_S^{n,c}}{\sum_{c=1}^{3} S_S^{n,c}/3} - 1\right)}{7} * 100 \tag{10}$$

In experiment B, several metrics were used to quantify the performance. The *completion rate* (CR) is the number of successful trials per total number of trials. The *movement time* (MT) is the duration of successful trials in seconds not including the one second hold time. The *average EMG amplitude* (EMG AMP) is a measure of effort based on the RMS of the EMG activity from each electrode (i) for each posture (p). AMP is a within subject measure and is calculated as the percent difference from the subject average RMS EMG amplitude for each controller (c, ((11)) [92]. Positive AMP occurs when the subject produces more EMG activity (i.e. – effort) for a controller/posture than the subject average and vice versa. The standardization of the EMG tuning methods, as detailed previously, ensured that the AMP metric accurately reflected the effort of the subject. EMG AMP was only calculated for experiment B since the manipulation tasks in experiment A caused compensatory EMG activity which was not of interest.

$$AMP = \left(\frac{RMS\ Average\ by\ posture}{Subject\ RMS\ Average} - 1\right) * 100 = \left(\frac{\left(\sum_{p=1}^{7}\left(\sum_{i=1}^{3} RMS_{i,p}/3\right)\right)/7}{\left(\sum_{c=1}^{3}\left(\left(\sum_{p=1}^{7}\left(\sum_{i=1}^{3} RMS_{i,p,c}/3\right)\right)/7\right)/3\right)} - 1\right) * 100 \tag{11}$$

Better performance in experiment A was quantified by higher S_S and S_D; better performance in experiment B was quantified by higher CR, lower MT, and lower EMG AMP. One-factor ANOVA's were used throughout and Bonferroni post-hoc corrections for multiple

comparisons were used when applicable with a significance level of 0.05. Experimental results report means ± standard error of the mean.

Results

The transformation of EMG signals to joint angle commands for the artificial (or virtual) hand for each MEC was shown as a comparison (Figure 24). The representative plots in Figure 24 depicted the differing logic performed by the three MECs while producing the same outputs. The control sequence for C1 showed a trigger command (vertical gray bar) into the TP state followed by extension, flexion, and extension EMG activity to cause HF, TP, and HF, respectively. The example for C2 showed a trigger command from the HF state into the OP state followed by a flexion and extension EMG activity to move between OP, TP, and OP. A second trigger command changed states from OP back to HF. The example for C3 showed predominately extension EMG activity that drives the hand posture from HF to TP followed by quiescent EMG activity which relaxes the hand posture back to HF.
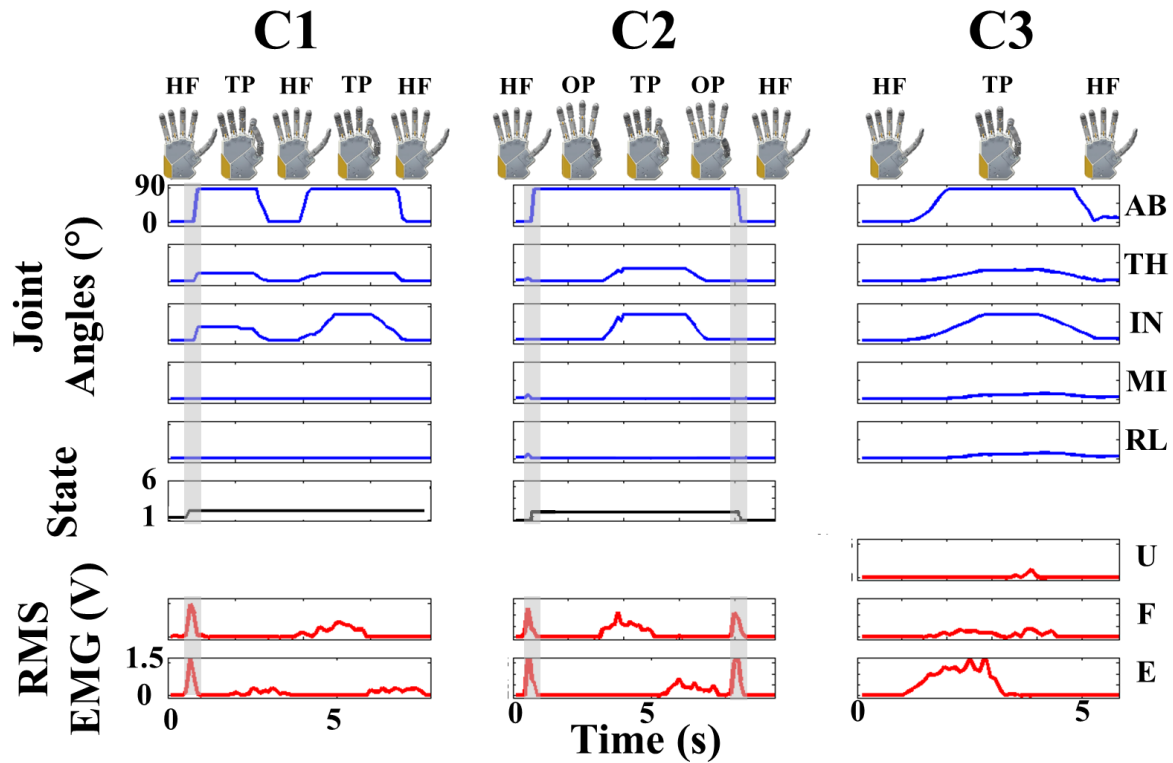
Figure 24 – The transformation of root mean square (RMS) EMG signals (E, F, and U) into five joint angles. The smoothed EMG signal in red from flexor digitorum (F), extensor digitorum (E), and extensor carpi ulnaris (U, only used in C3) showed the muscle activity after filtering and tuning. The joint angle traces from top to bottom for Thumb Abduction (AB), Thumb Flexion (TH), Index Flexion (IN), Middle Flexion (MI), Ring/Little Flexion (RL) in blue corresponded to the hand posture shown including tip prehension (TP), hand flat (HF), and opposition (OP). The state/posture of C1 and C2 (1-6) was depicted by the black trace and the co-contraction trigger signal was highlighted by the vertical gray bar. It should be noted that C3 did not require a trigger signal since the postural control architecture controls the hand posture in a continuous domain without discrete states.

Experiment A

The S_S's for each controller were equal to 38 ± 2.5, 41 ± 1.9, and 45 ± 1.0 for C1, C2, and C3 respectively (Figure 25, left panel). The S_S's were not significantly different across MECs ($p = 0.08$). However, the within subject average S_S ranged from 35 to 48 and was found to be significantly different ($p < 0.05$, not shown). In other words, some subjects were more

proficient at the SHAP than others irrespective of the controller. Therefore, the S_D was the preferred performance metric used since it normalized the S_S to the subject average. The mean S_D's across subjects were equal to -8.0% ± 2.6%, -0.6% ± 1.6%, and 8.6% ± 2.2% for C1, C2, and C3 respectively (Figure 25, right panel). Post-hoc analysis found that the S_D for C3 was significantly greater than both C1 and C2 ($p < 0.001$, $p < 0.05$) thereby suggesting that on average subjects performed the ADL's more proficiently using C3 than C1 or C2.
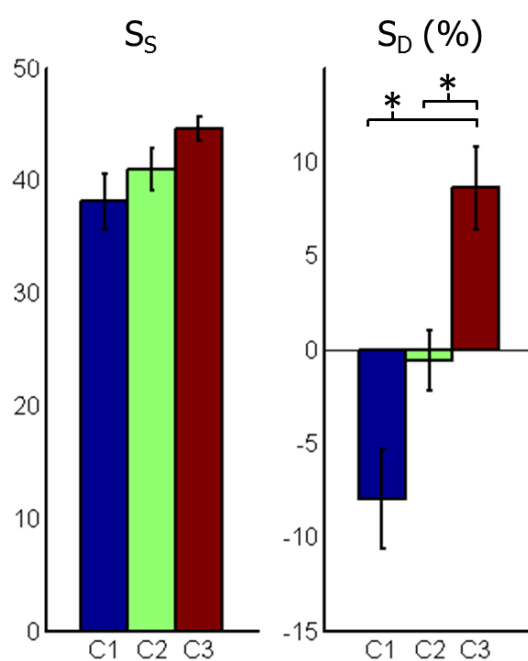
Figure 25 – Experiment A results for each controller. The S_S describes the artificial hand function where 100 equals able-bodied, hand function. The S_D is the percent difference of the S_S of each controller compared to the subject mean. * indicate p-values < 0.05.

Experiment B

The CR's equaled to 97% ± 1.4%, 99% ± 0.3%, and 86% ± 2.9% for C1, C2, and C3 respectively (Figure 26, left panel). Post-hoc analysis found that the CR for C3 was significantly

less than both C1 and C2 ($p < 0.01$, $p < 0.001$ respectively). The MT's equaled 3.9s ± 0.3s, 3.3s ± 0.2s, and 2.7s ± 0.4s for C1, C2, and C3 respectively (Figure 26, middle panel). There was no significant difference between the three controllers ($p = 0.06$), however there was strong trend where the MT decreased from C1 to C2 to C3. The EMG AMP equaled 25% ± 24%, -1% ± 26%, and -24% ± 13% for C1, C2, and C3 respectively (Figure 26, right panel). There was no significant difference between the three controllers ($p = 0.31$), however there was a trend where the EMG AMP decreased from C1 to C2 to C3. To summarize, C3 was the least accurate controller in reproducing the six target postures, however tended to be the fastest and least effortful controller.
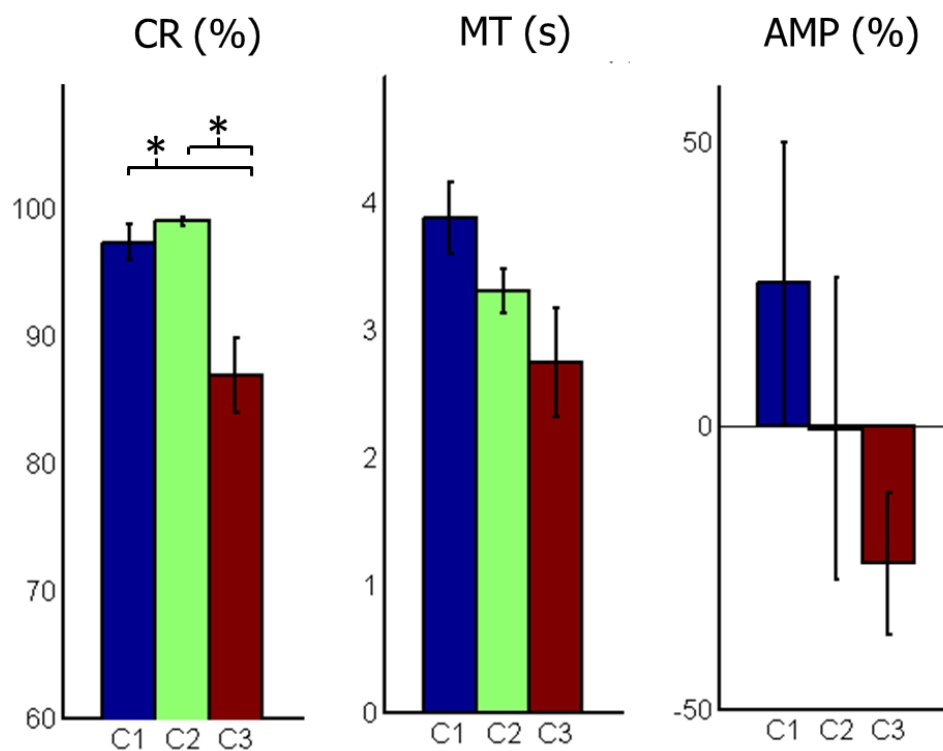
Figure 26 – Experiment B results averaged for each controller. The CR refers to percentage of successful attempts during the virtual hand posture matching task. The MT describes the time to completion during the virtual hand matching task. The EMG AMP is a measure of effort based on the RMS average of the EMG activity and is calculated as the percent difference from the subject average. Positive AMP describes more than average EMG activity. * indicate p-values < 0.05

The same results were sorted by target posture in order to analyze the intricacies of the PC architecture used in C3 (Figure 27). In C3, the target postures that require the activation of a single EMG site (PP, TP, and LP) are considered 1 degree of freedom (DoF) targets. The 2-DoF targets postures (HK, PT, and OP) require the activation of two EMG control sites (i.e. – a co-contraction). All target postures in C1 and C2 are considered 1-DoF since none require co-contraction. The CR for the 1-DoF trials equaled $97\% \pm 1.4\%$, $99\% \pm 0.3\%$, $96\% \pm 2.2\%$ for C1, C2, and C3 respectively. There was no difference in CR between the controllers for the 1-DoF trials ($p = 0.40$). However, the CR for C3 2-DoF trials equaled $78\% \pm 4.2\%$ and was significantly different ($p < 0.001$) than the 1-DoF trials. In other words, the failed attempts when using C3 occurred almost exclusively when the target posture required a co-contraction (a 2-DoF target). The MT for the 1-DoF trials equaled $3.9s \pm 0.3s$, $3.3s \pm 0.2s$, and $1.9s \pm 0.4s$ for C1, C2, and C3 respectively and the MT for the 2-DoF C3 trials equaled $3.8s \pm 0.4s$. The MT for the C3 1-DoF trials was significantly less than the MT for the C1, C2, and C3 2-DoF trials ($p < 0.001$). The EMG AMP for the 1-DoF trials equaled $25\% \pm 24\%$, $-1\% \pm 26\%$, and $-34\% \pm 11\%$ for C1, C2, and C3 respectively, and the EMG AMP for the C3 2-DoF trials equaled $-15\% \pm 15\%$. There was no significant difference between EMG AMP for the 1-DoF or 2-DoF trials ($p = 0.24$) however there was a trend where the EMG AMP decreased from C1 to C2 to C3 2-DoF trials to C3 1-DoF trials. In general, the C3 1-DoF trials were equally accurate, faster, and tended to be less effortful than C1 and C2. On the contrary, the C3 2-DoF trials were less accurate, equally timely, and were equally effortful as C1 and C2.
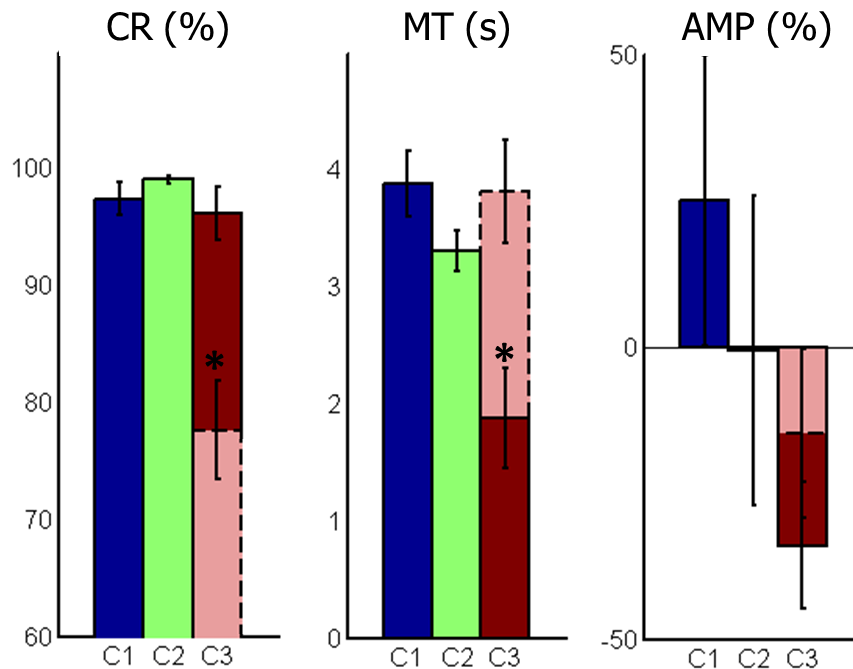
Figure 27 – Experiment B results sorted by target type and controller. Solid outlines indicate 1-DoF targets; dashed outline indicates 2-DoF targets. 2-DoF targets require the activation of two EMG signals (a co-contraction). * indicate p-values < 0.05

Further sorting was performed in order to provide insight into the EMG AMP required to produce the different target postures within each MEC (equation ((11 , Figure 28). It is worth recalling that a zero EMG AMP occurred when the posture required the average EMG activity for the subject. For C1 the EMG AMP monotonically increases from the initial target posture (TP) to the most distant one (OP). This finding is logical since a trigger command is required to sequentially move between states and thereby increases the required effort to reach the more distant target postures. For C2, the EMG AMP is significantly greater ($p < 0.001$) for target postures in the opposition state (OP,TP, and PP) than for the reposition state (PT,HK, and LP). Since the hand posture in experiment A was initialized to the HF state for all trials and MECs, the opposition state in C2 required an extra trigger command (more EMG activity) to switch

from the reposition state. For C3, the EMG AMP is significantly greater ($p < 0.001$) for the 2-DoF target postures (HK, OP, and PT) than for the 1-DoF target postures (PP, TP, and LP). This is a logical finding since modulation of two control sites (a co-contraction) is a more effortful task. While the controllers were equally effortful on average, the effort for each target posture differed significantly within each control architecture.

(a)   (b)   (c)
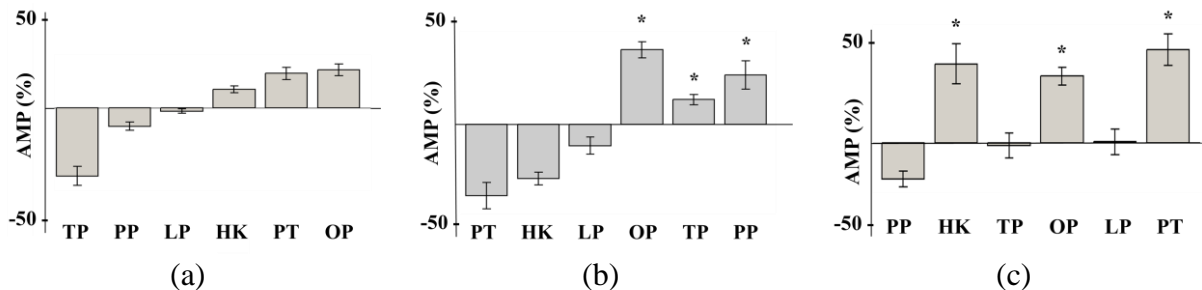
Figure 28 – AMP sorted by posture and controller for a) C1, b) C2, c) C3 where positive EMG AMP refers to postures that require more EMG activity than the subject average and vice versa. Postures are arranged along the x-axis based on the sequence of postures within each controller. * indicate p-values < 0.05.

Discussion

Significantly different results from both the physical and virtual assessment procedures were found. An asset of the present study was that it allowed for comparisons between MECs due to the standardized experimental design where the same interface and hardware was used for all conditions.

In experiment A, C3 was shown to be the best performing architecture as described by S_D (Figure 25). The trigger command used in C1 and C2, but not in C3, inherently retarded the completion of the ADL. Subjects were observed producing the trigger command during the reaching phase of the ADL in order to complete the task as quickly as possible when using C1 and C2. The absence of a trigger command in C3 proved to be advantageous. This finding

supported a similar study in which pattern recognition (without trigger commands) and state machine MECs were compared [93]. Furthermore, the architectures of C1 and C2 required extension EMG activity in order to release an object whereas C3 required quiescent EMG activity (i.e. – minimal activity). These traits resulted from the velocity control scheme in C1 and C2 compared to the position control scheme in C3. A velocity control scheme deciphered EMG activity as a speed and direction of hand movement and therefore quiescent EMG activity equated to no hand movement. EMG activity was necessary to close *and* open the hand. A position control scheme deciphered EMG activity as a position within the architecture. In C3, EMG activity was only necessary to close the hand; the hand opened when quiescent EMG activity was detected. However, the velocity control scheme used in C1 and C2 allowed the user to relax while grasping an object as opposed to in C3 which required continual EMG activity in order to maintain a grasp. This fact could cause fatigue (although not noticed here) and might need to be mitigated with switches or other logic within C3. In general, the need for extension activity in order to release an object in C1 and C2 seemed to slow the completion of the tasks compared to C3.

In experiment B, C3 was the least accurate (lowest CR) controller (Figure 26). We found that the dimensionality of the architectures affected the accurate reproduction of target postures. More specifically, the state machine architectures used in C1 and C2 restricted the subject to a linear arrangement of states, and therefore the posture matching task only required the modulation of one EMG signal at a time. This linear arrangement in C1 and C2 provided a more accurate interface. The PC architecture used in C3 presented the same postures in a planar, two-dimensional arrangement. Thereby, half of the target postures required the modulation of one EMG signal (1-DoF) and half required the modulation of two EMG signals (2-DoF) in order to

reproduce the target posture. The added dimension of the PC architecture in C3 (i.e. the need for co-contractions) negatively affected the CR of the MEC (Figure 27 – left panel). These results supported our previous findings that described a reduction in CR with an increase in dimensionality [87]. We believe that the dimensionality of the MEC is a major determining factor in the ability of a subject to control a prosthetic hand.

The MT metric in experiment B described the same trend seen in the S_S in experiment A (Figure 26). The MT tended to decrease from C1 to C2 to C3 which mirrored the S_S and S_D metrics. Furthermore, the MT for the C3-1DoF trials were significantly faster than the other controllers (Figure 27, middle panel). The similar trend between the S_S and the MT metric was logical since both are time-based metrics. This trend supported the fact that both the physical and virtual assessment protocols limited confounding variables and therefore produced similar result across assessment techniques.

The EMG AMP metric described the relative effort required for each controller/posture. While the controllers required equal effort on average (Figure 26, right panel), the effort for each target posture within each MEC differed significantly and was dependent on the controller architecture (Figure 28). In general, the sequential arrangement of states in C1 caused the closer postures to the initial position to be achieved more easily. Similarly in C2, the postures within the initial state (HF state) were achieved more easily than the postures not in the initial state (OP state). In C3, the EMG AMP metric highlighted the difficulty of commanding the 2-DoF target postures compared to the 1-DoF target postures. It should be noted that the EMG AMP metric was biased by controller architecture. The initial posture/state within each controller was the same for all trials in experiment B to ensure a standardized methodology across controllers. The reordering of states within C1 and/or the rearrangement of postures in the PC domain in C3

would have caused the EMG AMP values to differ for the specific postures. However, we concluded that the general insights still hold for all of the controllers; the effort increased with the number of trigger commands required in C1 and C2 and the 2-DoF postures in C3 required more effort than the 1-DoF postures.

The clinical implementation of the three controllers is feasible today. The EMG acquisition and processing was performed using clinically available hardware and standard processing techniques. Several five motor prosthetic hands are available today [10], and six motor devices are becoming available [20]. A clinical consideration when implementing the state-machine architectures (C1 and C2) is the design of the trigger signal. This work implemented the same trigger design as [67] for both C1 and C2, however more complex trigger designs including hold open, double impulse, and/or triple impulse are clinically available [20]. In general, the trigger design must balance the ease of use for the subject with the reliability of the trigger signal. Subject over-exertion and/or false triggers should be minimized in order to maintain a high quality control interface when using state-machine architectures. A clinical consideration when implementing the PC architecture (C3) is the availability of three independent surface EMG sites on the residual limb of persons with transradial amputation. Three control sites are preferable to two in order to span the entire PC domain using a radial mapping of EMG signals in the PC domain. Previous work by the authors [87] discussed two, three, and four-site EMG control interfaces using different maps in the PC domain. Anecdotally, the authors have found that three independent sites can be found on the residual limbs of both subjects with congenital limb loss and trauma-induced limb deficiency [76]. However, the two-site system used for both C1 and C2 is advantageous since it reduces cost of the prosthesis system compared to the three site-system required for C3.

The limitations of this work include the use of a left-handed prosthesis, the lack of training time, the lack of subjects with transradial amputation and the disregard for pattern recognition MECs. The experiments were performed using the left limb of the subjects due to the handedness of the physical prosthesis even though all seven subjects were right handed. We believe that the ability of subjects to use these MECs would change with additional training time, but that these results are robust to additional training and still describe the clear differences in MEC architectures. In the future, the authors plan to further test the PC architecture implemented in C3 within a population of persons with amputation. We did not test a pattern recognition based MEC in this work since we are not aware of an algorithm that can classify seven hand postures reliably during a clinically focused test like the SHAP. A surprising development from this work was the advantage to using a position control scheme as opposed to a velocity control scheme in the postural control architecture. In Chapter 4, the opposite preference was described when the PC scheme was used in a virtual center-out target acquisition task. In other words, the optimal parameters within the PC architecture are task-dependent; velocity control schemes are beneficial for target acquisition tasks (which do not require a 'release' action) while position control schemes are beneficial for physical tasks including object manipulation and other ADLs.

Here the postural controller was shown to be a valuable alternative to the state of the art finite state machine architecture for clinically viable MECs using virtual and physical assessment techniques with standardized protocols. Nonetheless, the remaining challenge in order to fully answer the overarching hypothesis is to prove clinical efficacy of the postural controller with persons with transradial limb loss. Able-limbed subjects were always used previously in order to simplify the experimental protocols. Now, the clinical complications like subject specific

musculature, lack of neural control, etc. must be overcome. Chapter 6 describes the process of

addressing and overcoming these complications.

Chapter 6 - Functional Assessment of Persons with Transradial Limb Loss Using a Myoelectric Postural Controller and Multi-functional Prosthetic Hand[10]

Introduction

The field of upper limb prosthetic design and control focuses on producing clinically relevant systems for use by persons with transradial amputation. However, the development of many prosthetic hand systems takes place using virtual environments and able-bodied people as experimental subjects like in Chapters 3-5 and [44], [45], [87]. Virtual environments simplify the experimental protocol by removing the need for physical devices like multi-functional prosthetic hands while still allowing in-depth study of the myoelectric interface [48], [67]. Able-bodied subjects ensure that the subject physiology is similar across subjects and are far more numerous than persons with transradial amputation. For these reasons among others, much of the studies in the field of upper limb prosthetic design and control avoid performing functional assessments of persons with limb loss while performing activities of daily living. However, here a functional assessment of persons with transradial limb loss using the postural controller to perform activities of daily living is first accomplished.

There are numerous challenges when investigating prosthetic systems using this type of experimental paradigm. The residual limb physiology is unique to each person and is dependent on the type of limb loss (amputation or congenital limb absence). During an amputation, the goal is to maintain as much limb length as possible and to conserve as much musculature as possible [15]. Various surgical techniques are used to achieve this goal. Myoplasty, connecting

---

[10] Intended publication with *Myoelectric Controls Symposium,* submitted March 2014 with co-authors Stephen Huddle, M.S. and Richard F. *ff.* Weir, Ph.D.

antagonist-agonist muscle groups at the distal end of the residual limb, and myodesis, connecting the muscle directly to the bone, can occur in unique ways depending on the amputation and thereby severely alter the amputation physiology compared to intact physiology [15]. The residual limb physiology for a person with congenital limb absence is unique to the person and dependent on the amount of in-utereo development.

Another challenge when implementing prosthetic systems on persons with transradial amputation is the weight of the system on the residual limb. The load on the residual limb is amplified due to a longer moment arm between the weight of the prosthesis and the limb in persons with limb loss. In result, greater muscular activity is required to suspend the load of the prosthesis off of the residual limb. The same musculature that stabilizes the limb is targeted by the MEC and thereby confounds the MEC's ability to decipher user intent. More generally, the reduction of weight of the prosthetic system is the number one concern for users of multi-functional prosthetic hands [9]. Finally, the recruitment of persons with transradial amputation is not a trivial task. For example, the Veteran Affairs Eastern Colorado Health Care System follows only 14 persons with transradial limb loss in all of Denver, Colorado[11]. Fortunately, there are only approximately 41,000 persons with major upper limb loss in the United States in 2005 [31]. In other words, only 0.01% of the U.S. population is available for subject recruitment. When these challenges are overcome, the functional assessment provides a more in-depth understanding to the true efficacy of the prosthetic system.

Here the postural controller developed in Chapters 4-6 was tested in order to determine if it was an effective method to control a multi-functional prosthesis for persons with trans-radial

---

[11] As described by email correspondence with Dr. Ryan Stephenson, Physical Medicine and Rehabilitation, Denver Veterans Affairs Medical Center

limb loss. Persons with transradial amputation or congenital limb absence performed the Southampton Hand Assessment Procedure (SHAP) using a multi-functional prosthetic hand with a postural controller. Able-bodied persons performed the same procedure using the identical hardware/software in order to provide a comparison. The aim of this study is to provide evidence of the efficacy of the postural controller for use with persons with trans-radial amputation or limb deficiency.

Methods

Prosthetic device

In order to implement the postural controller, the prosthetic hand required at least six DoA including an actuated thumb abduction joint. The Bebionic hand (RSL Steeper Inc., United Kingdom) was a commercially available five DoA, multi-functional prosthesis with a manually positioned thumb abduction joint (Figure 29a). This hand was modified into a six DoA device for this work by adding an actuator to adduct the thumb (Figure 29b). Both right and left handed devices were developed (Figure 29c). A 10mm DC motor, 1.75:1 spur gear train, and 256:1 planetary gearhead (MicroMo, Inc., Clearwater, FL) was embedded into the palm as shown in Figure 29b. The adduction drive allowed for 90° of rotation about the thumb axis and thereby could position the thumb in a hand flat and opposed positions. This function ensured that all functional grasps could be fully actuated using the postural controller including opposed grasps (tip prehension, palmar prehension) and lateral grasps (lateral prehension, hook, pointer).

(a)

(b)

(c)
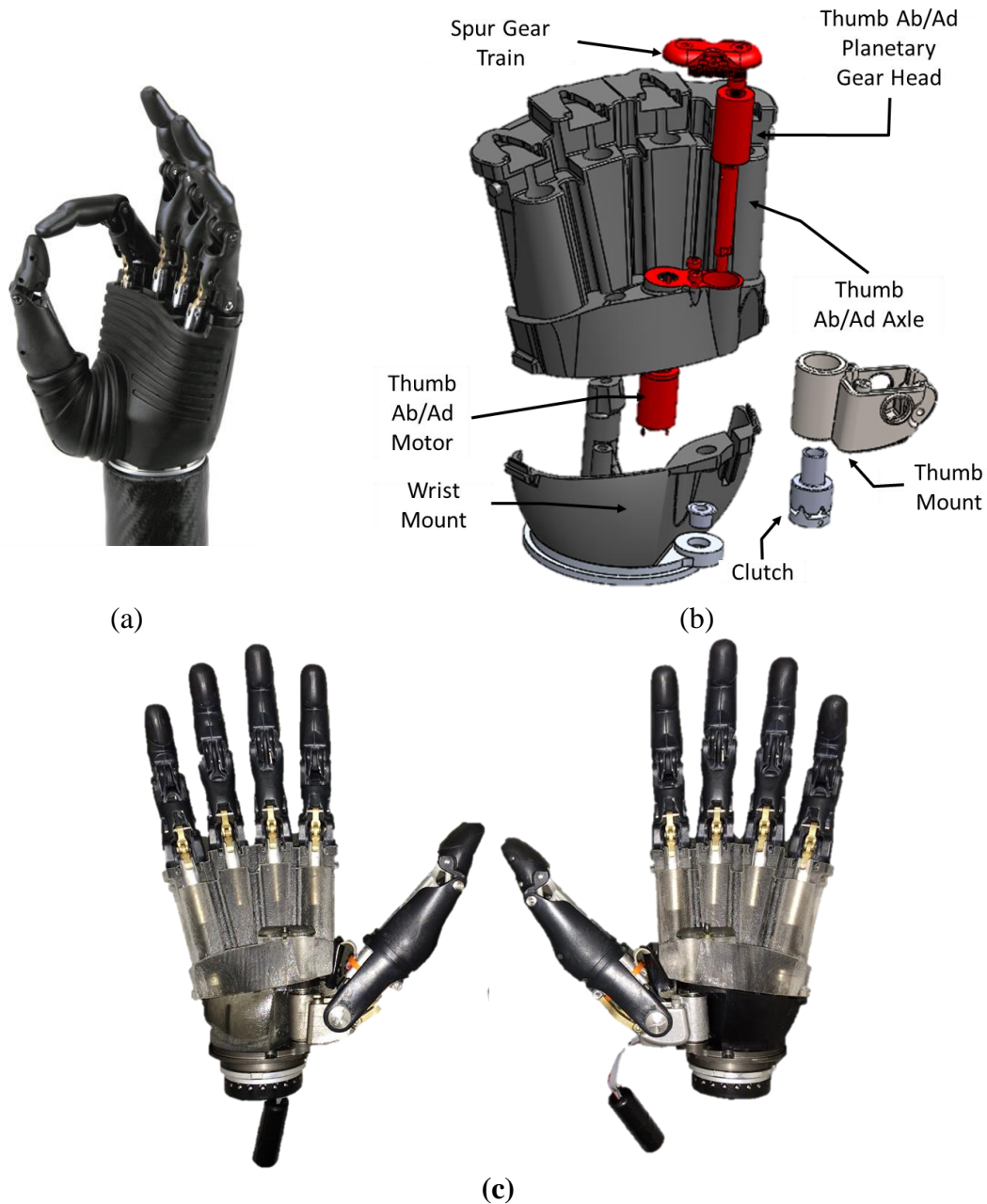
Figure 29 – (a) The Bebionic v2 by RSL Steeper, U.K. with five degrees of actuation. (b) A sixth degree of actuation was added in order to automate the positioning of the thumb ab/adduction. The actuator including motor, transmission, and clutch were embedded into the palm as shown in red. (c) Photos of the right and left hand configurations of the modified six degree of freedom Bebionic hand.

The electronics in the original Bebionic hand were replaced with a custom motor controller system (Sigenics Inc., Chicago, IL). The motor controller system included a controller

board and six satellite boards referred to as *penny boards*. The controller board consisted of an off-the-shelf Arduino microcontroller system (SparkFun Electronics, Inc., Boulder, CO) that translated serial communications from the USB connected personal computer to I2C commands for the penny boards. Each penny board was connected across a four-wire I2C bus and was each associated with an actuator. The penny board controlled the power provided to each actuator and deciphered the encoder information provided by each actuator. (The thumb abduction actuator did not include an encoder.)

For subjects with limb-loss, a temporary socket was built to mount the prosthesis to the residual limb (Figure 30). Bipolar electrodes (Motion Control Inc., Salt Lake City, UT) were placed on the skin, covered with cotton padding, and then wrapped with fiberglass casting tape (Ossur, Inc. Iceland). A modified quick disconnect wrist socket (Ottobock, Inc., Plymouth, MN) with laser-cut plastic struts was anchored to the residual limb by embedding the struts into the cast. The prosthesis was then mounted to the wrist socket which allowed for the subject to passively rotate the hand during the experiment. For able-bodied participants, a splint was built to mount the prosthesis distal to the physiological hand. The splint was strapped to the forearm of the participant distal to the surface electrodes. A handle was adjusted so that the wrist remained in a neutral posture. A modified quick disconnect wrist socket was anchored to the splint using metal struts.
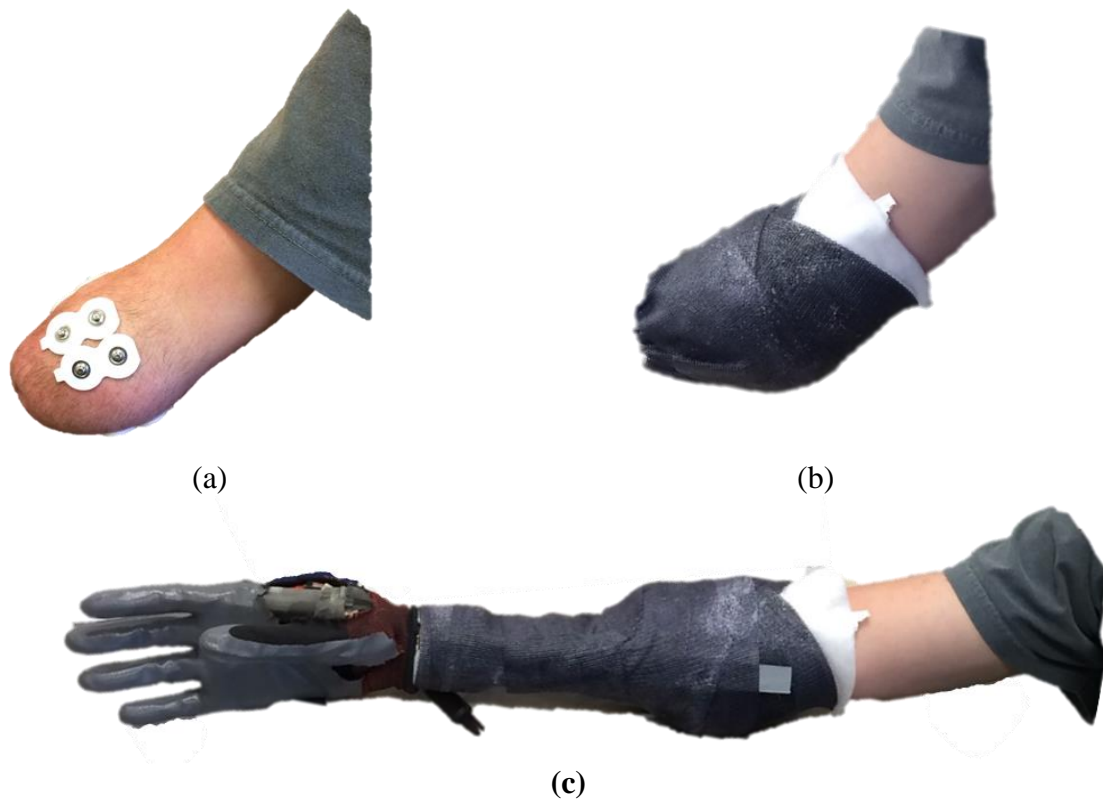
Figure 30 – (a) The residual limb of person with congenital limb loss. Three surface electrodes are placed on the limb (the third is not visible in image). (b) A temporary cast was formed around the residual limb. (c) The prosthesis is mounted to the temporary cast in a physiologically appropriate manner**.**

Postural controller

The postural controller was embedded into a custom LabVIEW program that communicated with the modified Bebionic hand. The custom LabVIEW program sent and received commands through the USB serial connection to and from the controller board. The program was responsible for the position control feedback loop including the desired position derived by the postural control algorithm, the measured position provided by the motor encoders, and the feedback loop gains for each actuator. The program performed the postural control algorithm including EMG processing and then communicated with all six actuators in series in

120ms. This update rate is sufficient for the control of myoelectric devices as determined by Farrell and Weir [53].

The program implemented was identical to the system described in Chapter 5 with a few exceptions including a dynamic EMG tuning algorithm and an optional two-site PC domain map. The dynamic EMG tuning algorithm was implemented in order to ensure stable grasps even in the presence of co-activity across the three EMG control sites. This algorithm implemented a 'first-on' principal in the postural control domain. When the cursor crossed the dynamic EMG threshold radius, the gains on the EMG signals (G_F, G_E, and G_U) were modulated as shown by PC domain map in Figure 31. When the cursor was within the green area, the EMG gains equated to the original gain (G_{Fo}, G_{Eo}, and G_{Uo}) for each EMG control signal. When the cursor was in the blue, red, and gray areas, the gains were adjusted so that only the local EMG signal was 'on'. The gains on the other two EMG control signals were set to zero in order to ignore any co-activity during the grasp. In effect, the dynamic EMG tuning algorithm implemented a 'first-on' principal to the PC domain where only the greatest EMG signal ('first-on') was utilized while the others are ignored.
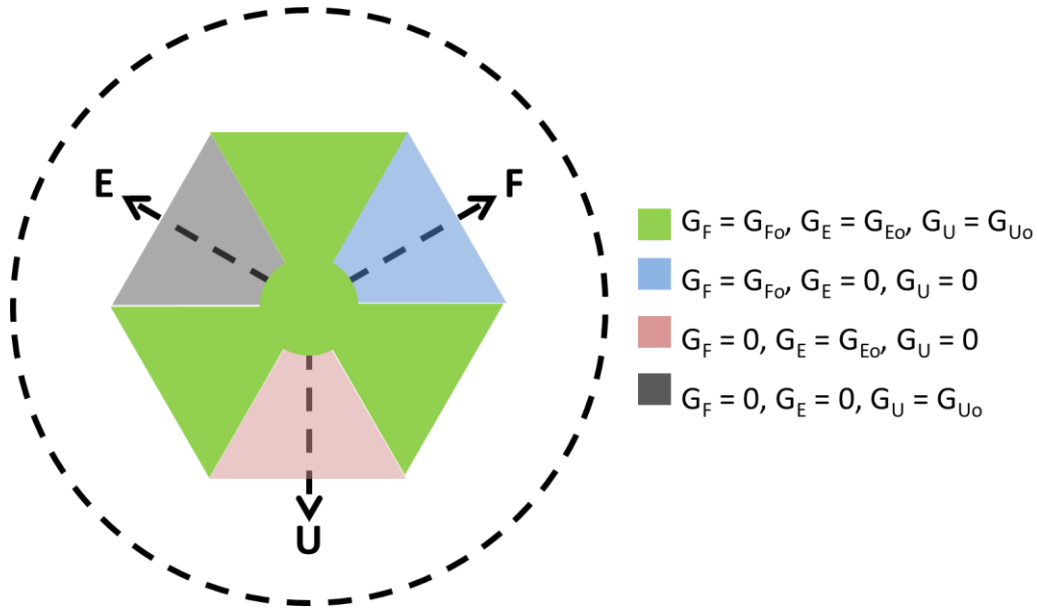
Figure 31 – Dynamic EMG tuning map in the PC domain. The EMG gains (G_I where *i* is the EMG signal) are determined by the location of the cursor in the PC domain. G*i*o refers to the original EMG gain value for the *ith* EMG signal.

In response to the various residual limb physiologies of the subjects, a two-site PC domain was designed. In some cases (two out of four subjects with limb loss), the residual limb physiology did not allow for the user to produce three independent EMG control sites; two independent EMG control sites were always available. The 2-site PC domain map required only the wrist flexion (F) and extension (E) EMG control sites (Figure 32). Only four functional postures were available to the user (palmar prehension, tip prehension, lateral prehension, and opposition) instead of the original seven. These grasps were chosen in order to provide the most necessary grasps for activities of daily living [16] and thereby the most necessary for the SHAP. Also, the opposition posture was located on the origin of the PC domain (as opposed to hand flat) in order to allow subjects to better align the thumb with the object being grasped.

<div align="center">(a)   (b)</div>
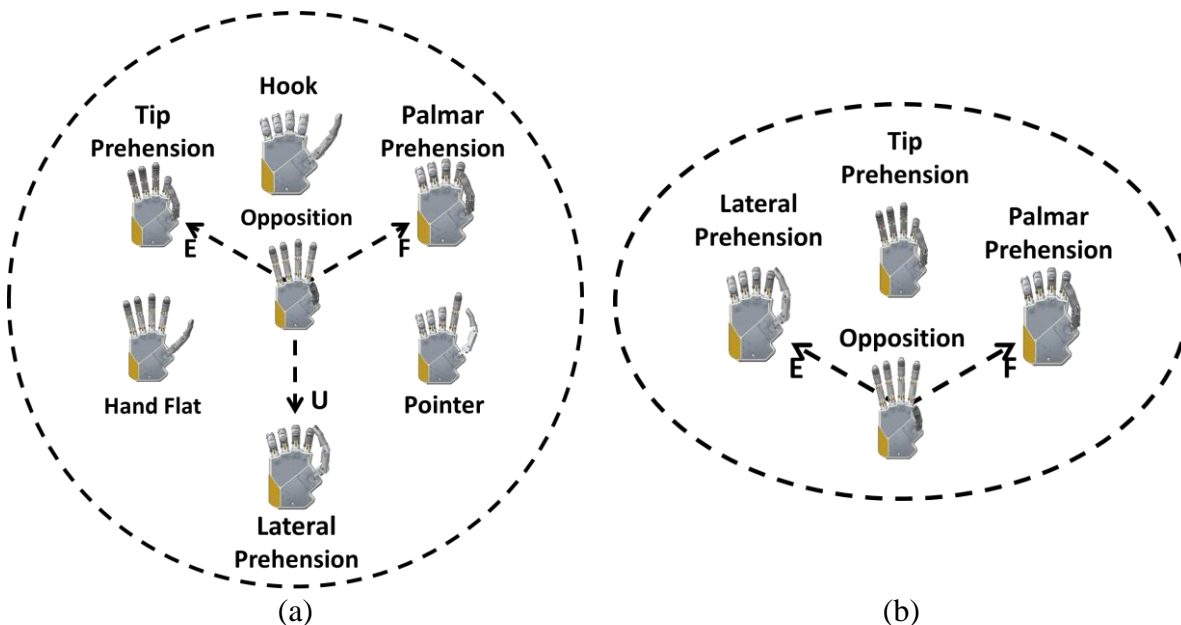
Figure 32 – Postural control maps. 3-site maps (a) were used by subjects A1,A4, and all able bodied subjects (S1-S4). 2-site maps were used by subjects A2 and A3.

Southampton Hand Assessment Procedure

The Southampton Hand Assessment Procedure (SHAP) is a standardized hand assessment procedure that measures the hand function relative to intact individuals using their intact limb by measuring the time-to-completion of 26 activities of daily living (ADLs) which span the functional grasps [18]. This protocol was shown to be reliable and validated so that results from independent investigators can be compared. The SHAP includes exact equipment and instructions for each of the tasks including the manipulation of abstract object tasks (moving cylinders, spheres, tabs, etc.) and ADLs (turning a door handle, picking up coins, moving containers, etc.) The tasks were performed as quickly as possible and were self-timed by the subject.

Participant details

Four persons with transradial limb loss (AMP, 3 men, 1 woman; age 44 years ± 16years, 1 with traumatic limb amputation, 3 with congenital limb absence) and four able-bodied control participants (ABLE, 3 men, 1 woman; age 34 years ± 3.9years) completed the experiment at the University of Colorado at Boulder. The University of Colorado at Boulder institutional review board approved the study, and written informed consent was obtained from all participants. The type of limb loss, affected side, length of residual limb, years with limb loss, typical type of prosthesis, and the number of control sites used during the experiment for each subject with limb loss are detailed in Table 7. The number of control sites used by the able-bodied control participants was always three and were placed on the skin over flexor digitorum, exetensor digitorum, and extensor carpi ulnaris. The number of control sites used by the persons with limb-loss was determined by empirically measuring the number of independent EMG signals prior to starting the SHAP. The control sites were localized based on normal anatomical locations and palpation of the limb.

Table 7 –Persons with limb loss subject specific details

Subject	Type of Limb Loss	Affected Side	Length of Residual Limb	Years with Limb Loss	Typical Type of Prosthesis	Number of Control Sites
A1	Amputation	Left	4" below elbow	43 years	Body-powered prehensor	3
A2	Congenital limb absence	Right	2" below elbow	34 years	Body-powered hook	2
A3	Congenital limb absence	Right	4" below elbow	51 years	None	2
A4	Congenital limb absence	Left	8"	27 years	Cosmetic	3

Performance Metrics

The *SHAP Score* (S_S) described the subject performance during the SHAP over all tasks (also referred to as the Index of Functionality [18]). The S_S was an integer between zero and 100 where a score of 100 correspo   nds to normal, able-bodied hand function while a score of zero corresponds to no hand function. The *functionality profile* (FP) scores described the subject performance during the SHAP specific to six functional grasps (spherical, power, tip, tripod, lateral, and extension) and used the same scale as the S_S. The FP provided detail on the performance of the subject when using specific grasps during the SHAP. Pair-wise t-tests and one-factor analysis of variances with Bonferroni corrected post-hoc analysis were used when

appropriate. Statistical tests were performed using a p-value of 0.05 and error bars represent standard error.

Results

Subject population comparison

The S_S equaled 56±1.0 and 55±1.8 on average for the subjects with limb loss and able-bodied subjects respectively. The S_S and FP for the subjects with limb loss were statistically equal to the able-bodied subjects (p's > 0.05, Figure 33). This result indicated that the modified Bebionic hand with postural controller restored approximately 55% of typical hand function. The FP scores ranged between 22 to 82. The whole hand grasp scores (67 ± 2.7 for spherical, power, and extension) produced significantly greater FP scores (p < 0.001) than the precision grasps (39 ± 3.5 for lateral, tripod, and tip) indicating the greater utility of the prosthetic system to manipulate larger, whole hand objects. The equal performance between populations indicated that the postural controller overcame the clinical challenges of persons with limb loss and was an effective control algorithm for myoelectric prosthetic hands.
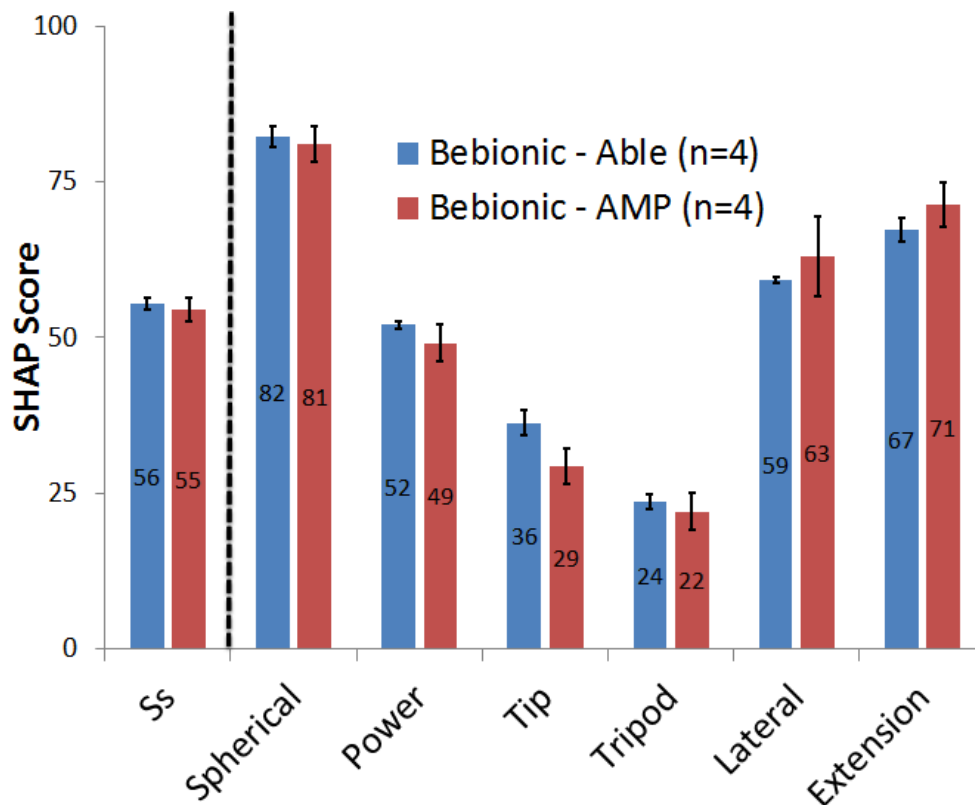
Figure 33 –The SHAP scores and functionality profile scores for subjects with limb loss (AMP) and able-bodied subjects (ABLE) when using the postural controller. All scores were statistically equal between two populations ($p > 0.05$).

Controller comparison

As a supplement to Chapter 5, the able-bodied subjects completed the SHAP using the same three MECs (C1, C2, and C3) with the modified Bebionic hand as opposed to the Azzurra robotic hand. The trend for the S_S across controllers was similar for both hands; the S_S for the Azzurra hand are reproduced from Chapter 5 (Figure 34). The S_S tended to increase from C1 to C2 to C3 (including C3 for persons with limb loss). In other words, the relative performance of the three controllers was robust to two different experimental apparatuses. However, the S_S when using the Bebionic hand ranged from 48 to 56 whereas the S_S for the Azzurra hand ranged

from 38 to 45. Independent of the controller, the S_S produced when using the Bebionic hand were greater than the Azzurra.

Also by deduction, this trend suggests that the C3 would perform better then C1 and C2 for persons with limb loss as well (even though no persons with limb loss were tested using C1 or C2 due to lack of available subjects). Hence, the postural controller may be a more effective and clinically robust interface compared to state of the art systems in the commercial (C1) and research (C2) realms for persons with transradial limb loss.
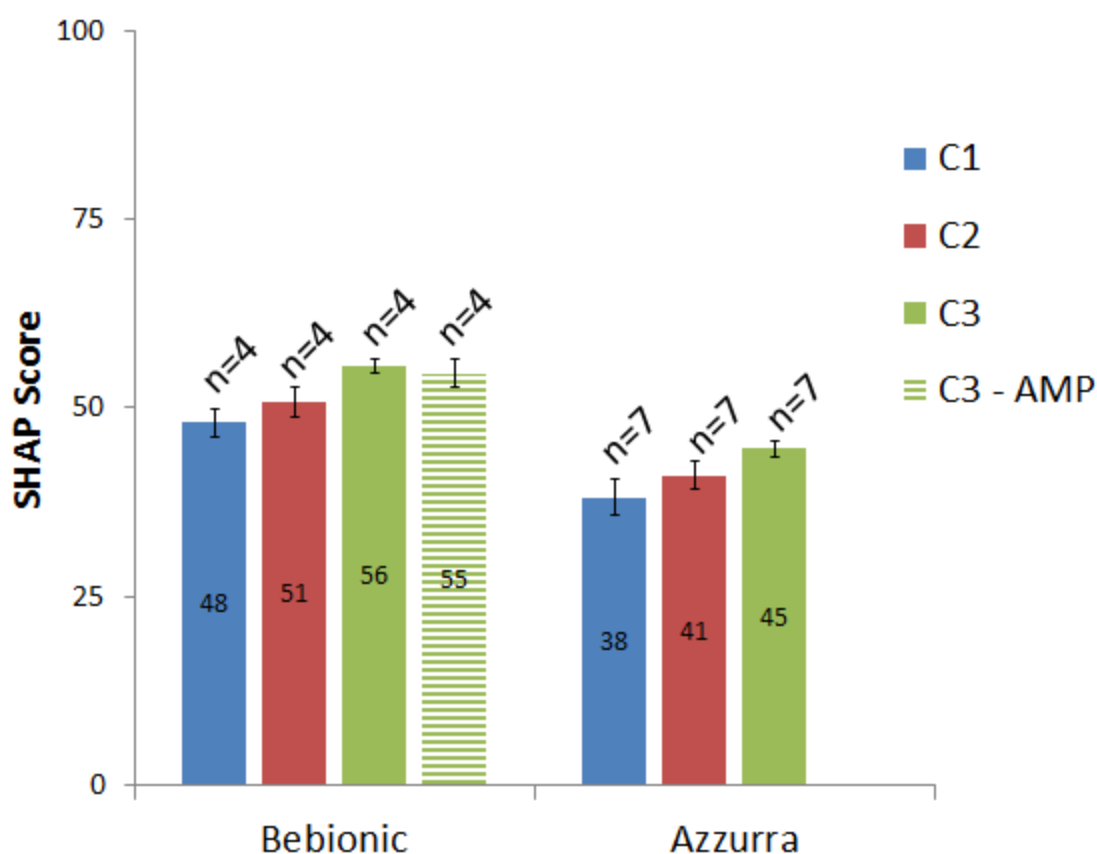
Figure 34 – The SHAP scores for the modified Bebionic and Azzurra hands for each myoelectric controller. The Azzurra SHAP scores are reproduced here from Chapter 5. The increasing SHAP score from C1 to C2 to C3 was similar across hands.

Prosthetic hand comparison

In order to further study the differences between the two prosthetic hands, S_S and FP scores across all controllers were averaged (Figure 35). The averaged S_S and FP scores emphasized the ways in which the hand (i.e. – hardware) affected the ability of subjects to perform activities of daily living independent of the MECs (i.e. – software). The S_S for the Bebionic hand (52 ± 1.1) was significantly greater ($p < 0.001$) than the S_S for the Azzurra hand (41 ± 1.2). Also, several grasps in the FP were significantly different (power, tip, and lateral prehension with $p < 0.001$, $p = 0.001$, and $p < 0.001$ respectively). The differences in the S_S and FP scores between hands indicate that the mechanical design of the prosthetic hand affected the ability of the subjects to perform activities of daily living.
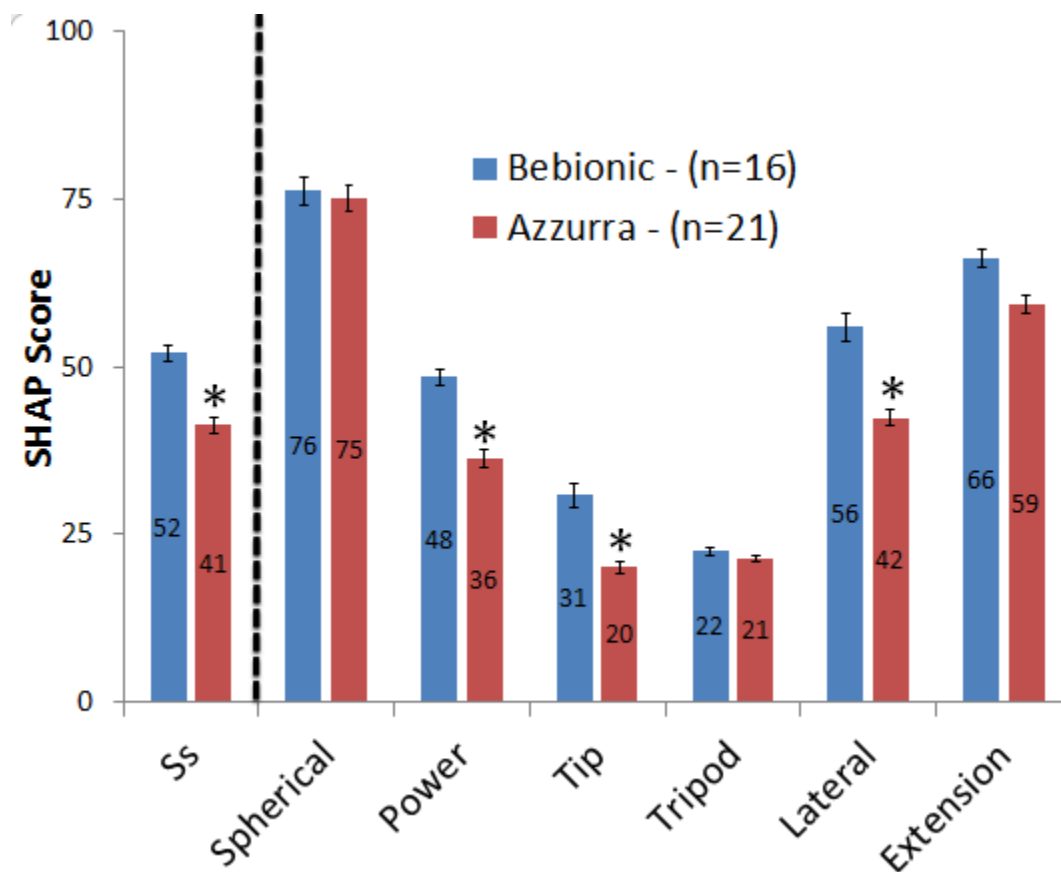
Figure 35 – The average SHAP and functionality profile scores for the modified Bebionic and Azzurra hands averaged across all controllers. The SHAP score and several functionality profile scores were significantly different indicating that the mechanical design of the hand affected the ability of subjects to perform the SHAP test.

The SHAP protocol ensured that independent experimental results could be compared. Table 8 compared S_S and FP scores from two independent studies [54], [67] and the work described here. The VMG & MMC hand was a three degree of actuation prosthetic hand with the Vanderbilt state machine control system (the motivation for C2) and outperformed the other prosthetic systems. The DMC was a 1 degree of actuation prehensor from Otto Bock Inc. The i-LIMB is a five degree of actuation prosthetic hand which uses a state machine control system (the motivation for C1). The S_S and FP for the Azzurra hand with postural controller (reproduced from Aim 3) and the modified Bebionic hand with postural controller are most

similar to the i-LIMB results. In general, the whole hand grasps (spherical, power, and extension) produced higher scores than the precision grasps (tip, tripod, and lateral) as observed previously with the modified Bebionic hand.

Table 8 – SHAP scores and functionality profiles for various prosthetic hands and control systems. The standardized protocol demanded by the SHAP allows for robust comparisons of SHAP results across independent studies.

Functionality Profile	VMG & MMC (n=1)	DMC (n=1)	i-LIMB (n=1)	Azzurra & Postural Controller (n=7)	Bebionic & Postural Controller (n=8)
S_S	81	74	52	45±1.0	55±1.0
Spherical	87	90	90	81±1.9	82±1.3
Power	85	75	51	40±0.8	51±1.2
Tip	59	39	42	19±2.3	33±2.6
Tripod	71	76	32	23±0.5	23±1.3
Lateral	88	69	23	46±1.0	61±2.4
Extension	89	81	55	63±2.5	69±1.6

Discussion

This chapter asked whether the postural controller was an effective method to control a multi-functional prosthesis for persons with trans-radial limb loss. The postural controller was easily learned by the subjects (less than 10 minutes of practice before performing the beginning the SHAP) and it was robust to the varied residual limb physiology of the 4 subjects with limb loss. Also, it was possible to tune the postural controller so that the limb position effects and dynamic motion effects including co-activity among EMG control sites were overcome. The results indicated that 55% of typical hand function was restored using the modified Bebionic

hand with postural controller for persons with trans-radial limb loss as shown by the S_S metric. The ability of the subjects with limb-loss to complete 26 activities of daily living within a single experimental session was an existence proof of the efficacy of the postural control as a myoelectric control system for persons with transradial limb loss.

The fact that the S_S and FP for persons with limb loss were statistically equal to able-bodied subjects (Figure 33) indicated that the postural controller was robust to differences in the residual limb physiology. Many experimental factors were inherently different among the two subject populations including the placement of EMG control sites on the residual limb, the neural control of the residual limb musculature, and the mounting of the prosthesis with the quick-fit socket. The placement of EMG sites on the residual limb varied among all subjects with limb loss. As opposed to able-limbed subjects, those sites were identified by palpating the residual limb since the residual limb physiology was unfamiliar especially for subjects with congenital limb loss. The neural control of the residual limb musculature was especially interesting for subjects with congenital limb loss since the hand never existed. They described a variety of strategies including imagining wrist flexion/extension, pronation/supination, pressing against points within the socket, etc. These strategies were developed by the subjects as they became accustomed to the postural control interface and were beneficial in their ability to control the prosthesis. The temporary socket was not completely self-suspending and thereby the weight of the prosthesis was loaded onto the residual limb. The mechanical loading of the residual limb changed the EMG signals by pressing or lifting the socket away from the surface electrodes, however the postural controller proved to be robust to these affects. Here, we found that the postural controller withstood the inherent differences among persons with limb-loss compared to able-bodied persons.

The trend of increasing S_S when using C1 to C2 to C3 from Aim 3 was reproduced using different hardware. This reproduction further corroborates the results found in Aim 3. The increase in absolute value of the S_S when using the Bebionic hand irrespective of the controller further indicated that the S_S was influenced by both the controller and mechanical device. When averaged over all the controllers used, the S_S for the Bebionic hand was greater than the S_S for the Azzurra hand (Figure 35). The mechanical design of the hands had a substantial effect on the S_S and FP. The Bebionic digits are actuated using a linear ball screw and rigid body kinematic linkage system whereas the Azzurra digits are actuated using a linear ball screw and cable-pulley system. The mechanical performance of the hand (i.e. – grip strength, reliability, back-drivability, etc.) was dependent on the efficiency of the actuation systems implemented (for more details see review paper by the authors [10]). Several grasps especially benefitted from the mechanical design of the Bebionic hand (power, tip, and lateral, Figure 35). During tip and lateral prehension, only one actuator/digit produces the force on an object as opposed to five actuators/digits. The drive system in the Bebionic significantly improved the ability of the subjects to perform these grasps as compared to the Azzurra.

Table 8 indicated that the S_S and FP when using the postural controller were similar to previously published SHAP results using the commercially available i-LIMB hand. However, the S_S and FP of the Vanderbilt Multigrasp (VMG) hand with Multigrasp Myoelectric Controller (MMC) overwhelmed the scores when using the postural controller. The previous literature cited referred to a single subject experiment (n=1) whereas the postural controller scores were averaged over seven and eight subjects (n = 7 and 8). It should be noted that the mechanical device used in all the SHAP results listed were different (the VMG hand, DMC hand, i-LIMB

hand, Azzurra hand, and modified Bebionic hand). The S_S and FP when using the postural controller would hopefully increase when using a more effective device like the VMG hand.

The major design adjustment in this work to the postural controller was the implementation of a 2-site PC domain map (Figure 32). Previously, the authors found that three independent control sites could be found on trans-radial amputees [76]. However, the limb length and residual limb musculature for several subjects with limb loss (A2 and A3) did not allow for three independent sites. We noticed a high level of co-activity in the residual limbs of A2 and A3 when suspending the prosthesis and/or manipulating objects. Therefore, the 2-site PC domain map was beneficial since it ignored the co-activity of the third control site and provided a simpler control interface. The disadvantage of the 2-site PC domain map was the decrease in hand postures available to the subject. The ability of the postural controller to adjust to clinical considerations like the number of independent control sites makes the system even more clinically applicable.

Conclusion

Here the clinical efficacy of the postural control system was tested using a modified Bebionic hand with persons with limb loss. The results provide an existence proof that the postural controller is an effective myoelectric control interface for persons with trans-radial limb loss. The real world experimental demands of the SHAP ensured that the control system would be challenged. The SHAP score and functionality profile were equivalent between the subjects with limb-loss and able-bodied subjects. This result indicated that the postural controller was robust to the musculature, neural control, and residual limb size of persons with trans-radial limb loss. Additionally, previously studied state machine control systems were compared to the

postural controller and the modified Bebionic hand was compared to the previously utilized Azzurra hand. Therefore, the overarching hypothesis that postural control systems provide a more effective and clinically robust interface compare to the state-of-the-art systems in the commercial and research realms for persons with transradial limb loss has been verified.

<u>Chapter 7 - Conclusions</u>

This dissertation describes the development of a myoelectric prosthetic hand controller across four aims. The MEC design progressed using typical techniques like brainstorming, prototyping, testing, analyzing, and iterating upon the design. This process occurred throughout each aim and is summarized below.

Specific Aim 1: Based upon the work of Santello et al. [11], a two-dimensional domain was developed using a principal component analysis of human grasping. EMG control signals were mapped onto this domain in various orientations. The mappings used two, three, or four EMG signals and were tested by 10 able-bodied subjects during a virtual hand posture matching experiment. The preferred map used only two EMG control signals and was oriented similarly to the distribution of the postures within the domain as shown by Santello et al. The findings from this aim motivated the design of a customizable two-dimensional domain with functional grasps deliberately positioned with respect to the EMG control signals.

Specific Aim 2: Here we designed and tested a novel postural control algorithm. The algorithm was motivated by the findings of Aim 1 and included a customizable two-dimensional domain, the postural control (PC) domain, with functional grasps deliberately positioned with respect to the EMG control signals. New features in the postural control algorithm were developed here including the position and velocity cursor control schemes and gravity wells. Experiments were conducted using able-bodied subjects using a virtual hand interface. Several parameters of the algorithm were decided upon empirically including the preferred number of surface electrodes (three) and cursor control scheme (velocity control for center-out target acquisition tasks). Also the ability to learn the controller system was shown to take only a single one-hour training session. The findings from this aim identified certain design parameters

(number of electrodes, cursor control scheme, amount of training) and provided encouraging results with respect to the clinical efficacy of the postural control scheme.

Specific Aim 3: Here the postural control scheme was first implemented on a physical device and compared to other state-of-the-art myoelectric control schemes. The postural controller used the preferred design parameters as determined by Aim 2. The experimental protocol entailed able-bodied subjects using the Azzurra IH2 robotic hand to perform the Southampton Hand Assessment Procedure (SHAP). Three experimental sessions took place where a different myoelectric controller (i.e. – software) was used with the same experimental apparatus (i.e. – hardware) thereby allowing for direct comparisons between the controllers. Also, a virtual hand posture matching exercise was performed. The results showed that the postural control scheme was advantageous compared to the other controllers during activities of daily living, but was less adept during virtual hand matching exercises. Again, these findings were encouraging in that they indicated the utility of the postural controller to control a prosthetic hand in real time and manipulate objects successfully.

Specific Aim 4: Here the postural control scheme was used by persons with limb loss for the first time. A functional assessment was performed by persons with limb loss using a modified Bebionic hand and the SHAP. Able-bodied subjects performed the same experiment for comparison. The results substantiate several initial assumptions about the ability of persons with limb loss to use the postural control scheme. Without training, persons with limb loss were able to control the prosthesis and perform activities of daily living to the same ability of able-bodied persons using the identical prosthesis. In other words, the postural controller is robust to differences in musculature, neural control, and limb size between able-bodied and persons with limb loss. Also, by deduction, it was found that the postural controller would perform better than

the state of the art MECs in the commercial and research realms by persons with transradial limb loss. Therefore, the overarching hypothesis that postural control systems provide a more effective and clinically robust interface has been verified.

This work was fundamentally a design project. The technology itself was being developed in parallel with the experiments performed in Specific Aims 1-4. In result, various aspects of the postural controller were modified, revised, and revisited in order to adapt the design to the new experiences and data. The most noticeable example of this process should be highlighted. The preference for a position cursor control scheme as opposed to a velocity control scheme during activities of daily living was found in Specific Aims 3 and 4. This preference disagrees with the finding from Specific Aim 2 that the velocity control scheme was preferred during a center-out target acquisition task. This apparent discrepancy informs the design of the postural controller by highlighting the fact that the preferred cursor control scheme is task dependent. Tasks within a virtual environment like in Specific Aim 2 simply required the maneuvering of a cursor within the PC domain and do not require the user to acquire objects, produce force against objects, and release objects. Physical manipulation tasks like in Specific Aims 3 and 4 required the user to interact with the world during which users anecdotally preferred the position control technique. Of course, both techniques are possible within the postural control architecture and throughout our study we were able to discern the benefits and pitfalls of each. As with any design process, testing and analysis informs future improvements. The postural control architecture is a work in progress and the findings reported here, even when describing an apparent discrepancy, are useful in the design process.

Future Ideas

The postural control algorithm provides a valuable platform upon which exciting concepts can be implemented. Throughout the design process, many design concepts were discussed but not implemented since they were outside the scope of this dissertation. Two exciting future applications using the postural control platform are described here.

Simultaneous myoelectric wrist and hand postural control for persons with transradial limb loss

The utility of the wrist in performing activities of daily living is well documented [94], [95] however the simultaneous control of hand and wrist posture is not clinically available. Several groups have implemented simultaneous control of the wrist and hand using state-of-the-art research techniques including pattern recognition algorithms [63] and/or implantable myoelectric sensors, but these technologies have not left the laboratory. I would like to use standard of care surface electrodes to drive a cursor in a two-dimensional postural control domain which would simultaneously morph the wrist and hand posture. A possible wrist and hand PC domain map is shown in Figure 36. The postural control algorithm can be easily modified to include wrist joint angles (simply increase the dimensionality of the joint angle transform), however experimentation must be performed in order to determine what wrist postures should be coupled to each hand posture. Able-bodied experiments will be performed where both hand and wrist postures are measured during activities of daily living. These empirical results will drive the design of the PC domain to couple wrist and hand posture.
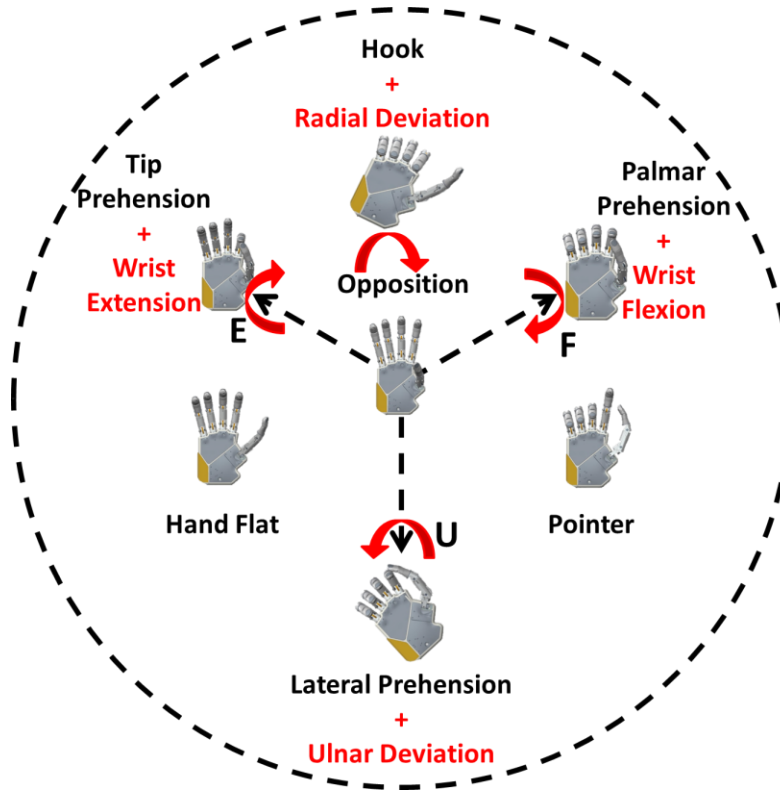
Figure 36 – A possible simultaneous wrist and hand PC domain map. Red text distinguishes the added simultaneous wrist degrees of freedom that are controlled. Red arrows indicate the direction of wrist movement.

Intrinsic sensory feedback for stable force controlled grasping using myoelectric postural control

The use of sensory feedback in our intact limbs has been shown to be critical to our ability to perform dexterous tasks with our hands [96], [97] however prosthetic hands do not have the sense of touch. Many fingertip sensors have been developed for robotic applications [98], [99], but not for a prosthesis. Here we will develop a multi-functional prosthetic hand with fingertip sensors based on the modified Bebionic hand used in Chapter 6. A novel control algorithm using the postural control platform will then integrate the sensory feedback provided by the fingertip sensors into the robotic control loop (intrinsic feedback). Using the force

feedback from the fingertip sensors, the postural control algorithm can be modified to control force as well as position thereby forming more stable grasps. After the development of the sensing prosthetic hand and novel force control paradigm within the postural control algorithm, experiments will test the ability of subjects to perform activities of daily living with and without intrinsic feedback. The experimental apparatus developed here could then be used in more advanced extrinsic sensory feedback studies where the user is provided the sensory information using advance human-machine interfaces [5], [100].

Novel Contributions

This work contributed novel concepts to the field of upper limb prosthetic control. Research in the field of upper limb prosthetic control has been dominated by the study of pattern recognition and state machines control algorithms. Both techniques are well-developed (over 20+ years of research) however still contain well-known benefits and pitfalls. Pattern recognition techniques provide an intuitive interface however perform poorly in a clinical setting due to limb position affects, electrode shift, sweat, etc. State machine algorithms provide a robust interface however require an unintuitive trigger command in order to change the function of the device. The postural controller is a novel alternative to these standard-bearers. This work indicated that the postural controller is easily learned, customizable, and an effective interface to control myoelectric prosthetic hands in a clinical setting for persons with transradial limb loss. It is robust to limb position affects, electrode shift, sweat, etc. It also does not require any trigger commands. The customizable postural control domain can be arranged in order to make the most intuitive interface for the person. The postural controller is an innovative contribution to a field that has been focused mainly on two other methods for 20+ years.

More specifically, the postural controller is a novel compilation of control techniques applied within the PC domain. In general, these control techniques are well known within the field of upper limb prosthetic control; however this is the first time they have been compiled in this arrangement.

- Customizable PC domain – Several other groups have used a two-dimensional domain in the control of hand posture [73], [82], however here is the first development of a customizable two-dimensional domain where hand postures can be arranged in any way with respect to the EMG control signals. The mathematics entails a simple linear transform between the cursor position and the joint angle vector (see Chapter 4). In addition, the logic in order to determine the modified PC cursor coordinate is a simple percent difference calculation in radial coordinates. The result is a continuously varying hand posture as the cursor maneuvers within the PC domain.

- Position and velocity control schemes – The interpretation of the EMG control signals with respect to the cursor in the PC domain was studied using both a position and velocity control scheme. The position control scheme equates to 'spring-return' where the cursor moves away from the origin of the PC domain with EMG activity and then 'spring-returns' when the EMG signal is quiescent. The velocity control scheme equates the EMG activity with a speed and a direction so that quiescent EMG activity causes the cursor to become stationary within the PC domain. Both types of schemes have been used in the control of myoelectric prehensors previously, but this is the first implementation in this manner.

- Potential wells – Potential wells are localized position feedback loops within the PC domain and can be visualized as depressions within the PC domain. In

essence, the potential wells add a third dimension to the two-dimensional PC domain. The potential wells preferentially attract the cursor to certain areas within the PC domain where the functional postures are positioned. This is the first implementation of such a concept in the control of upper limb prosthetic devices.

- Dynamic EMG tuning – The dynamic EMG tuning technique was applied in order to compensate for co-activity within the musculature especially for persons with limb loss. This technique is similar to the first-on procedure used in standard two-site myoelectric devise, however is applied to the EMG signals in the PC domain. In result, more stable grasps can be achieved and the controller is more robust to limb position affects.

Although not novel, the testing of this algorithm with persons with limb loss is a substantial contribution to the field. Myoelectric control algorithms are too often tested only with intact individuals and/or virtual testing environments. The clinical realities of persons with limb loss need to be addressed in order to invent devices and algorithms that benefit users of prosthetic devices. I know that experiments with able-bodied subjects and/or virtual environments do not allow for a full understanding of the technology. I feel that our field needs to stay grounded in the clinics and stay focused on providing the best technology to persons with limb loss. We need to translate the research from the lab bench to the clinic. This work attempted to do that by using standard of care techniques/equipment and by performing experiments requiring real-world tasks by persons with limb loss. My interactions with subjects with limb loss were the most valuable experiences of my degree, and I hope to continue in this pursuit of providing innovative technology to persons with upper limb loss as a scientist in this field.

Final Thoughts

The human hand is a complex mechano-sensory system capable of a wide range of functions from fine precision to powerful grasps. The challenge of replacing a lost limb demands technology from interdisciplinary fields like mechanical design, biomedical signal analysis, control theory, and many other specialties. Myoelectric control systems offer the best opportunities to provide more functional and intuitive prosthetic limbs. This project follows in that pursuit in the development of a postural controller for advanced myoelectric prosthetic hand. The controller developed has demonstrated encouraging performance compared to other state-of-the-art MEC as well as in a functional assessment by persons with limb loss. Hopefully, research in the field of prosthetic design will continue to absorb the best practices of related fields and continue to produce improved prostheses for those in need.

Bibliography

[1]   L. R. Hochberg, D. Bacher, B. Jarosiewicz, N. Y. Masse, J. D. Simeral, J. Vogel, S. Haddadin, J. Liu, S. S. Cash, P. van der Smagt, and J. P. Donoghue, "Reach and grasp by people with tetraplegia using a neurally controlled robotic arm," *Nature*, vol. 485, no. 7398, pp. 372–375, May 2012.

[2]   L. R. Hochberg, M. D. Serruya, G. M. Friehs, J. A. Mukand, M. Saleh, A. H. Caplan, A. Branner, D. Chen, R. D. Penn, and J. P. Donoghue, "Neuronal ensemble control of prosthetic devices by a human with tetraplegia," *Nature*, vol. 442, no. 7099, pp. 164–171, Jul. 2006.

[3]   M. A. Nicolelis and M. A. Lebedev, "Principles of neural ensemble physiology underlying the operation of brain–machine interfaces," *Nature Reviews Neuroscience*, vol. 10, no. 7, pp. 530–540, 2009.

[4]   D. J. Tyler and D. M. Durand, "Functionally selective peripheral nerve stimulation with a flat interface nerve electrode," *IEEE Transactions on Neural Systems and Rehabilitation Engineering*, vol. 10, no. 4, pp. 294–303, Dec. 2002.

[5]   D. Tan, M. Schiefer, M. W. Keith, R. Anderson, and D. J. Tyler, "Stability and selectivity of a chronic, multi-contact cuff electrode for sensory stimulation in a human amputee," in *Neural Engineering (NER), 2013 6th International IEEE/EMBS Conference on*, 2013, pp. 859–862.

[6]   G. S. Dhillon and K. W. Horch, "Direct Neural Sensory Feedback and Control of a Prosthetic Arm," *IEEE Transactions on Neural Systems and Rehabilitation Engineering*, vol. 13, no. 4, pp. 468–472, Dec. 2005.

[7]   T. A. Kuiken, G. Li, B. A. Lock, R. D. Lipschutz, L. A. Miller, K. A. Stubblefield, and K. B. Englehart, "Targeted muscle reinnervation for real-time myoelectric control of multifunction artificial arms," *JAMA: the journal of the American Medical Association*, vol. 301, no. 6, pp. 619–628, 2009.

[8]   R. F. Weir, P. R. Troyk, G. A. DeMichele, D. A. Kerns, J. F. Schorsch, and H. Maas, "Implantable Myoelectric Sensors (IMESs) for Intramuscular Electromyogram Recording," *IEEE Transactions on Biomedical Engineering*, vol. 56, no. 1, pp. 159–171, Jan. 2009.

[9]   E. Biddiss, D. Beaton, and T. Chau, "Consumer design priorities for upper limb prosthetics," *Disability & Rehabilitation: Assistive Technology*, vol. 2, no. 6, pp. 346–357, Jan. 2007.

[10]   J. T. Belter, J. Segil, A. M. Dollar, and R. F. Weir, "The Mechanical Design and Performance Specifications of Anthropomorphic Prosthetic Hands," *Journal of Rehabilitation and Development*, 2012.

[11]   M. Santello, M. Flanders, and J. F. Soechting, "Postural hand synergies for tool use," *The Journal of Neuroscience*, vol. 18, no. 23, pp. 10105–10115, 1998.

[12]   J. R. Napier and R. Tuttle, *Hands*. Princeton University Press, 1993.

[13]   K. L. Moore and A. F. Dalley, *Clinically Oriented Anatomy, 4th Edition*, 4th ed. Lippincott Williams & Wilkins, 1999.

[14]   D. U. Silverthorn, *Human Physiology: An Integrated Approach*, 5th ed. Benjamin Cummings, 2009.

[15]   D. S. Childress and R. F. Weir, "Control of limb prostheses," *Atlas of Limb Prosthetics*, vol. 2, pp. 175–198, 2004.

[16] A. Keller, C. Taylor, and V. Zahn, "Studies to Determine the Functional Requirements for Hand Arm Prosthesis." University of California Los Angeles, Jul-1947.

[17] M. R. Cutkosky, "On grasp choice, grasp models, and the design of hands for manufacturing tasks," *IEEE Transactions on Robotics and Automation*, vol. 5, no. 3, pp. 269–279, Jun. 1989.

[18] C. M. Light, P. H. Chappell, and P. J. Kyberd, "Establishing a standardized clinical assessment tool of pathologic and prosthetic hand function: normative data, reliability, and validity," *Archive of Physical Medicine and Rehabilitation*, vol. 83, pp. 776–783, 2002.

[19] "Bebionic v2 Brochure," *RSL Steeper*. [Online]. Available: http://rslsteeper.com/uploads/files/159/bebionic-ukrow-product-brochure-rsllit294-issue-21.pdf.

[20] "iLIMB Ultra Revolution Clinician Manual." Touch Bionics, Inc., Apr-2013.

[21] N. A. Bernstein, M. L. Latash, and M. Turvey, *Dexterity and its development*. Taylor & Francis, 1996.

[22] J. P. Scholz and G. Schöner, "The uncontrolled manifold concept: identifying control variables for a functional task," *Experimental Brain Research*, vol. 126, no. 3, pp. 289–306, 1999.

[23] M. L. Latash, J. P. Scholz, and G. Schöner, "Motor control strategies revealed in the structure of motor variability," *Exercise and sport sciences reviews*, vol. 30, no. 1, pp. 26–31, 2002.

[24] E. Todorov and M. I. Jordan, "Optimal feedback control as a theory of motor coordination," *Nature neuroscience*, vol. 5, no. 11, pp. 1226–1235, 2002.

[25] M. C. Tresch and A. Jarc, "The case for and against muscle synergies," *Current Opinion in Neurobiology*, vol. 19, no. 6, pp. 601–607, Dec. 2009.

[26] A. B. Ajiboye and R. F. Weir, "Muscle synergies as a predictive framework for the EMG patterns of new hand postures," *Journal of neural engineering*, vol. 6, p. 036004, 2009.

[27] M. H. Schieber, "Hand function: peripheral and central constraints on performance," *Journal of Applied Physiology*, vol. 96, no. 6, pp. 2293–2300, Jun. 2004.

[28] A. Bicchi, M. Gabiccini, and M. Santello, "Modelling natural and artificial hands with synergies," *Phil. Trans. R. Soc. B*, vol. 366, no. 1581, pp. 3153–3161, Nov. 2011.

[29] P. A. Parker and R. N. Scott, "Myoelectric control of prostheses," *Crit Rev Biomed Eng*, vol. 13, no. 4, pp. 283–310, 1986.

[30] D. D. Frey and L. E. Carlson, "A body powered prehensor with variable mechanical advantage," *Prosthet Orthot Int*, vol. 18, no. 2, pp. 118–123, Aug. 1994.

[31] K. Ziegler-Graham, E. J. MacKenzie, P. L. Ephraim, T. G. Travison, and R. Brookmeyer, "Estimating the prevalence of limb loss in the United States: 2005 to 2050," *Archives of physical medicine and rehabilitation*, vol. 89, no. 3, pp. 422–429, 2008.

[32] D. Atkins, D. Heard, and W. Donovan, "Epidemiologic Overview of Individuals with Upper Limb Loss and Their Reported Resarch Priorities." Institute of Rehabilitation and Research, 1996.

[33] P. Parker, K. Englehart, and B. Hudgins, "Myoelectric signal processing for control of powered limb prostheses," *Journal of electromyography and kinesiology*, vol. 16, no. 6, pp. 541–548, 2006.

[34] D. S. Childress, "Historical aspects of powered limb prostheses," *Clinical prosthetics and orthotics*, vol. 9, no. 1, pp. 2–13, 1985.

[35] T. W. Williams III, "Progress on stabilizing and controlling powered upper-limb prostheses.," *Journal of rehabilitation research and development*, vol. 48, no. 6, p. ix, 2011.

[36] M. Zecca, S. Micera, M. C. Carrozza, and P. Dario, "Control of multifunctional prosthetic hands by processing the electromyographic signal," *Critical reviews in biomedical engineering*, vol. 30, no. 4–6, p. 459, 2002.

[37] A. Fougner, O. Stavdahl, P. J. Kyberd, Y. G. Losier, and P. A. Parker, "Control of Upper Limb Prostheses: Terminology and Proportional Myoelectric Control—A Review," *IEEE Transactions on Neural Systems and Rehabilitation Engineering*, vol. 20, no. 5, pp. 663–677, Sep. 2012.

[38] A. Harris, K. Katyal, M. Para, and J. Thomas, "Revolutionizing Prosthetics software technology," in *2011 IEEE International Conference on Systems, Man, and Cybernetics (SMC)*, 2011, pp. 2877–2884.

[39] P. A. Parker, J. Stuller, and R. Scott, "Signal processing for the multistate myoelectric channel," *Proceedings of the IEEE*, vol. 65, no. 5, pp. 662–674, 1977.

[40] D. Dorcas and R. Scott, "A three-state myo-electric control," *Medical and Biological Engineering and Computing*, vol. 4, no. 4, pp. 367–370, 1966.

[41] "Electric Terminal Device (ETD)," *Motion Control - Utah Arm*. [Online]. Available: http://www.utaharm.com/ETD-Sales-Sheet.pdf.

[42] "Hosmer Terminal Device," *Hosmer Prosthetics and Orthotics*. [Online]. Available: http://www.hosmer.com/products/hooks/pdfs/PR108-Hooks_Brochure.pdf.

[43] "System Electric Hand," *Otto Bock*. [Online]. Available: http://www.ottobock.com/cps/rde/xchg/ob_us_en/hs.xsl/6952.html.

[44] A. Birdwell, "Investigation of Extrinsic Finger and Thumb Muscles to Command Invididual Digits on a Multi-Functional Artificial Hand," PhD Dissertation, Northwestern University, 2011.

[45] C. Cipriani, J. L. Segil, J. A. Birdwell, and R. F. Weir, "Dexterous control of a prosthetic hand using fine-wire intramuscular electrodes in targeted extrinsic muscles," *IEEE Transactions on Neural Systems and Rehabilitation Engineering*, vol. (accepted), Jan. 2014.

[46] S. Dalley, H. Varol, and M. Goldfarb, "A Method for the Control of Multigrasp MyoelectricProsthetic Hands," *Neural Systems and Rehabilitation Engineering, IEEE Transactions on*, no. 99, pp. 1–1, 2011.

[47] L. Hargrove, Y. Losier, B. Lock, K. Englehart, and B. Hudgins, "A Real-Time Pattern Recognition Based Myoelectric Control Usability Study Implemented in a Virtual Environment," in *29th Annual International Conference of the IEEE Engineering in Medicine and Biology Society, 2007. EMBS 2007*, 2007, pp. 4842–4845.

[48] A. M. Simon, L. J. Hargrove, B. A. Lock, and T. A. Kuiken, "Target Achievement Control Test: Evaluating real-time myoelectric pattern-recognition control of multifunctional upper-limb prostheses," *The Journal of Rehabilitation Research and Development*, vol. 48, no. 6, p. 619, 2011.

[49] P. Kyberd and W. Hill, "Upper Limb Prosthetic Outcome Measures (ULPOM) Group," 2008.

[50] L. A. Miller and S. Swanson, "Summary and Recommendations of the Academy's State of the Science Conference on Upper Limb Prosthetic Outcome Measures," *Journal of Prosthetics*, vol. 21, no. 9, 2009.

[51] F. V. Bs. Wright, "Measurement of Functional Outcome With Individuals Who Use Upper Extremity Prosthetic Devices: Current and Future Directions," *Journal of Prosthetics*, vol. 18, no. 2, pp. 46–56, 2006.

[52] L. A. Miller, K. A. Stubblefield, R. D. Lipschutz, B. A. Lock, and T. A. Kuiken, "Improved Myoelectric Prosthesis Control Using Targeted Reinnervation Surgery: A Case Series," *IEEE Transactions on Neural Systems and Rehabilitation Engineering*, vol. 16, no. 1, pp. 46–50, 2008.

[53] T. R. Farrell and R. F. Weir, "The Optimal Controller Delay for Myoelectric Prostheses," *IEEE Transactions on Neural Systems and Rehabilitation Engineering*, vol. 15, no. 1, pp. 111–118, Mar. 2007.

[54] O. Van Der Niet Otr, H. A. Reinders-Messelink, R. M. Bongers, H. Bouwsema, and C. K. Van Der Sluis, "The i-LIMB hand and the DMC plus hand compared: A case report," *Prosthetics and Orthotics International*, vol. 34, no. 2, pp. 216–220, Jun. 2010.

[55] S. A. Dalley, D. A. Bennett, and M. Goldfarb, "Preliminary functional assessment of a multigrasp myoelectric prosthesis," in *Engineering in Medicine and Biology Society (EMBC), 2012 Annual International Conference of the IEEE*, 2012, pp. 4172–4175.

[56] B. Hudgins, P. Parker, and R. N. Scott, "A new strategy for multifunction myoelectric control," *IEEE Transactions on Biomedical Engineering*, vol. 40, no. 1, pp. 82–94, 1993.

[57] K. Englehart and B. Hudgins, "A robust, real-time control scheme for multifunction myoelectric control," *IEEE Transactions on Biomedical Engineering*, vol. 50, no. 7, pp. 848–854, Jul. 2003.

[58] Guanglin Li, A. E. Schultz, and T. A. Kuiken, "Quantifying Pattern Recognition—Based Myoelectric Control of Multifunctional Transradial Prostheses," *IEEE Transactions on Neural Systems and Rehabilitation Engineering*, vol. 18, no. 2, pp. 185–192, Apr. 2010.

[59] E. Scheme and K. Englehart, "Electromyogram pattern recognition for control of powered upper-limb prostheses: state of the art and challenges for clinical use," *J Rehabil Res Dev*, vol. 48, no. 6, pp. 643–659, 2011.

[60] A. J. Young, L. J. Hargrove, and T. A. Kuiken, "Improving Myoelectric Pattern Recognition Robustness to Electrode Shift by Changing Interelectrode Distance and Electrode Configuration," *IEEE Transactions on Biomedical Engineering*, vol. 59, no. 3, pp. 645–652, 2012.

[61] C. Cipriani, R. Sassu, M. Controzzi, and M. C. Carrozza, "Influence of the weight actions of the hand prosthesis on the performance of pattern recognition based myoelectric control: Preliminary study," in *2011 Annual International Conference of the IEEE Engineering in Medicine and Biology Society,EMBC*, 2011, pp. 1620–1623.

[62] A. Fougner, E. Scheme, A. D. C. Chan, K. Englehart, and O. Stavdahl, "Resolving the Limb Position Effect in Myoelectric Pattern Recognition," *IEEE Transactions on Neural Systems and Rehabilitation Engineering*, vol. 19, no. 6, pp. 644–651, 2011.

[63] A. J. Young, L. H. Smith, E. J. Rouse, and L. J. Hargrove, "Classification of Simultaneous Movements Using Surface EMG Pattern Recognition," *IEEE Transactions on Biomedical Engineering*, vol. 60, no. 5, pp. 1250–1258, 2013.

[64] B. A. Lock, A. M. Simon, K. Stubblefield, and L. J. Hargrove, "Prosthesis-Guided Training For Practical Use Of Pattern Recognition Control Of Prostheses," 2011.

[65] P. J. Kyberd and P. H. Chappell, "The Southampton Hand: an intelligent myoelectric prosthesis," *J Rehabil Res Dev*, vol. 31, no. 4, pp. 326–334, Nov. 1994.

[66] P. J. Kyberd, O. E. Holland, P. H. Chappell, S. Smith, R. Tregidgo, P. J. Bagwell, and M. Snaith, "MARCUS: A two degree of freedom hand prosthesis with hierarchical grip control," *Rehabilitation Engineering, IEEE Transactions on*, vol. 3, no. 1, pp. 70–76, 1995.

[67] S. A. Dalley, H. A. Varol, and M. Goldfarb, "A Method for the Control of Multigrasp Myoelectric Prosthetic Hands," *IEEE Transactions on Neural Systems and Rehabilitation Engineering*, vol. 20, no. 1, pp. 58–67, Jan. 2012.

[68] C. Cipriani, M. Controzzi, and M. C. Carrozza, "The SmartHand transradial prosthesis," *Journal of neuroengineering and rehabilitation*, vol. 8, no. 1, p. 29, 2011.

[69] "iLIMB User Manual," *Touch Bionics*. [Online]. Available: http://www.touchbionics.com/media/58279/i-limb_digits_user_manual_ma01063.pdf.

[70] N. A. Alshammary, S. A. Dalley, and M. Goldfarb, "Assessment of a multigrasp myoelectric control approach for use by transhumeral amputees," in *2012 Annual International Conference of the IEEE Engineering in Medicine and Biology Society (EMBC)*, 2012, pp. 968–971.

[71] M. T. Ciocarlie and P. K. Allen, "Hand Posture Subspaces for Dexterous Robotic Grasping," *The International Journal of Robotics Research*, vol. 28, no. 7, pp. 851–867, Jun. 2009.

[72] G. C. Matrone, C. Cipriani, E. L. Secco, G. Magenes, M. C. Carrozza, and others, "Principal components analysis based control of a multi-dof underactuated prosthetic hand," *Journal of neuroengineering and rehabilitation*, vol. 7, no. 1, p. 16, 2010.

[73] G. C. Matrone, C. Cipriani, M. C. Carrozza, and G. Magenes, "Real-time myoelectric control of a multi-fingered hand prosthesis using principal components analysis," *Journal of NeuroEngineering and Rehabilitation*, vol. 9, no. 1, p. 40, 2012.

[74] G. Matrone, C. Cipriani, M. Carrozza, and G. Magenes, "Two-channel real-time EMG control of a dexterous hand prosthesis," in *Neural Engineering (NER), 2011 5th International IEEE/EMBS Conference on*, 2011, pp. 554–557.

[75] J. Segil, R. F. Weir, and D. Reamon, "Design Of A Myoelectric Controller For A Multi-Dof Prosthetic Hand Based On Principal Component Analysis," in *Proceeding of the MyoElectric Controls/Powered Prosthetics Symposium*, Fredericton, New Brunswick, 2011, pp. 205–209.

[76] A. B. Ajiboye and R. F. H. Weir, "A Heuristic Fuzzy Logic Approach to EMG Pattern Recognition for Multifunctional Prosthesis Control," *IEEE Transactions on Neural Systems and Rehabilitation Engineering*, vol. 13, no. 3, pp. 280–291, Sep. 2005.

[77] R. L. Lieber, "Statistical significance and statistical power in hypothesis testing," *Journal of Orthopaedic Research*, vol. 8, no. 2, pp. 304–309, 1990.

[78] A. R. Tilley and H. D. Associates, *The Measure of Man and Woman: Human Factors in Design*. Wiley, 2001.

[79] L. Y. Chang and Y. Matsuoka, "A kinematic thumb model for the ACT hand," in *Robotics and Automation, 2006. ICRA 2006. Proceedings 2006 IEEE International Conference on*, 2006, pp. 1000–1005.

[80] D. Giurintano, A. Hollister, W. Buford, D. Thompson, and L. Myers, "A virtual five-link model of the thumb," *Medical engineering & physics*, vol. 17, no. 4, pp. 297–303, 1995.

[81] A. de Rugy, G. E. Loeb, and T. J. Carroll, "Muscle Coordination Is Habitual Rather than Optimal," *Journal of Neuroscience*, vol. 32, no. 21, pp. 7384–7391, May 2012.

[82] T. Pistohl, C. Cipriani, A. Jackson, and K. Nazarpour, "Abstract and Proportional Myoelectric Control for Multi-Fingered Hand Prostheses," *Annals of Biomedical Engineering*, vol. 41, no. 12, pp. 2687–2698, Aug. 2013.

[83] S. M. Radhakrishnan, S. N. Baker, and A. Jackson, "Learning a Novel Myoelectric-Controlled Interface Task," *Journal of Neurophysiology*, vol. 100, no. 4, pp. 2397–2408, Aug. 2008.

[84] A. W. Salmoni, R. A. Schmidt, and C. B. Walter, "Knowledge of results and motor learning: A review and critical reappraisal," *Psychological Bulletin*, vol. 95, no. 3, pp. 355–386, 1984.

[85] N. Jiang, H. Rehbaum, I. Vujaklija, B. Graimann, and D. Farina, "Intuitive, Online, Simultaneous, and Proportional Myoelectric Control Over Two Degrees-of-Freedom in Upper Limb Amputees," *IEEE Transactions on Neural Systems and Rehabilitation Engineering*, vol. 22, no. 3, pp. 501–510, May 2014.

[86] J. L. Segil and R. F. ff Weir, "Derivation of Optimal Surface Electrode Control Sites Using Untargeted Electrode Array for Myoelectric Control of Prosthetic Hands," in *Rocky Mountain American Society of Biomechanics*, Estes Park, CO, 2013.

[87] J. L. Segil and R. F. Weir, "Design and Validation of a Morphing Myoelectric Hand Posture Controller based on Principal Component Analysis of Human Grasping," *IEEE Transactions on Neural Systems and Rehabilitation Engineering*, vol. Early Access Online, 2013.

[88] C. Cipriani, F. Zaccone, S. Micera, and M. C. Carrozza, "On the Shared Control of an EMG-Controlled Prosthetic Hand: Analysis of User–Prosthesis Interaction," *IEEE Transactions on Robotics*, vol. 24, no. 1, pp. 170–184, Feb. 2008.

[89] "Michelangelo Hand User Manual." Otto Bock, Inc., 2012.

[90] J. L. Segil and R. F. Weir, "A Novel Architecture for a Postural Controller of Multi-functional Myoelectric Prosthetic Hands," *Journal of Neural Engineeringand Rehabilitatio*, vol. (in submission), Oct. 2013.

[91] SHAP Business Enterprise, "Assessor's SHAP Protocol," University of Southampton, Manual, 2012.

[92] J. V. Basmajian, *Muscles alive: their functions revealed by electromyography*. Williams & Wilkins, 1974.

[93] S. M. Wurth and L. J. Hargrove, "Real-time comparison of conventional direct control and pattern recognition myoelectric control in a two-dimensional Fitts' law style test," in *Engineering in Medicine and Biology Society (EMBC), 2013 35th Annual International Conference of the IEEE*, 2013, pp. 3630–3633.

[94] P. J. Kyberd, E. D. Lemaire, E. Scheme, C. MacPhail, L. Goudreau, G. Bush, and M. Brookeshaw, "Two-degree-of-freedom powered prosthetic wrist," *The Journal of Rehabilitation Research and Development*, vol. 48, no. 6, p. 609, 2011.

[95] F. Montagnani, M. Controzzi, and C. Cipriani, "Preliminary design and development of a two degrees of freedom passive compliant prosthetic wrist with switchable stiffness," in *Robotics and Biomimetics (ROBIO), 2013 IEEE International Conference on*, 2013, pp. 310–315.

[96] R. S. Johansson and J. R. Flanagan, "Coding and use of tactile signals from the fingertips in object manipulation tasks," *Nature Reviews Neuroscience*, vol. 10, no. 5, pp. 345–359, May 2009.

[97] R. S. Johansson and B. B. Edin, "Predictive feed-forward sensory control during grasping and manipulation in man," *BIOMEDICAL RESEARCH-TOKYO-*, vol. 14, pp. 95–95, 1993.

[98] J. Ulmen and M. Cutkosky, "A robust, low-cost and low-noise artificial skin for human-friendly robots," in *Robotics and Automation (ICRA), 2010 IEEE International Conference on*, 2010, pp. 4836–4841.

[99] M. C. Jimenez and J. A. Fishel, "Evaluation of force, vibration and thermal tactile feedback in prosthetic limbs," in *Haptics Symposium (HAPTICS), 2014 IEEE*, 2014, pp. 437–441.

[100] C. Cipriani, J. L. Segil, F. Clemente, R. F. Weir, and B. Edin, "Discrete Event Sensory Feedback during Teleoperation of a Prosthetic Hand," *(pending publication).*